UNIVERSITÀ DELLA CALABRIA

UNIVERSITA' DELLA CALABRIA

Dipartimento di Biologia, Ecologia e Scienze della Terra (DiBest)

Dottorato di Ricerca in

Scienze della Vita

Indirizzo

Biotecnologie

XXIX CICLO

Structure/function relationships of the human heterodimeric amino acids transporter 4F2hc/LAT1

Settore Scientifico Disciplinare: BIO/10 BIOCHIMICA

Coordinatore: Ch.mo Prof. Marcello Canonaco

Firma

Supervisore/Tutor: Ch.mo Prof. Cesare Indiveri

Firma

Co-Tutor: Dott.ssa Mariafrancesca Scalise

Firma

Dottoranda: Dott.ssa Lara Napolitano

Firma

CONTENTS

Abstract

Amino acids transport in mammalian cells is mediated by different amino acid transporters whose activity allow the flow of an important source for metabolic need of cells. Moreover, some amino acids such as Gln, Arg and Leu work as signalling molecules and their availability and concentration represent key factors in the regulation of intracellular signalling pathways responsible of cellular growth. Thus, amino acids flow, which is important under physiological condition, becomes particularly relevant under pathological conditions such as in tumours cells to satisfy their unique metabolic and proliferative needs. Therefore, since in tumours upregulation of amino acids transporters is an important step to satisfy the increased demand for these nutrients, the same transporters are potential drug targets for cancer therapy. However, the certainty that a specific transporter could be a target in human therapy requires its functional characterization and the knowledge of the enchanting structure/function relationships. In this context, an important transporter that became of particular interest for its overexpression in many tumours is LAT1, and the aim of this work has been that to shed light on still unclear aspects of its function.

hLAT1 belongs to SLC7 family and into the plasma membrane forms heterodimers with the glycoprotein 4F2hc (also known as CD98 in mice), member of SLC3 family. Studies conducted in intact cells showed that 4F2hc/LAT1 complex catalyses amino acids transport; however, in this experimental model it was not possible to clarify whether one or both subunits are competent for transport activity and substrate recognition. Thus, aimed to unravel the dark side of 4F2hc/LAT1 mediated transport, different experimental strategies were adopted allowing to demonstrate that LAT1 is the sole transport competent unit of the heterodimer. Indeed, using western blot analyses and transport assays in liposomes reconstituted with proteins extracted from SiHa cells and in liposomes reconstituted with recombinant LAT1, it has been demonstrated that neither the covalent interaction nor the association of 4F2hc with LAT1 influence transport and specificity of LAT1. Moreover, the suitability of proteoliposome model used for reconstitution of recombinant LAT1, allowed to identify a functional asymmetry of this transporter which, on a physiological point of view, exhaustively elucidates the reciprocal correlation between the transport activity of LAT1 and that of another important amino acids transporter overexpressed in tumours cells, ASCT2. To the same extent, proteoliposome tool together with bioinformatics and site-directed mutagenesis have been useful to probe critical residues of the substrate binding site of LAT1. These results laid the groundwork for deciphering molecular mechanism of LAT1 function and for setting up studies aimed to identify new potent and specific inhibitors great for human health.

Riassunto

Il trasporto di amminoacidi nelle cellule umane è mediato da diverse proteine di trasporto la cui attività consente il flusso, attraverso la membrana, di un'importante classe di nutrienti necessari a soddisfare le richieste metaboliche delle cellule stesse. Alcuni amminoacidi, quali Gln, Arg and Leu, fungono anche da molecole segnale perciò la loro disponibilità e concentrazione rappresentano fattori chiave per il controllo di vie di segnalazione intracellulari responsabili della crescita cellulare. Per tale ragione, il flusso di amminoacidi è rilevante sia in contesti fisiologici che patologici. Le cellule tumorali, ad esempio, presentano un incremento del flusso di amminoacidi necessari a sostenere la loro proliferazione. Per soddisfare l'aumentato flusso di nutrienti, le cellule tumorali over-esprimono sistemi di trasporto di amminoacidi che, quindi, divengono potenziali target nella terapia anticancro. Tuttavia, perché una specifica proteina di trasporto possa essere studiata come target farmacologico, è necessaria una profonda conoscenza delle sue caratteristiche funzionali e cinetiche nonché del rapporto struttura funzione. Per raggiungere tale scopo, nel presente lavoro di dottorato è stato studiato uno specifico trasportatore umano, LAT1, over-espresso in molti tumori.

hLAT1 appartiene alla famiglia SLC7 e forma, nella membrana plasmatica, eterodimeri con la glicoproteina 4F2hc (anche nota come CD98) appartenente alla famiglia SLC3. L'attività del complesso 4F2hc/LAT1, come riportato in letteratura, è stata studiata in cellule intatte, tuttavia, tale modello sperimentale non ha consentito di chiarire se una o entrambe le subunità del complesso fossero necessarie per l'attività di trasporto e per il riconoscimento del substrato. Per tale ragione, al fine di rivelare gli aspetti poco chiari del trasporto mediato dal complesso 4F2hc/LAT1, sono state adottate differenti strategie sperimentali che hanno consentito di dimostrare che LAT1 è l'unica unità competente del complesso. Analisi di western blot e studi di trasporto condotti in proteoliposomi hanno consentito di dimostrare che né il trasporto né la specificità del trasportatore LAT1 sono influenzate dall'interazione covalente o dall'associazione con la glicoproteina 4F2hc. Questi risultati sono stati ottenuti sia usando le proteine estratte da cellule SiHa, sia la proteina ricombinate LAT1. La corrispondenza di risultati ottenuti con la proteina nativa e quella ricombinante ha permesso di dimostrare la validità del modello sperimentale di ricostituzione in liposomi del trasportatore LAT1. Il sistema LAT1 è un antiport di amminoacidi Na^+ e pH indipendente che mostra una preferenza per grandi amminoacidi quali Trp, Phe Tyr ed His, ma anche amminoacidi più piccoli quali Met, Val, Leu, Ile risultano essere trasportati. Nel modello sperimentale della ricostituzione in liposomi è stata dimostrata anche l'asimmetria funzionale e cinetica di LAT1 che, da un punto di vista fisiologico, chiarisce la reciproca correlazione tra l'attività di trasporto mediata da LAT1 e quella mediata da ASCT2, un altro trasportatore di amminoacidi ampiamente espresso nelle cellule tumorali. Allo stesso modo, la ricostituzione in liposomi della proteina ricombinante LAT1, in associazione a studi di bioinformatica e all'uso della mutazione sito-diretta per ottenere proteine ricombinanti mutate, hanno consentito di verificare il coinvolgimento di specifici residui amminoacidici nel riconoscimento, legame e traslocazione del substrato. In particolare è stato dimostrato che F252, S342 e C335 sono cruciali nel riconoscimento del substrato, mentre C407 svolge un ruolo marginale. I risultati ottenuti, rappresentano una base solida per decifrare il meccanismo molecolare del trasportatore oggetto di studio che

è di tipo random simultaneo in cui i due substrati legano nello stesso momento il sito interno ed esterno del trasportatore. I risultati complessivamente ottenuti nel presente lavoro di dottorato costituiscono le basi per effettuare studi volti all'identificazione di nuovi potenti e specifici inibitori importanti per la salute umana.

Abbreviations

AdiC	L-arginine/agmatine antiporter
APC	Amino acid-polyamine-organocation (APC) superfamily
ApcT	Proton-coupled broad-specificity amino acid transporter
BBB	Blood brain barrier
BCH	2-aminobicyclo-(2,2,1)-heptane-2-carboxylic acid
$C_{12}E_8$	Octaethylene glycol monododecyl ether
CD98	Cluster of differentiation 98
DDM	N-Dodecyl β-D-maltopyranoside
DTE	Dithioerythritol
E. coli	*Escherichia coli*
GST	Glutathione-S-transferase
LATs	Light subunits of amino acid transporters
LeuT	Na^+-coupled leucine transporter
mTOR	Mammalian target of rapamycin
MTSEA	2-Aminoethyl methanethiosulfonate hydrobromide
NEM	N-ethylmaleimide
SLC	Solute carrier
TEMED	Tetramethylethylenediamine
TMD	Transmembrane domain
TX-100	Triton X-100

Chapter I

Introduction

1.1. Biological membranes and transport activity

Biological membranes represent a permeability barrier that divide the cytoplasmic from the extracellular space in all cells, establishing and discerning the biochemical identity of a single cell from the external environment. Therefore, biological membranes govern substance traffic between the internal and the external environments of cells, safeguarding nutrient assumption, metabolic intermediates retention and scrap product ejection.

Biological membranes consist of a continuous phospholipids bilayer in which many membrane proteins are included, indeed, a pure phospholipidic bilayer would impede the access of ions, amino acids, sugars and other hydro soluble molecules. In this contest transport proteins guarantee selective transport of molecules. In the past, it was believed that a large number of molecules could diffuse through membranes. It is now well established that transmembrane proteins are necessary for translocating virtually all the molecules with the exception of very few molecules such as oxygen [1, 2].

In particular, transport proteins mediate entry of nutrients into the cytoplasmic compartment, allowing metabolism of exogenous sources of carbon, nitrogen, sulfur, phosphorus, ions, micronutrients and, then, elimination of end products of metabolic pathways. Transporters allow also uptake and efflux of drugs and other toxic compounds. Active transport of ion species is important to maintain a membrane potential given by ion concentration gradients. Transporters are also directly involved in the elimination of many physiological molecules produced by the cell metabolism, such as lipids, proteins, and complex carbohydrates into and beyond the cytoplasmic membrane. Sometimes, transport proteins work in conjunction with extra cytoplasmic receptors or with cytoplasmic energy-coupling and regulatory proteins forming protein complex [3].

Transporters are also important for metabolite exchange among different sub-cellular compartments, allowing completion of biochemical pathways.

1.2. Membrane transport proteins

Given their essential role for uptake, elimination, and intracellular traffic of all nutrients and metabolites, transport proteins are fundamental for life, indeed they represent a significant fraction of all proteins encoded in the genomes of both simple and complex organisms.

Transport proteins can be classified using different criteria based on functional, molecular or evolutionary aspects. On a functional point of view, in both prokaryotes and eukaryotes, transport systems can be classified in two main groups: channels and permeases.

I. **Channels** are transmembrane proteins, which catalyse ion transport with an high turnover rates. The driving force for transport derives from ion concentration gradients.

II. **Permeases** catalyse transport of different compounds with a lower turnover than channels and are active transporters, which utilize diverse energy-coupling mechanisms [4]. In particular, on the basis of the origin of the transport driving force, permeases can be subdivided into primary and secondary active transporters.

- **Primary active transporters** contain ATPase domains or subunits which generate free energy from ATP hydrolysis coupled to the transport process.
- **Secondary active transporters**, which constitute the largest group, can be classified in three categories (uniporters, symporters and antiporters) on the basis of the number of substrates and of transport direction. The driving force for this group of transporters is generated, by concentration gradients of the transported substrates (uniporters), coupling to a co-transported ion such as Na^+ or H^+ (symporters), or coupling to a counter substrate, which is transported in the opposite direction (antiporters) (Fig. 1) [1].

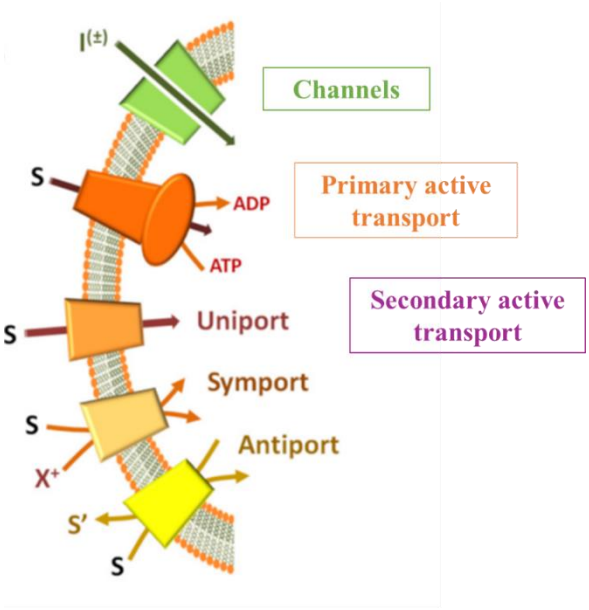

Fig. 1: Functional classification of membrane proteins. (Adapted from Scalise et al., Proteoliposomes as Tool for Assaying Membrane Transporter Functions and Interactions with Xenobiotics, 2013).

1.3. Amino acid metabolism and transport

Protein's share through diet is about 30% in a typical western diet. Protein degradation, in their constituent amino acids, takes place in the gastrointestinal segment. Indeed, after their digestion, the resulting dipeptides and amino acids are efficiently absorbed by the enterocytes of the small intestine where dipeptides are metabolized. Most of globular proteins from animal sources are almost completely degraded in free amino acids [2].

Amino acids derived from intracellular or diet proteins degradation, are distributed to tissues and metabolized in liver. Amino acids are an important biological molecule class whose oxidation gives a significant, but variable, contribution to metabolic energetic request of cells. In particular oxidative degradation of amino acids require a phase in which the amino group is separated from carbon skeleton and sent to specialized pathway for amino group metabolism, whereas, carbon skeletons are channelled into citric acid cycle to obtain energy from oxidation. Amino acids are also necessary for synthesis of proteins and bioactive molecules and they are delivered to all tissues through the blood [2, 5]. The flow of these important nutrients, across the plasma membrane, is mediated and strictly controlled by specific transport proteins.

1.4. Mammalian amino acid transporters

Researches on mammalian amino acid transporters have been introduced in 1960 by Christensen's group, to identify functional characteristics, which allow to discern different transporter. Indeed, using radiolabelled amino acids and amino acid analogues, Christensen and colleagues observed that amino acid transporters accept groups of amino acid rather than single amino acids. Functional characteristics, such as substrate specificity, kinetic and regulatory properties, ion dependence and pH sensitivity, distinguish specific transporters [6]. On the basis of the differential characteristics emerged from these studies, the main criteria adopted to classify amino acid transporters has been the type of amino acid (acidic, zwitterionic or hydrophobic) and the thermodynamic properties of the transport. Moreover, amino acids transport activity was commonly defined "system", term used to indicate a transport activity functionally identified and very similar in different cell types.

In particular, Christensen's work identified:

- **System L** which includes amino acid transporters that prefer leucine and other large hydrophobic neutral amino acids;
- **System A** for alanine and other small neutral amino acids;
- **System ASC** for alanine, serine, and cysteine;
- **System y^+** for cationic amino acids;
- **System X^{-AG}** for anionic amino acids;

All amino acid transporters are divided into two categories, Na^+-dependent and Na^+-independent.

- **Na^+-dependent amino acid transporters** utilize the energy present across the membrane established by Na^+ electrochemical gradient which is mainly maintained by the Na^+/K^+-ATPase, to drive the uptake of amino acids across the membrane.
- **Na^+-independent amino acid transporters** drive the selective movement of amino acids across the plasma membrane independently of Na^+.

The nomenclature used for mammalian amino acid transporters terms Na^+-dependent systems in uppercase letters and Na^+-independent systems in lowercase letters. Only the Na^+-independent transporter System L has maintained its uppercase designation for historical reasons [7].

Even though the above described classification is still considered effective on a functional point of view, the growing knowledge of structural data obtained on transporters, together with bioinformatics, introduced a classification of amino acid transporters based on the sequence homology. In the latest two decade, in silico methodologies gave additional information on eukaryote amino acid transporters deriving from homology modelling based on prokaryotic template structures [8]. These studies start from the outset that similar amino acid sequences in proteins reflect similar three-dimensional structures and mechanisms of action; thus by determining the structure and function of at least one member of each protein family, it is possible obtain information about structures, substrate specificities and function of other proteins belonging to the same family [2, 54].

1.5. The APC superfamily

One of the major transporter groups is the amino acid/polyamine/organocation (APC) superfamily, which is represented in each of the life domains (eukaryotes, bacteria and archea). The APC superfamily includes 10 families for which literature data report phylogenetic/sequence analyses defining the evolutionary relationships of the proteins to each other as well as the phylogeny of each of the 10 families within the APC superfamily [9-11]. The members of these 10 families function as solute:cation symporters and solute:solute antiporters. The families belonging to APC superfamily are: EAT (ethanolamine transporter) family; AAT (amino acid transporter) family; YAT (yeast amino acid transporter); LAT (l-type amino acid transporter) family; CAT (cationic amino acid transporter) family; APA (basic amino acid/polyamine transporter) family; ACT (amino acid/choline transporter) family; ABT (archaeal/bacterial transporter) family; GGA (Glutamate:GABA antiporter) family; SGP (Spore germination protein) family. The substrate specificities of some APC superfamily transporters have been carefully studied revealing that while some have exceptionally broad specificity for amino acids, others are restricted to just one or a few amino acids.

The majority of homologous integral membrane APC permease polypeptide chains, vary in size from about 400 to 800 amino acid residues. According to hydropathy profile analysis and biochemically established topological features of most prokaryotic and eukaryotic APC superfamily members, both the N- and C-termini of the proteins are located in the cytoplasm with a 12-transmembrane segment topology, with some exception [9-11].

1.6. The solute carrier SLC7 family

One family of the APC transporter superfamily have human members involved in relevant physiological functions. This family is the solute carrier SLC7 family whose members belong to two subfamily: the cationic

amino acid transporters (CATs, SLC7A1–4 and SLC7A14) and the L-type amino acid transporters (LATs, SLC7A5-13 and SLC7A15). The latter are also called light chains or catalytic subunits of the heteromeric amino acid transporters (HATs) or glycoprotein-associated amino acid transporters (the gpaAT family) (Fig.2).

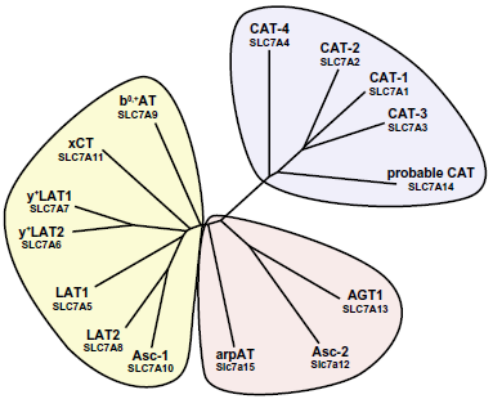

Fig. 2: Phylogenetic tree of SLC7 family members. The SLC7 family is composed of the CATs and the light subunits of HATs. (Adapted from Fotiadis D. et al., The SLC3 and SLC7 families of amino acid transporters, 2013).

CATs are the principal entry path for cationic amino acids, playing an important role in nitric oxide synthesis by delivering L-arginine for nitric oxide synthase. These transporters are N-glycosylated and have 14 putative transmembrane domains (TMDs) with cytosolic N- and C-termini in line with transmembrane topology prediction and experimental evidence [12].

LATs are not N-glycosylated and the peculiar property of this group of proteins consists in forming covalent heterodimer with larger polypeptides belonging to the SLC3 family, a small group of type II membrane glycoproteins. LATs only have 12 TMDs, which show significant similarity to the first 12 TMDs of CATs.

As indicated from sequence analyses both, CATs and LATs, originate from an ancestral 12 TMD protein and the duplication of the last two TMDs of this ancestral protein is the origin of the 14 TMD CAT structure. An estimation indicates that this duplication happened about 2.6 billion years ago [13]. Homologous CAT and LAT proteins are found in prokaryotes, but the cysteine residue of the LATs involved in the disulphide bridge with polypeptides belonging to the SLC3 family is not conserved [14]. SLC3 proteins and HATs are only found in metazoans [12].

1.7. The heteromeric amino acid transporters HATs

The heteromeric amino acid transporters, HATs, are composed of a light and a heavy subunit linked by a disulphide bridge. The heavy subunits are the SLC3 members, whereas the light subunits are the eukaryotic LATs from the SLC7 family of amino acid transporters. For SLC3 members, the cysteine residue participating in the disulphide bridge with the corresponding light subunit is four to five amino acids away from the TMD,

whereas for LATs the cysteine residue involved in the disulphide bridge with the heavy subunit is located between TMD III and IV (Fig. 3).

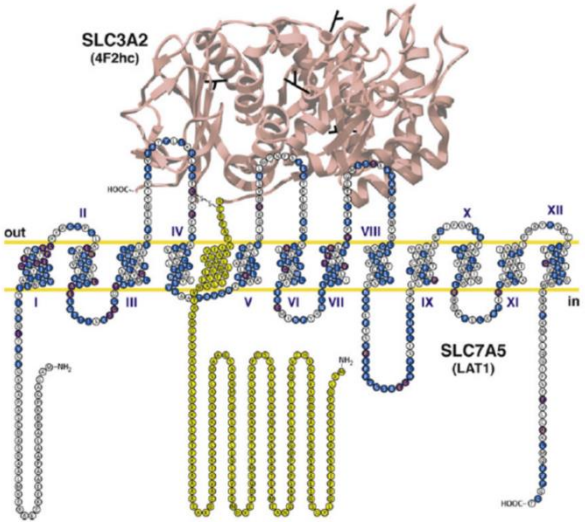

Fig. 3: Model of human heterodimer 4F2hc/LAT1 proteins. (Adapted from Fotiadis D. et al., The SLC3 and SLC7 families of amino acid transporters, 2013).

1.7.1. HATs and their heavy subunits

The SLC3 family includes two members: rBAT (SLC3A1) and 4F2hc (SLC3A2, also named CD98) (Table 1).

Human gene	Protein	Aliases	Predominant substrates	Transport type	Tissue distribution and cellular / subcellular expression	Link to disease	Human gene locus
SLC3A1	rBAT	NBAT D2	Heterodimerizes with light subunit $b^{0,+}$ AT (SLC7A9): amino acid transport system $b^{0,+}$	Exchanger (see SLC7 table for details)	Epithelial cells in kidney and small intestine, liver, pancreas. In epithelial cells, apical plasma membrane	Classic cystinuria type I	2p16.3-p21
SLC3A2	4F2hc	CD98hc	Amino acid transport systems L, y^+ L, x_c^- and asc with light subunits SLC7A5-8 and SLC7A10-11	Exchanger (see SLC7 table for details)	Ubiquitous. In epithelial cells, basolateral plasma membrane		11q13

Table 1: SLC3 family (Adapted from Palacin, M., Kanai, Y., 2004. The ancillary proteins of HATs: SLC3 family of amino acid transporters).

The two proteins share about 20% amino acid sequence identity and both are N-glycosylated with a molecular mass of ~94 and ~85 kDa for rBAT and 4F2hc, respectively [12]. In particular, SLC3 proteins are type II membrane glycoproteins with a single transmembrane domain and the C-terminal located outside the cell. The large extracellular domain of SLC3 members has sequence and structural homology with bacterial α-glucosidases and the insect maltases. In this regard, a bioinformatics study describing a comparison of all

available rBAT and 4F2hc sequences with GH13 enzyme family is reported in literature [15]. The crystal structure of the extracellular domain of human 4F2hc has been solved at 2.1 Å resolution, and it has been observed that the protein has the characteristic fold of these enzymes, a $(\beta\alpha)_8$ barrel and a C-terminal, anti-parallel β_8 sandwich [16]. However, despite this structural similarity, 4F2hc lacks the key catalytic residues necessary for glucosidase activity [16]. The atomic structure of the rBAT extracellular domain has not been solved.

rBAT was identified by expression in *Xenopus* oocytes and in 1999, $b^{0,+}$AT (SLC7A9) was identified as the light subunit that co-expresses with rBAT. This complex mediates the antiport of cystine and dibasic amino acids with neutral amino acids. The rBAT/$b^{0,+}$AT heterodimer is defective in cystinuria, a recessive disease, and the most common primary inherited aminoaciduria, characterized by hyperexcretion of dibasic amino acids and cystine in urine [17].

4F2hc was originally identified as a lymphocyte activation antigen through a monoclonal antibody 4F2 and is a ubiquitous multifunctional protein [17]. 4F2hc, indeed, could associate with different transporters (see Table 1 and below) over-expressed in many tumours and in activated lymphocytes suggesting a role of 4F2hc and the associated transporters in cell growth. Furthermore, 4F2hc mediates β-integrin signalling and cell fusion. Thus, given the dual function exerted by 4F2hc, it is possible to hypothesize that this protein plays a key role in integrating integrin signalling and amino acid transport [12].

In agreement with the different roles of both heavy subunits, rBAT/$b^{0,+}$AT expression is restricted to the apical domain of the plasma membrane of epithelial cells of the small intestine and of the renal proximal tubule, whereas 4F2hc-associated transporters are almost ubiquitously expressed. Moreover, 4F2hc is expressed in the basolateral plasma membrane of epithelial cells (Fig. 4) [18].

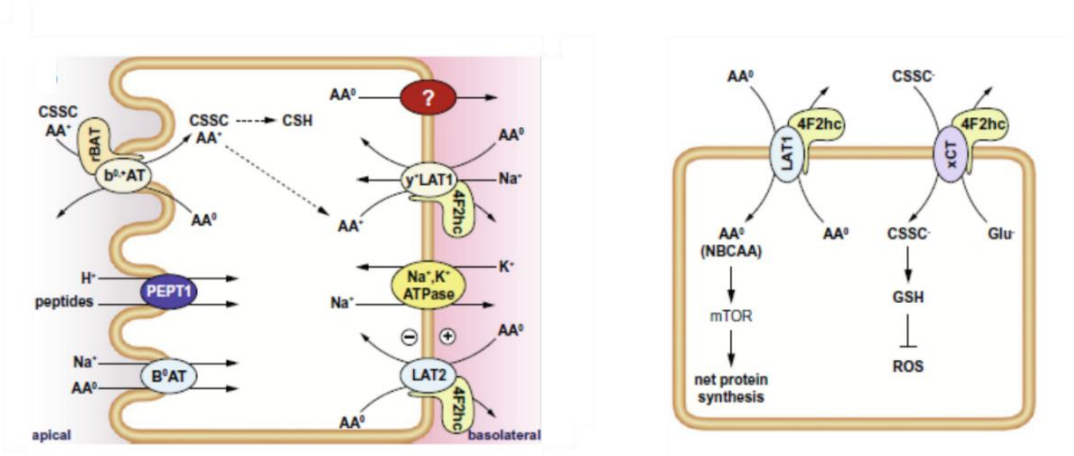

Fig. 4: Physiology of HATs. (Adapted from Fotiadis D. et al., The SLC3 and SLC7 families of amino acid transporters, 2013).

1.7.2. HATs and their light subunits

The eukaryotic LATs from the SLC7 family of amino acid transporters that represent the light subunit of HATs are seven transporter, which differ each other for substrate selectivity, ion coupling and tissue distribution (Fig. 4 and Table 2). As above described, only the amino acid transporter $b^{0,+}$AT (SLC7A9) forms heterodimers with rBAT, whereas six of these transporters form heterodimers with 4F2hc: LAT1 (SLC7A5), LAT2 (SLC7A8), y^+LAT1 (SLC7A7), y^+LAT1-2 (SLC7A6) and the cystine/glutamate antiporter xCT (SLC7A11) and ASC-1 (SLC7A10) (Table 2). (The same table contain also SLC7A13 associated with an unknown protein and SLC7A14 an orphan transporter).

Human gene	Protein name	Aliases [assoc. with]	Predominant substrates	Transport type	Tissue distribution and cellular / subcellular expression	Link to disease	Human gene locus
SLC7A5	LAT1	[4F2hc], 4F2lc, system L	Large neutral Lamino acids, T3, T4, LDOPA, BCH	E (similar intra- and extracellular selectivities, lower intracellular apparent affinity)	Brain, ovary, testis, placenta, spleen, colon, blood–brain barrier, fetal liver, activated lymphocytes, tumor cells	Cancer	16q24.3
SLC7A6	y^+LAT2	[4F2hc], system y^+L	Na^+ indep.: cationic amino acids; Na^+/ large neutral amino acids	E (preferentially intracellular cationic amino acid against extracellular neutral amino acid/ Na^+)	Brain, small intestine, testis, parotids, heart, kidney, lung, thymus/basolateral in epithelial cells		16q22.1
SLC7A7	y+LAT1	[4F2hc], system y^+L	Na^+ indep.: cationic amino acids; Na^+/ large neutral L-amino acids	E (preferentially intracellular cationic amino acid against extracellular neutral amino acid/ Na^+)	Small intestine, kidney, spleen, leucocytes, placenta, lung/basolateral in epithelial cells	Lysinuric protein intolerance (LPI)	14q11.2
SLC7A8	LAT2	[4F2hc], system L	Neutral L-amino acids, T3, T4, BCH	E (similar intra- and extracellular selectivities, lower intracellular apparent affinity)	Small intestine, kidney, lung, heart, spleen, liver, brain, placenta, prostate, ovary, fetal liver, testis, skeletal muscle/basolateral in epithelial cells		14q11.2
SLC7A9	$b^{0,+}$AT	[rBAT], system $b^{0,+}$	Cationic amino acids, large neutral amino acids	E (preferentially extracellular cationic amino acid and cystine against intracellular neutral amino acid)	Kidney, small intestine, liver, placenta/apical in epithelial cells	Cystinuria and isolated cystinuria	19q13.1
SLC7A10	Asc-1	[4F2hc], system asc	Small neutral amino acids	Preferentially E	Brain, CNS, lung, small intestine, heart, placenta, skeletal muscle and kidney		19q13.1
SLC7A11	xCT	[4F2hc], system xc^-	Cystine (anionic form), L-glutamate	E (preferentially extracellular cystine against intracellular glutamate)	Macrophages, brain, retinal pigment cells, liver, kidney/basolateral in epithelial cells		4q28.3
SLC7A13	AGT-1	XAT2	L-Aspartate and L-glutamate	E	Proximal straight tubules and distal convoluted tubules (basolateral)		8q21.3
SLC7A14				O	Highly expressed in CNS/intracellular localization		3q26.2

E: exchanger; O: orphan transporter

Table 2: SLC7 family (Adapted from Fotiadis D. et al., The SLC3 and SLC7 families of amino acid transporters, 2013).

A characteristic of HATs is that they function as obligatory antiporters with the exception of system Asc that also mediate facilitated diffusion [19]. The differing tissue localizations of HATs appear to complete them each other [20] but at the same time, they are quite diverse in terms of substrate selectivity [21]. Their selectivity ranges from large neutral amino acids (LAT1-2) to small neutral amino acids (ala, ser, cys-preferring, Asc-1), negatively charged amino acid (xc^-) and cationic amino acids plus neutral amino acids (y^+L and $b^{0,+}$-like). The (obligatory) antiporters equilibrate the concentrations of their substrate amino acids across membranes. In particular, these transporters uses the driving force provided by a transmembrane gradient of one amino acid, accumulated by a parallel transport process. Nevertheless, the transport of specific amino acids is guaranteed by the intrinsic asymmetry of these antiporters. The fact that genetic defects of the epithelial $b^{0,+}$AT and y^+LAT1 cause non-type I cystinuria and lysinuric protein intolerance, respectively, demonstrates that these HATs perform transport of specific amino acids in vivo [20-22].

1.8. 4F2hc (SLC7A2)

The 4F2hc heavy chain of HATs (also called CD98 in mice) has been originally identified in 1981 by a murine monoclonal antibody (mAb4F2) raised against the human T-cell tumor line HSB-2 [23]. Initial studies utilizing anti-4F2 antibodies revealed that the antigen is present on all established human cell lines and the majority of malignant human cells [24]. The gene has been identified on chromosome 11 and seems to be more ubiquitously expressed than the other human heavy chain rBAT. 4F2hc gene codified a protein constituted by 630 amino acids with a theoretical mass of ~85 kDa [12, 17, 25].

1.9. LAT1 (SLC7A5)

LAT1 is the first member of HATs that has been identified in 1998 [26, 27]. The LAT1 subunit in humans is a 507 amino acid long hydrophobic polypeptide with a molecular mass of 55.0 kDa. The protein is predicted to be constituted by 12 transmembrane segments. The high hydrophobicity that characterize this protein is responsible of its apparent molecular mass in SDS-PAGE of ~40 kDa. The higher electrophoretic mobility is probably due to a more compact form of the protein induced by partial oxidation and formation of disulphides among some of the 12 Cys residues present in hLAT1 amino acidic sequence [25].

As member of HATs LAT1 forms heterodimers with 4F2hc stabilized by a conserved disulphide between residues C164 of LAT1 and C109 of 4F2hc (Fig. 3). The role of LAT1/4F2hc heterodimer in mediating amino acid transport across the plasma membrane has been extensively studied in cell systems. Available literature data describe LAT1/4F2hc heterodimer mediated transport as a sodium independent amino acid antiport with preference for neutral amino acids with large, branched or aromatic side chains such as Phe, Tyr, His and Trp, and smaller amino acids such as Met, Val, Leu, Ile [27, 28]. LAT1/4F2hc has been also described as a transporter of non amino acid substrates, such as L-DOPA, gabapentin and thyroid hormones [29, 30]. As

other member of LATs subfamily, i.e. LAT2, LAT1 is inhibited by BCH commonly used to discriminate its activity from that of other amino acid transporters in cells [31].

LAT1 is broadly expressed and mainly localized in basolateral membranes of polarized epithelia [7, 28, 32]. Important exceptions are the luminal and abluminal membranes of BBB (blood–brain barrier) and the brush border membranes of placenta, i.e. maternal side [29]. More specifically SLC7A5 gene coding for hLAT1 is expressed in the placenta > the brain > the spleen > the testes and the colon [27]. Literature data suggest that in the inner blood-retinal barrier LAT1 plays an important role in transporting large neutral amino acids and neurotransmitters [33], as well as in placental membranes nourish fetus and placenta with thyroid hormones and amino acids [12, 29]. Moreover, an intracellular localization of LAT1/4F2hc heterodimer in lysosomes has been described [34].

1.10. Amino acids, LAT1 and tumours cells

The distinctive traits of tumour cells are rapid growth and proliferation that could be achieved by facilitation of cell cycle and resistance to apoptosis. The first step to enhance cell proliferation is an increased demand for nutrients used as building blocks for the synthesis of macromolecules and as carbon source for generation of metabolic energy. Thus, different nutrients are necessary, i.e. glucose, amino acids, vitamins, fatty acids, micronutrients, and, tumours cells adopt particular mechanisms to satisfy their increased demand for them. One of these is the vasculogenesis to increase the availability of nutrients, whereas upregulation of specific transporters allow entry of the nutrients into tumour cells. In some instances, the same signalling events that promote vascularization participate also in the upregulation of nutrient transporters, thus coordinating the availability of nutrients with their entry into tumour cells [35].

Nevertheless all nutrient are important to support growth and proliferation of tumour cells, the latter have an unique metabolic need for amino acids. Amino acids, indeed, are essential for protein synthesis but also as carbon and nitrogen source for purine and pyrimidine nucleotides, amino sugars, and glutathione synthesis. Moreover, the regulation of intracellular signalling pathways responsible of cellular growth involves upstream sensing of concentration of certain amino acids. The consequent scenario is that although the primary function of the amino acids is to serve as the building blocks for protein synthesis, some amino acids have specific signalling functions. Glutamine, glycine, and aspartate are needed for nucleotide biosynthesis, a process critical for proliferation of tumour cells. Serine plays an important role as a one-carbon source that is critical in nucleotide synthesis and DNA methylation. Leucine, glutamine, and arginine serve as signalling molecules [36].

The two best-studied nutrient signalling cascades in higher eukaryotes, important under physiological conditions, are the GCN (general control non-derepressible) and mTOR (mammalian target of rapamycin) pathways, both of which are regulated by mechanisms that include upstream sensing of intracellular amino acids concentrations.

One protein involved in the first nutrient signalling cascade is the GCN2 protein kinase. GCN2 appears to monitor intracellular amino acids concentration from the level of tRNA charging. In particular, uncharged tRNA accumulation correlated to a low concentration of amino activates GCN2, which phosphorylates and inactivates the initiation factor eIF2α (eukaryotic initiation factor 2α). As consequence, the global mRNA translation is suppressed, but occur the translation of the transcription factor ATF4 (activating transcription factor 4) which allow the induction of genes for amino acids biosynthesis and transport [37].

The mTOR pathway, in contrast, is stimulated by cellular amino acids supplementation and activates mRNA translation, promoting cell growth. This pathway regulates many major cellular processes thus it became particular relevant in tumours cells. mTOR is the target of a molecule named rapamycin which is a macrolide produced by *Streptomyces Hygroscopicus* bacteria that kept attention because of its antiproliferative properties. In the early 1990s, genetic screens in budding yeast identified TOR1 and TOR2 as mediators of the toxic effects of rapamycin on yeast. Successively biochemical approaches in mammals led to purification of mTOR and its discovery as the physical target of rapamycin. mTOR is an atypical serine/threonine protein kinase belonging to the phosphoinositide 3-kinase (PI3K)-related kinase family and interacts with several proteins to form two distinct complexes named mTOR complex 1 (mTORC1) and 2 (mTORC2) (Fig. 5) [38].

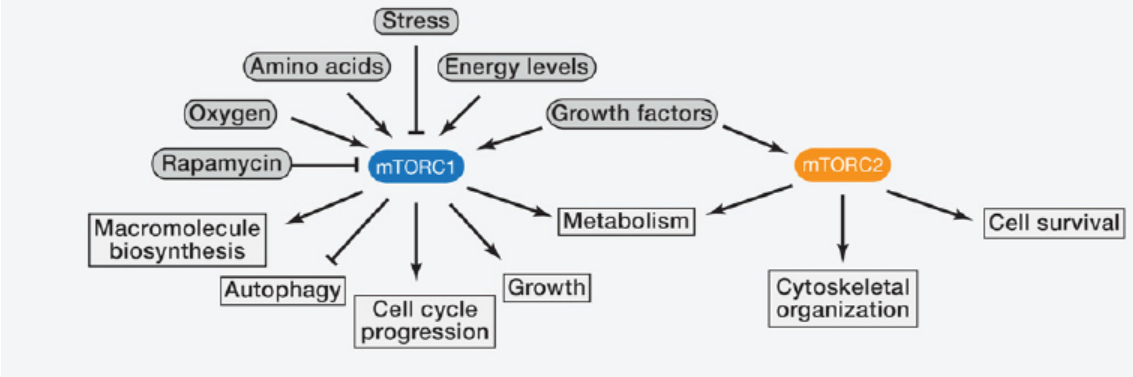

Fig. 5: mTORC1 and mTORC2 Complexes. (Adapted from Mathieu Laplante and David M. Sabatini, mTOR Signaling in Growth Control and Disease, 2012).

Amino acids are required for the activation of mTORC1, but not mTORC2 [39]. Although not yet fully resolved, the field of mTORC1 activation by amino acids has rapidly progressed [40]. mTORC1 activation occurs at the lysosomal membrane through an inside-out model of amino acid sensing, in which amino acids accumulate in the lysosomal lumen and initiate signalling through a mechanism that requires the vacuolar H^+-adenoside triphosphate ATPase (V-ATPase). At the surface of the lysosome, the V-ATPase directly interacts with the Ragulator, a pentameric complex important for amino acids regulation of mTORC1. The Ragulator serves as a scaffold protein complex and possess guanine nucleotide exchange factor (GEF) activity linked to Rag GTPases a group of four GTPases (RagA, RagB, RagC and RagD) that can recruit and activate mTORC1

at the lysosomal surface. Upon amino acid stimulation, the GEF activity of the Regulator promotes the loading of RagA or RagB with GTP in a V-ATPase-dependent manner allowing RagA or RagB to interact with RAPTOR component of mTORC1. This interaction results in the recruitment of mTORC1 at the lysosomal surface, where its endogenous activator Rheb resides [40].

In particular, a relevant role in activating mTORC1 is fulfilled by Leu and leucine-sensing mechanisms. Therefore, it is not unexpected that LAT1, which is predominantly expressed in tumours cells, is of particular interest in the contest of mTORC1 signalling [37, 40]. Indeed, on one hand the overexpression of LAT1 at the plasma membrane of tumours cells together with other amino acid transporters, such as ASCT2, allow to supply cell with Leu. On the other hand, the recent work by Milkereit and colleagues, which identified that LAPTM4b recruits LAT1/4F2hc to lysosomes, suggested a novel mechanism based on leucine lysosomal sensing (fig. 6) [34].

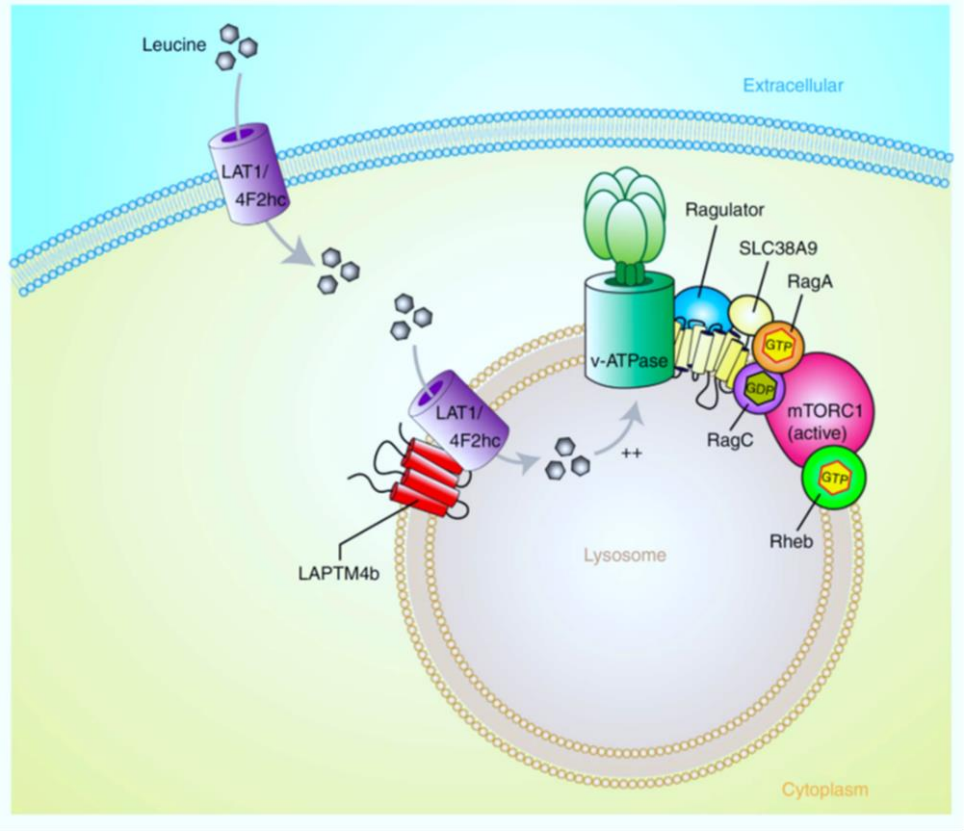

Fig. 6: Proposed role of LAPTM4b in activation of mTORC1 via recruitment of the Leu transporter to lysosomes. (Adapted from Milkereit et al., LAPTM4b recruits the LAT1-4F2hc Leu transporter to lysosomes and promotes mTORC1 activation, 2015).

LAPTM4b recruits the Leu transporter LAT1/4F2hc to lysosomes, enhances Leu uptake into lysosomes and stimulates mTORC1 activation via V-ATPase. These findings not only identify a functional Leu transporter at the lysosomal membrane, but also help solve the puzzle of how mTORC1 is activated by amino acids in the lysosome by an inside-out mechanism (intra-lysosomal stimulation of V-ATPase) originally noted by Sabatini et al. as described above. Being LAT1/4F2hc an antiport intra-lysosomal neutral amino acids would be

necessary as exchange substrates to sustain LAT1/4F2hc antiport function. Possible sources of lysosomal amino acids include uptake of large neutral (non-essential) amino acids such as Gln into lysosomes via directional/accumulative amino-acid transporters. Candidate transporters could be in particular SLC38A3 and SLC38A5 [34]. Another transporter presents in lysosomal membrane is SLC38A9 that transport Gln and Arg with low-affinity, indeed its peculiar role is that to function as a transceptor to sense Arg which allow to bind directly to Ragulator and Rag proteins. Thus, SLC38A9 participates in mTORC1 activation at the lysosome rather than contributing to the import of extracellular amino acids at the plasma membrane [41].

1.11. SLC7A5 genetic variants in Autism Spectrum Disorder

Beyond the vast literature data that give to LAT1/4F2hc heterodimer a prominent role in tumour survival, very recently, inherited mutations of SLC7A5 have been described as responsible of Autism Spectrum Disorder (ASD) a group of disorders often overlapping with other neurological conditions. This interesting study evidenced that in mice, deletion of SLC7A5 from the endothelial cells of the BBB leads to atypical brain amino acid profile. Furthermore, the same study has identified several patients with autistic traits and motor delay carrying homozygous mutations in the SLC7A5 gene. In particular, two genetic variants have been identified and mapped onto a homology model of SLC7A5. The first, A246V mutation, changes a highly conserved alanine affecting the transporter's structure. A246 is located in transmembrane helix 6 in proximity to the extracellular side and to the channel, and its substitution with the slightly larger residue valine has been experimentally demonstrated that impair transport activity by disrupting helix-helix packing and ligand transport. The second mutation identified, P375L, instead, leading to the change of the conserved proline in position 375 to a leucine. P375 is located in transmembrane helix 9 in close proximity to the cytoplasmic side. Proline often plays a key role in allowing conformational changes important for transporter function. Thus, mutation of this residue to leucine is likely to disrupt the flexibility required for transport by SLC7A5. Also for this mutant, this possible effect has been evaluated measuring transport activity, and it has been observed that the mutation P375L impairs the driving force for taking up SLC7A5 substrates. Thus, this study demonstrated that the substitution of the SLC7A5 alanine 246 into a valine, or of the proline 375 into a leucine, is sufficient to significantly reduce the SLC7A5-mediated BCAA uptake. This is an important feature because the fine-tuning of brain BCAA concentrations is critical for normal brain function, and mutations affecting genes contributing to BCAA homeostasis and the downstream signalling cascade may underlie a larger subgroup of ASD [42].

1.12. The intriguing role of 4F2hc in the intrinsic transport activity of LAT1

Although there are many literature data about transport properties of LAT1/4F2hc heterodimer, the precise role of 4F2hc in the intrinsic transport activity of LAT1 is still an open issue. The heavy subunit may be involved in trafficking the light chain to the plasma membrane or, together with the light subunit may catalyse

the transporter function [17, 21]. The two proteins as well as HATs proteins form a heterodimer interacting via a disulphide bridge. However, if there were other possible interaction between the proteins of the heterodimers and if both these and the disulphide bridge are critical and/or essential for the stability of the heterodimer and/or for the transport are intriguing aspects, thus many literature data are present on this issue. Some authors declaim that the absence of disulphide bond does not preclude, but only decreases transport surface expression and/or function. The heterodimer interaction takes place also in absence of disulphide bridge formation and this interaction is stable enough to allow cell surface expression of the light chain [43]. Other authors suggest that despite the disulphide bridge is not necessary for the functional association, in absence of the covalent bridge, the C-terminal of the heavy chain is necessary for a functional transport competence [44]. Moreover, seemingly conflicting results published on 4F2hc/LAT1 interaction, declaimed the importance of the N-terminal part of 4F2hc or alternatively, the role of the extracellular part of 4F2hc [45, 46]. Whereas, other authors deduced that the interaction of the heavy chain 4F2hc with the light chain LAT1 involves all domains of 4F2hc [47].

Studies performed in intact cells considered 4F2hc crucial for LAT1 transport activity [27, 48]. There again, other authors, claimed that involvement of 4F2hc in transport is linked to maturation and trafficking of LAT1 protein in plasma membrane [26, 47, 49, 50]. In particular, it is reported that rat LAT1 remains in Golgi area in absence of the heavy subunit [49], thus the heavy chain is necessary for trafficking LAT1 to the plasma membrane. Moreover, in mouse hepatocarcinoma cells, over-expressed LAT1 has been showed to mediate leucine transport without involvement of 4F2hc [51].

Therefore, considering that in intact cell, which is the only system used until now, 4F2hc is always present, it is difficult to understand if 4F2hc is only necessary for maturation, trafficking and/or surface residence of LAT1 or it is essential for LAT1 transport function. Thus, this aspect remain unclear.

1.13. Pharmacological approaches for LAT1

The over-expression of LAT1 in tumour cells made this human transporter an interesting pharmacological target. Indeed, as for other amino acids transporters over-expressed in tumour cells compared to normal cells, compounds with the ability to inhibit the cellular pathways responsible for their induction or to block the function of the induced transporters would have potential effects as chemotherapeutic agents. Indeed, since tumour cells induce these transporters specifically for their unique metabolic needs, normal cells are expected to be relatively resistant to the therapeutic actions of such compounds, thus reducing undesirable side effects [35]. In this regard, many authors are involved in the research of inhibitors of this transporter useful as potential anticancer drugs. More specifically literature data report two approaches for anticancer therapies involving LAT1. The first regard the capacity of this transporter to mediate the uptake of several amino acid-derived anticancer drugs, thus this approach is based on the notion that LAT1 could be involved in the cellular internalization of these anticancer drugs. The second approach is a novel strategy based on the inhibition of

LAT1 activity to reduce tumour proliferation and progression but the targeting of amino acid transporters in cancer is under development and there are few specific inhibitors available. Thus, the development of more effective inhibitors of LAT1 will change the scenario. However, identification or design of potent inhibitors to be proposed as potential drugs, requires a deep knowledge of the target structure and action mechanism that, in the case of LAT1, are still missing [52-55].

The described roles employ by LAT1 justify the growing number of literature works regard this fascinating protein. Nevertheless, the study of transport proteins is not of simple realization. Given their hydrophobic nature, transport proteins require different devices for their study.

1.14. X-ray crystallography state for transmembrane protein and bioinformatics approaches

As described above, the three-dimensional structure of the C-terminal of the heavy chain has been solved [16], while crystals of LAT1 are not available, as for all the mammalian amino acid transporters. The lateness in the possibility to obtain stable crystals for transmembrane proteins is due to their hydrophobicity; moreover, resolution of the structure needs large-scale purified transport proteins. The lack of crystal structure of transport proteins makes difficult the understanding of the structure/function relationships and the mechanisms of interaction with xenobiotics, a very important issue connected with drug discovery and toxicity.

Nevertheless, the increasing study of atomic structure of homologues prokaryotic transporter allowed unravelling their molecular mechanisms. In particular, the prokaryotic amino acid transporters AdiC, whose structure has been solved by x-ray crystallography, is the closest homologue of the mammalian LAT transporters (amino acid sequence identity ranging from 14% to 20%) [56-60]. These transporters share the protein fold named 5+5 inverted repeat fold (also known as LeuT-fold). Proteins with the LeuT-fold, although differing each other in the total number of TM helices, are characterized by two structurally similar repeats, each containing a core of five consecutive TMs. The feature of this fold is that the first TM in each of the two inverted repeats (TM1 and 6) is discontinuous and consists of two short alpha helices connected by a highly conserved unwound segment. This structural feature is important for the transport mechanism of transporters with the LeuT-fold as it is part of the substrate coordination site in crystallized amino acid transporters with this fold [59, 60]. Indeed, in absence of crystal structure for LATs transporter, elucidation of the structure of closely related prokaryotic homologues of human LAT1 transporters and the generation of structural models from these crystal structures through a bioinformatics approach could be useful to make a step forward in the understanding of the structure/function relationship. Nevertheless, the silico methodologies represent only a tile in the complex mosaic of the structure/function relationship of LAT1.

1.15. The study of transport proteins through a multidisciplinary approach

Even though the building of structural model using in silico methodologies could represent an important feature for advancing the knowledge of a specific transport protein, on the other hand, transport measurements

are essential to validate, experimentally, the in silico predictions. Nevertheless, to measure transport activity the best way is to use different system that could confirm each other the results obtained. Indeed, measuring transport activity both in intact cells and in an isolated environment such as that offered by proteoliposomal tool, is possible to obtain more clear information. However, the use of proteoliposomal tool requires the heterologous expression of the protein object of study, an important methodology that, together with site direct mutagenesis, allowing to obtain also mutants of the protein of interest with consequent possibility of better understanding of the involvement of specific residues in transport activity.

Thus, the better way to obtain trustworthy results is develop a multidisciplinary approach, which confirm each other the made observation allowing to shedding light in the complex mosaic of the structure/function relationship of the studied transport protein.

1.16. Experimental methods to study transport proteins

Two different methods could be used for measuring transport activity of a protein of interest.

1.16.1. Intact cell systems

The study on transport proteins started in 1970' and the first model adopted was that of intact cells. In particular, transport functions was studied following the flux of labelled compounds through native membranes of intact cells, isolated organelles (such as mitochondria) or microsomes, derived from endoplasmic reticulum. Intact cell models are still broadly used as tools for studying the functional properties of transport systems. Different cells lines are used, expressing endogenous transporters or over-expressing specific transporters after transient transfection by appropriate plasmids. *X. laevis* oocytes over-expressing a specific transporter are also used in some studies. The over-expression procedure offers the advantage of increasing the amount of the protein of interest. In this system, the activity of the over-expressed protein should overcome that of the endogenous ones, leading to a better resolution of the transport activity measurement.

Nevertheless, the use of intact cell systems, disclose some limits. Indeed the impossibility to control the intracellular compartment limits the kinetic characterization of the transporter especially on the internal side. Moreover, intracellular enzyme pathways can readily metabolize the substrates used for measuring the transport activity and the presence of many similar transporters in the same membrane is responsible of interferences. Therefore, the use of intact cell systems as unique method is not suitable for a comprehensive functional characterization of a transporter and even less for revealing structure/function relationships.

1.16.2. Proteoliposomes

An alternative model for studying transport proteins is the proteoliposomes. Liposomes were initially produced for encapsulating and delivering enzymes or pharmaceutical compounds [61-63], and then, used as

a tool for studying membrane transporters [64, 65], which are inserted into the membrane bilayer to obtain active proteoliposomes. Transport proteins could be extracted from biological samples in non-ionic detergent, but a more recent and effective method is that of producing recombinant proteins by over-expression in heterologous systems and purification by affinity chromatography. Production of recombinant proteins offer the advantage of excluding any kind of interference and, in addition, to obtain human proteins that, obviously, cannot be extracted from tissues. This method offers several advantages with respect to intact cells: 1) the possibility to control internal and external compartments as well as the internal and the external site of the transport protein allowing detailed kinetic analysis; 2) the possibility to construct specific mutants in which selected amino acid residues are substituted, thus allowing the study of structure/function relationships; 3) the study of interaction with chemicals and potential drugs, that can be well characterized with respect to their mechanism of action [1].

1.17. Proteoliposomes as method to reveal xenobiotic-transporter interaction mechanisms

When the interest is that of characterizing the interaction between a transport protein and xenobiotic compounds such as environmental contaminants or drugs, IC50 or Ki parameters have to be measured with a good confidence. The threshold fixed for considering an interaction of interest is 30μM [1].

Using both intact cell system and proteoliposomes different and complementary information can be obtained. Intact cell system, including the case of cell lines over-expressing specific transporters, gives information on vitality of the cells after exposition to a specific compound and only a general alteration of the transport activity. On the contrary, the suitability of the proteoliposomal method allow the description of the mechanism of the interaction at the molecular level. Indeed the possibility to make extensive kinetic analysis of the transporter-xenobiotic interaction gives information both on the constants, i.e. Ki, and on the type of interaction competitive, non-competitive or mixed inhibition. Moreover, when a homology structural model is available and possibly validated by site-directed mutagenesis, information on the involvement of amino acid residues could be obtained.

Thus, the use of proteoliposomes together with intact cells as method to study transporter function, kinetics and interactions is an example of how a multidisciplinary approach, including bioinformatics allow obtaining detailed and trustworthy results on the structure/function relationship of a transport protein (Fig. 7).

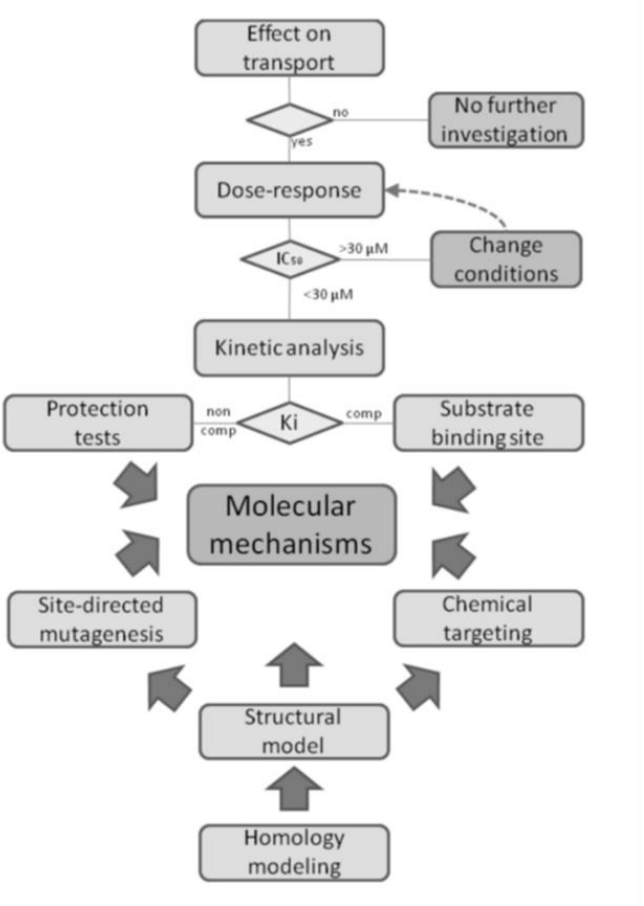

Fig. 7: Work plan for xenobiotic-transporter interaction studies in proteoliposomes. (Adapted from Scalise et al., Proteoliposomes as Tool for Assaying Membrane Transporter Functions and Interactions with Xenobiotics, 2013)

Chapter II

Materials and Methods

2.1. Materials

2.1.1. RIPA Buffer 1X

- 20 mM Tris-HCl (pH 7.5)
- 150 mM NaCl
- 1 mM Na_2EDTA
- 1 mM EGTA
- 1% NP-40
- 1% sodium deoxycholate
- 2.5 mM sodium pyrophosphate
- 1 mM β-glycerophosphate
- 1 mM Na_3VO_4
- 1 µg/ml leupeptin

2.1.2. Buffers for h4F2hc purification

2.1.2.1. Binding buffer for h4F2hc purification

- 5% Glycerol
- 1% Triton X-100
- PBS pH 7.4
- 5 mM DTE

2.1.2.2. Washing buffer for h4F2hc purification

- 0.1% Triton X-100
- PBS pH 7.4

2.1.3. Washing buffer for hLAT1 pellets

- 0.1 M Tris-HCl pH 8

2.1.4. FPLC buffers for hLAT1 purification

2.1.4.1. Equilibration buffer

- 20 mM Tris-HCl pH 8
- 200 mM NaCl
- 10% Glycerol
- 0.1% Sarkosyl

2.1.4.2. Washing buffer

- 20 mM Tris-HCl pH 8
- 200 mM NaCl
- 10% Glycerol
- 0.05% DDM
- 3 mM DTE

2.1.4.3. Elution buffer

- 20 mM Tris-HCl pH 8
- 200 mM NaCl
- 10% Glycerol
- 0.05% DDM
- 3 mM DTE
- 400 mM Imidazole

2.1.5. Desalt buffer for purified hLAT1

- 20 mM Tris-HCl pH 8
- 0.05% DDM
- 10 mM DTE

2.1.6. Running buffer for PAGE 10X

- 250 mM Tris
- 14.4 % Glycine
- 1% SDS or 1% Sarkosyl

2.1.7. Loading dye for PAGE 3X

- 0.2 M Tris-HCl pH 6.8
- 7.5% SDS or 7.5% Sarkosyl
- 3% Glycerol
- 0.01% Bromophenol blu
- 100 mM DTE (when indicated)

2.1.8. Coomassie Brilliant Blue

- 0.25 g Coomassie Brilliant Blue
- 45 mL Methanol
- 45 mL Distilled H_2O
- 10 mL Acetic acid

2.1.9. Destaining solution

- 10% Acetic acid
- 40% Methanol
- 50% H_2O

2.1.10. Washing buffer for western blot analysis

- 50 mM Tris-HCl pH 7
- 150 mM NaCl

2.1.11. Lowry's solution

- 4 mg/mL NaOH and 20 mg/mL Na_2CO_3 in water
- 10 mg/mL Potassium Sodium Tartrate

- 5 mg/ mL $CuSO_4$
- 1% SDS

2.2. Experimental procedures

2.2.1. Protein purification by affinity chromatography

Affinity chromatography is a separation method based on a specific binding interaction between an immobilized ligand and its binding partner. This technique is commonly used for purification of recombinant proteins genetically modified in order to harbour specific tag(s) for affinity binding. In the case of the proteins studied in this work, glutathione-S-transferase (GST) or hexahistidine (6His) were used as tags. GST has an affinity for glutathione, which is commercially available immobilized as glutathione agarose. Histidine tags have an affinity for nickel or cobalt ions, which have been immobilized by forming coordinate covalent bonds with a chelator, incorporated in the stationary phase. The elution of the protein with a 6-His tag is performed using an excess amount of a compound able to act as a metal ion ligand, such as imidazole.

2.2.2. Gel Filtration Chromatography

Gel filtration chromatography is commonly used to separate molecules in a mixture on the basis of their sizes. The molecules move through a bed of porous beads and diffuse into the beads to greater or lesser degrees. In particular, smaller molecules diffuse more slowly than larger molecules, which do not enter or enter the beads to a lesser extent. Gel filtration chromatography may be used for different purposes. In our case, this approach has been used to separate proteoliposomes from the external substrate both after reconstitution procedure and transport assay, or for salt removal from the protein.

2.2.3. Reconstitution into liposomes

The reconstitution into liposomes of a transport protein can be performed with two main procedures, which differ for the efficiency. The first is the freeze-thaw-sonication procedure that consists of three steps: i) a fast freezing of a mixture of liposomes, transport protein and non-ionic detergent; ii) a slow thawing of this sample; iii) a final sonication for sealing formed proteoliposomes. After freezing, liposomes are broken due to ice formation and, during the slow thawing, the protein inserts into the phospholipid bilayer. This procedure has the disadvantage that the detergent is not removed and can impair the complete sealing of proteoliposomes. The second procedure, instead, is based on the removing of detergent from mixed micelles of protein, detergent and phospholipids. In particular, the remove of detergent from mixed micelles can be performed by cyclic chromatography of the reconstitution mixture on hydrophobic column for 10–20 cycles, or by the batch-wise procedure. In the latter, the mixed micelles are incubated with an hydrophobic resin for a time sufficient to remove virtually all the detergent. The main advantage of detergent removal is that the proteoliposomes are more sealed, unilamellar and, hence, virtually impermeable to hydrophilic compounds. Moreover, by mean of

detergent removal procedure the protein is inserted with an unidirectional orientation, which in most cases, corresponds to that of the transporter in the native membrane. This is due to the feature of the starting micelles that have a relatively small radius: this property forces the asymmetric protein to insert into the micelles with a right side-out orientation (Fig. A).

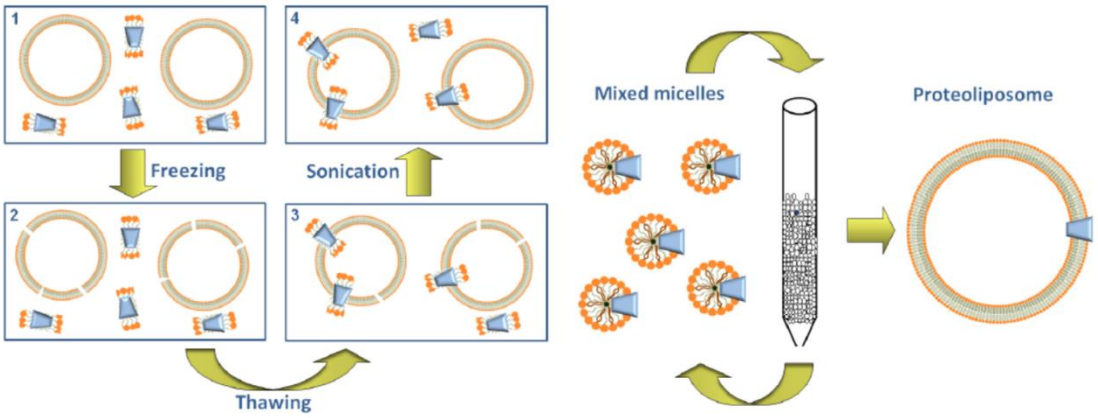

Fig. A: Sketch of methodologies for proteoliposome preparation. (Adapted from Scalise et al., Proteoliposomes as Tool for Assaying Membrane Transporter Functions and Interactions with Xenobiotics, 2013).

Given the suitability of the detergent removal method, it has been adopted in this work using the batch-wise procedure. This initial mixture contains primarily the protein of interest, which has been previously solubilized from cell extracts (in our case from SiHa cells) or purified through affinity chromatography (recombinant proteins overexpressed in *E.Coli*). Subsequently, non-ionic detergent (octaethylene glycol monododecyl ether $C_{12}E_8$), egg yolk phospholipids (w/v) (in the form of liposomes prepared through sonication), substrate, buffer and water in a final volume of 700 µL are added to complete the mixture. This mixed mixture is then incubated at room temperature with a hydrophobic resin (Amberlite XAD-4) for a time sufficient to remove virtually all the detergent and obtain active proteoliposomes.

2.2.4. Ultracentrifugation of proteoliposomes

To evaluate the insertion of the protein into liposome membranes, after reconstitution the ultracentrifugation of the proteoliposomes can be performed. After gel filtration chromatography, 500 µL of obtained samples are subjected to two consecutive ultracentrifugation steps for 90 min 110,000 × g at 4°C. The first one is performed in order to separate the fraction containing proteoliposomes from that of empty liposomes, i.e. vesicles which did not incorporate the protein during reconstitution. The separation is achieved because proteoliposomes are heavier than empty liposomes and, after the first ultracentrifugation, are present in the pellet. The same pellet is then washed with a saline buffer and the sample obtained is subjected to a second ultracentrifugation. The pellet obtained after this second ultracentrifugation, is solubilized with 3% of detergent such as Sarkosyl or SDS, according to experimental needs, and can be used for PAGE or western blot analyses.

2.2.5. Cross-link

Cross-link strategy is used to bind one polymer chain to another. These bonds can be covalent or ionic and the polymer chains can be synthetic or natural polymers such as proteins. In our case, the covalent bond of interest is a disulphide bridge between two cysteine residues of the proteins and this strategy has been adopted to evaluate the possible formation of a dimeric structure of the protein. The formation of a disulphide bridge from two thiol groups (-SH) is a two-electron reaction that require an oxidizing agent or electron acceptor. These disulphide bridges can form spontaneously in vitro downstream the loss of electrons by two cysteine residues together with the acquisition of the same electrons by an electron acceptor such as the molecular oxygen. If the electron acceptor is the molecular oxygen, a catalyst is necessary, such as a transition metal, to overtake the slow association of the oxygen with the thiol groups of the proteins. Thus, the formation of the disulphide bridge between the two proteins could be performed in vitro placing the purified proteins in the presence of molecular oxygen and of a catalyst for an interval of time. In particular, in the cross-link strategy adopted to our purpose 1 or 2 mM copper phenanthroline (Cu^{++}-phenanthroline) has been used as catalyser and the formation of the disulphide bridge has been evaluated on PAGE under non-reducing conditions (in absence of reducing DTE during gel run).

2.2.6. Polyacrylamide gel electrophoresis (PAGE)

To separate biological macromolecules, such as proteins, according to their mobility, a technique diffusely used is polyacrylamide gel electrophoresis (PAGE). The mobility of the protein depends on their molecular weight, conformation and charge and on PAGE the proteins can be run either in their native or denatured state. Sodium dodecyl sulfate (SDS) is the most common ionic detergent applied to protein samples to linearize them and to confer a negative charge triggering proteins to be separates on the basis of their mass/charge ratio. This application is called SDS-PAGE. Moreover, using the ionic detergent N-Lauroylsarcosine sodium salt (Sarkosyl), with lower denaturation power respect to SDS, a gel under mild-denaturating condition can be performed. The polyacrylamide gels typically consist of acrylamide, bisacrylamide, the denaturant (SDS or Sarkosyl), and a buffer with adjusted pHs. A source of free radicals and a stabilizer, i.e. ammonium persulfate and TEMED are added to initiate polymerization. TEMED accelerates the rate of formation of free radicals from persulfate and these, in turn, catalyze polymerization. The polymerization reaction creates a gel because of the bisacrylamide, which can form cross-links between two polyacrylamide molecules. The acrylamide concentration of the gel can also be varied, generally in the range from 5% to 25%. In our case, the concentration was 10% or 12%. Lower percentage gels are better to separate higher molecular weight molecules, while much higher percentages are needed to resolve smaller proteins. The protein samples were solubilized with loading dye (Materials, section 2.1.7.) and then ran using running buffer (Materials, section 2.1.6.). The gels were stained using Coomassie staining (Materials, section 2.1.8.) or Silver staining. In the Coomassie staining, gel was incubated with Coomassie solution for 30 min and then washed with destaining

solution (Materials, section 2.1.9.) to remove the unbound Coomassie and detect the protein as blue bands. In the Silver staining gel was incubated 20' with destaining solution (Materials, section 2.1.9.), 15' with 10% glutaraldehyde, 15' with water, 15' with 0.16 mM DTE, 20' with 0.1% silver nitrate and the dection of proteins was performed with 30 mM sodium carbonate plus 0.03% formaldehyde.

2.2.7. Western blot

To identify specific proteins in sample derived from tissue extract, homogenate or protein extracts, a diffusely technique used is the western blot also known as immunoblot. In our case, the proteins derived from cell extracts (SiHa cells) or obtained through affinity chromatography (recombinant purified proteins). For western blot analysis, different steps are required. First of all the proteins present in the sample of interest are separated through PAGE (SDS-PAGE or Sarkosyl-PAGE). In a second step, the proteins are transferred to a nitrocellulose membrane where the same proteins are stained using specific antibodies for the target proteins. The proteins subjected to an electric field move from the gel onto the membrane maintaining the organization that they had within the gel. Then, the incubation with the specific antibody is performed. During the incubation, to prevent the non-specific binding of the antibody, a solution of 3% Bovine serum albumin (BSA) and a minute percentage (0.1%) of detergent such as Tween 20 is used. The membrane is then washed with washing buffer (Materials, section 2.1.10.) to remove the unbound antibody. A further incubation with a secondary antibody, linked to a reporter enzyme (peroxidase), is necessary for the detection of reaction. This is performed by using Electro Chemi Luminescence (ECL) (Fig B).

More specifically, in our purpose western blot analyses were performed using anti-4F2hc antibody 1:2000 to immuno-detect h4F2hc and anti-LAT1 antibody 1:2000 or anti-His antiserum 1:1000 to immuno-detect hLAT1. The reaction has been performed over night at 4°C for anti-4F2hc and anti-LAT1 antibody and detected by Electro Chemi Luminescence (ECL) assay after an incubation of 1 h with secondary antibody anti-rabbit 1:5000. For anti-His HRP conjugate the reaction has been performed for 1 h at room temperature and detected by Electro Chemi Luminescence (ECL) at the end of incubation.

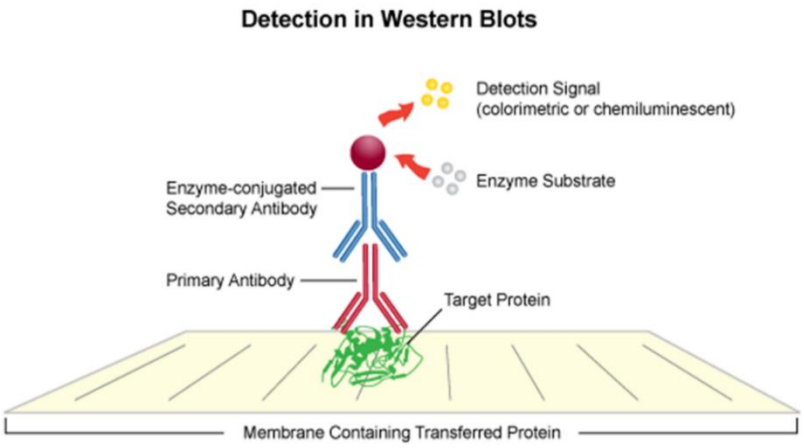

Fig. B: Schematic representation of western blotting technique (Adapted from http://www.leinco.com/).

2.3. Extraction of 4F2hc/LAT1 complex from SiHa cells

SiHa pellets were adopted to recover native 4F2hc/LAT1 complex for western blot analysis and reconstitution into liposomes. More specifically, 4F2hc/LAT1 was solubilized from these pellets with RIPA buffer and an incubation for 30 min on ice was performed. The sample were than subjected to centrifugation (12,000 g, 4°C, 15 min) and the proteins were quantified using Lowry method for following analysis. More specifically to 5µL of the sample plus 45 µL of water were added 1 mL of Lowry's solution (Materials, section 2.1.11.) and 100 µL of 1.0N Folin's Phenol reagent.

2.4. Recombinant GST-h4F2hc purification

The purification of recombinant h4F2hc overexpressed in *E.Coli* with a GST (Glutathione S-transferases) tag at the N-terminal was optimized respect data previously reported [25]. In the case of this work, the purification was performed through affinity chromatography in batch using Glutathione Sepharose 4B resin. This resin forms a bed of porous beads with immobilized GSH able to link the GST tag of the protein. The protocol optimized for this purification consisted of different steps. First of all, 500 µL of the resin were washed with degassed water and equilibrated with five volume of Binding Buffer (see Materials section 2.1.2.) to favour the interaction with the protein. After that, 400 µL of the soluble fraction (supernatant), obtained after 1 mL of lysate centrifugation (12,000g, 4°C, 10 min) was added to the resin and an incubation on Stuart tube rotator at 4°C overnight was performed. At the end of the incubation, the sample was subjected to centrifugation (500g, 4°C, 5 min) to remove the supernatant containing the unbound recombinant proteins and all the other bacterial proteins. At this point, the resin was incubated with 2U of thrombin (37 °C, 5 hours). Indeed, a cut site for thrombin is present between the GST tag and the protein exploited to separate the protein of interest from its tag. After the incubation, 4F2hc was recovered by centrifugation using test-tube with filter. In particular, on one test-tube pre-incubated aliquots were added and subject to centrifugation (500g, 4°C, 2 min); the filter retained the resin with the linked GST tag, whereas 4F2hc lacking its tag, crossed the same filter and was recovered. 4F2hc was used for following analyses.

2.5. Recombinant 6His-hLAT1 purification

hLAT1 over-expressed in *E. Coli* with a 6His tag at the N-terminal was purified with some modifications respect data previously reported [25]. For purification of hLAT1, cell lysate pellets were adopted. In particular, after washing the pellets with washing buffer (see Materials section 2.1.3.), the proteins were solubilized with 100 mM DTE, 3.5 M urea, 0.8% sarkosyl, 10% glycerol, 200 mM NaCl and buffered at pH 8.0 with 10 mM Tris-HCl. After centrifugation (12,000 × g, 4°C, 10 min) supernatant was recovered and applied on a His Trap HP column (5 ml NiSepharose) for purification using ÄKTA start. The same column was equilibrated with 10 mL buffer (Equilibration buffer, Materials section 2.1.4.) and supernatant was applied onto the column.

Unbound bacterial proteins were washed out by using 10 mL of the same buffer. Elution of the protein was then obtained by using the same buffer plus imidazole 400 mM (Elution buffer, Materials section 2.1.4.); 2.5 mL of purified hLAT1 were recovered. This pool of purified protein was then desalted on a PD-10 column using 3.5 mL of a desalt buffer (Materials, section 2.1.5.)

2.6. Reconstitution into liposomes of extracted 4F2hc/LAT1 complex

4F2hc/LAT1 complex extracted from SiHa cells pellets was adopted for reconstitution into liposomes. The samples were pre-treated or not with DTE to obtain the reconstitution of the single proteins constituting the complex or the reconstitution of the intact complex respectively. The reconstitution in liposomes was achieved by detergent removal method using batch-wise technique. The initial mixture used for this purpose included: 150 µg of cell extract, 100 µL of 10% $C_{12}E_8$, 100 µL of 10 % phospholipids, 20 mM Tris–HCl pH 7.5, 10 mM L-His in a final volume of 700 µL and incubated with 0.5 g Amberlite XAD-4 at room temperature for 40 min (see section 2.2.3. for details). Internal substrate was opportunely changed for specific purposes, such as experiments of functional characterization or added at different concentration for kinetic analyses.

2.7. Reconstitution into liposomes of purified h4F2hc or hLAT1

Reconstitution into liposomes was adopted also for recombinant proteins using the same protocol as for native protein. In particular 4 µg of the purified h4F2hc and hLAT1 were used in the mixture. Also in this case, internal substrate was opportunely changed for specific purposes, such as experiments of functional characterization or added at different concentration for kinetic analysis.

2.8. Transport assay

To measure transport activity, 600 µL of proteoliposomes were subjected to gel filtration chromatography to remove the excess of external substrate. In particular, the sample was applied onto a Sephadex G-75 column (0.7 cm diameter × 15 cm height) pre-equilibrated with 20 mM Tris–HCl pH 7.5 and sucrose at an appropriate concentration to balance internal osmolarity. At this point, the pool of proteoliposomes obtained was used for transport measurements, which can be performed either as uptake or efflux of radiolabelled substrate.

2.8.1. Uptake experiments

For uptake experiments, after passage through Sephadex G-75 column, 5 µM of [^{3}H]His were added to 100µL of eluted proteoliposomes to start transport. For functional characterization, the transport activity was measured in 30 or 60 minutes, whereas kinetic analysis were performed measuring transport activity for 10 minutes within the initial linear range of [^{3}H]His. After the specific time, transport activity was stopped by adding as inhibitors 100 µM BCH (2-amino-2-norbornanecarboxylic acid) and 1.5 µM $HgCl_2$. In controls, inhibitors were added at time zero according to the inhibitor stop method [66]. After the transport, 100 µL of

proteoliposomes were subjected to gel filtration chromatography using a Sephadex G-75 column (0.6 cm diameter × 8 cm height). In this case, gel filtration was adopted to separate the external from the internal radioactivity. The elution of loaded proteoliposomes was performed with 1 mL 50 mM NaCl and added to 4 mL scintillation mixture to be counted by a Liquid Scintillation Counter.

2.8.2. Efflux experiments

To perform efflux measurements, an uptake step was performed for 60 minutes to preload proteoliposomes with 5 µM [^{3}H]His [67]. After uptake assay, external radioactivity was removed by another passage through Sephadex G-75 and efflux was started by adding 5 mM of substrates on the extraliposomal space of the preloaded proteoliposomes. Efflux measurements could be performed in 10 minutes within the initial linear range of [^{3}H]His or in time course, and also in the case of efflux experiments, the inhibitor stop method was adopted to stop transport activity.

2.9. Elaboration of experimental data

Experimental values, obtained from Liquid Scintillation Counter, were corrected by subtracting controls in the case of uptake measurements and by subtracting radioactivity present in proteoliposomes at time zero for efflux measurements. The same values were then elaborated using Grafit software (Grafit® 5.0). In particular, different equations were adopted in line with experimental purposes.

First Order Rate Equation: used where a process increases with time following a 1st order rate law:

$$A_t = A_\infty(1-e^{-kt})$$

Single Exponential Decay: is the equation for a single exponential decay:

$$y = A_0.e^{-kt}$$

Michaelis-Menten Equation: used to calculate kinetics parameters:

$$v = \frac{V_{max}.[S]}{K_m + [S]}$$

Lineweaver Burk Equation: the Lineweaver Burk transformation was used to produce a double-reciprocal plot of the data:

$$1/V_0 = [Km / (V_{max}\cdot[S])] + 1/V_{max}$$

IC50 Fully Range Corrected: dose–response equation to calculate IC50 value:

$$y = \frac{100\%}{1 + \left(\frac{x}{\mathrm{IC}_{50}} \right)^{s}}$$

Chapter III

Results

3.1. Functional characterization of LAT1 mediated transport

3.1.1. 4F2hc and LAT1 are linked through a disulphide bridge in cell membrane

Proteins extracted from pellets of SiHa cells, were subjected to western blot analysis to identify 4F2hc/LAT1 complex. Considering that the two proteins are linked by a disulphide bridge, to observe the entire complex (4F2hc/LAT1) or both single proteins (4F2hc or LAT1), the samples were run on SDS-PAGE under oxidizing or reducing conditions, i.e., in absence or presence of the reducing agent DTE, respectively. The immuno-detection of the 4F2hc/LAT1 complex proteins was carried out using both anti-4F2hc (Fig. 8 A) and anti-LAT1 antibodies (Fig. 8 B).

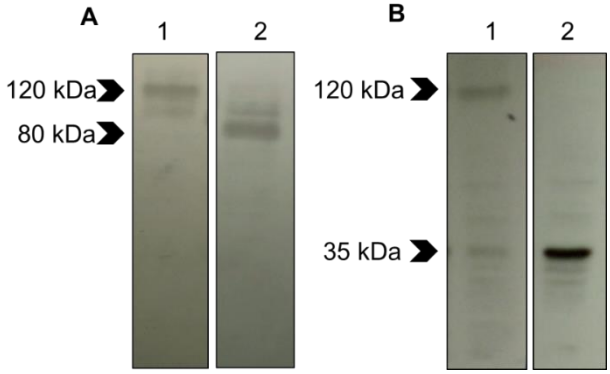

Fig. 8: Western blot analysis of h4F2hc/hLAT1 complex from SiHa cells. Cell membranes were solubilized with buffer without DTE (*lanes 1*) or with DTE (*lanes 2*). Western blot analyses were conducted using anti-4F2hc (A) and anti-hLAT1 (B) antibodies. The images (A-B) are representative of at least two independent experiments.

As shown in Fig. 8 both antibodies identified, under oxidizing conditions (lane 1 of both A and B), a band of 120 kDa which corresponds to the sum of the apparent molecular mass of 4F2hc plus LAT1. Whereas, under reducing conditions, the apparent molecular mass of the proteins diminished to about 80 kDa (Fig. 8A lane 2) when immuno-detected with anti-4F2hc and to about 35 kDa when immuno-detected with anti-LAT1 (Fig. 8B lane 2). As above described (Introduction sections 1.8., 1.9.), these are approximately the molecular masses of the two separate proteins, i.e., 4F2hc (about 80 kDa) or LAT1 (about 35 kDa). The obtained result confirmed that 4F2hc/LAT1 heterodimer is present in SiHa cells membranes and that the two proteins are linked by a disulphide in the same membranes. Indeed, the presence of reducing agent DTE caused the disruption of the disulphide and the immuno-detection of both proteins at their own molecular mass. The smaller amount of unlinked proteins observed also under oxidizing conditions is probably due to the reducing action of physiological reducing agents present in cells.

3.1.2. Purification of recombinant h4F2hc and hLAT1

Recombinant h4F2hc and hLAT1 had been previously over-expressed in *E. coli* [25]. Purification of these proteins was optimized as described in Materials and Methods.

The purification of 4F2hc was performed in batch as well as the incubation with thrombin (Materials and Methods section 2.4.), allowing to obtain a protein lacking its GST tag useful for subsequent analysis (Fig. 9).

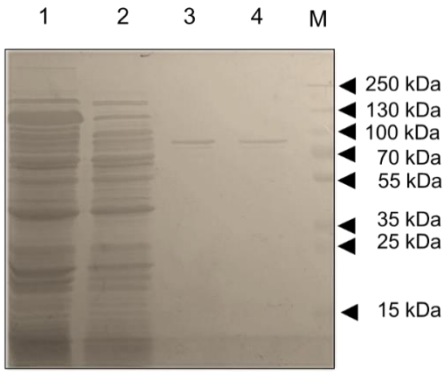

Fig. 9: SDS-PAGE of recombinant h4F2hc purification. *Lane 1* cell lysate (80µg), *lane 2* pass through after incubation with resin, *lanes 3-4* purified 4F2hc lacking its GST tag after treatment with thrombin, *lane M* molecular mass markers.

In particular, Fig. 9 shows both 4F2hc in the initial lysate and after treatment with 2U of thrombin. A band was present at about 130 kDa (lanes 1-2) corresponding to the sum of 4F2hc plus its GST tag either in the lysate (lane 1) and in the pass through after incubation overnight with Glutathione Sepharose 4B resin (lane 2). Whereas the band at about 80 kDa (lanes 3-4) corresponded to 4F2hc lacking its GST tag after treatment with thrombin. The latter purified proteins was used for reconstitution into liposomes.

The purification of hLAT1 was modified with respect to the previously published protocol [25], using FPLC chromatography by ÄKTA start (Materials and Methods section 2.5.). Fig. 10 shows a chromatogram profile and a SDS-PAGE of a typical purification of hLAT1. In particular, panel A represents an example of a chromatogram in which, after the peak of unbound proteins, a second peak containing hLAT1 was eluted, as indicated by the arrow (1). This fraction is shown by SDS-PAGE of panel B (lane 1). Lane 2 of the same panel shows the protein after desalting procedure for removing imidazole as described in Materials and Methods.

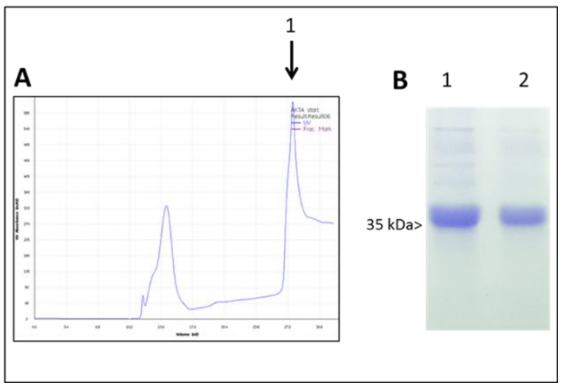

Fig. 10: Chromatogram profile and SDS-PAGE of recombinant hLAT1 purification. (A) Chromatogram of hLAT1 purification, the arrow represents the pick containing hLAT1. (B) SDS-PAGE of eluted protein (*lane 1*) and corresponding desalted protein (*lane 2*).

3.1.3. Transport assay of native (4F2hc)/LAT1 in proteoliposomes

The proteins, extracted from cell lysates or purified from *E. coli* were then adopted for reconstitution into liposomes as described in Materials and Methods (section 2.6. and 2.7.).

The proteins extracted from SiHa cells were pre-treated, or not, with 10 mM DTE and then reconstituted in liposomes for transport assay. Treatment with DTE was performed to separate LAT1 from 4F2hc in order to observe the transport activity of LAT1 alone or (samples not treated with DTE) in complex with 4F2hc.

Transport activity was measured as homologous antiport [^{3}H]His$_{ex}$/His$_{in}$ as function of time. His was used as preferred substrate to reduce interferences by other transporters which are present in SiHa cell extracts, but have lower affinity for His than for neutral amino acids. As shown in Fig. 11, DTE strongly activates [^{3}H]His transport. Transport equilibrium was reached after 30 min with an initial transport rate of 0.68±0.03 pmol·min^{-1}·mg protein^{-1} in liposomes reconstituted with proteins extract not treated with DTE and of 7.02±2.86 pmol·min^{-1}·mg protein^{-1}, in liposomes reconstituted with proteins extract treated with DTE. As mainly discussed beyond, this discrepancy is probably due to the redox state of the protein extract not treated with DTE.

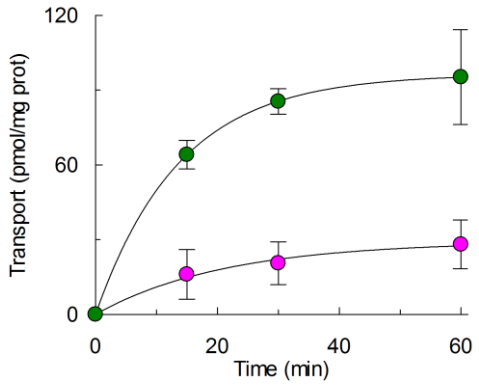

Fig. 11: Time course of [^{3}H]His uptake in liposomes reconstituted with SiHa cells extract treated (●) or not (●) with 10 mM DTE. Transport reaction was stopped at indicated times as described in Section 2.8.1. Results are mean ± S.D. from three experiments.

To verify if the measured transport activity was actually due to the reconstitution of the complex or of LAT1 alone, and to confirm whether the SiHa cell heterodimer was cleaved and inserted into liposomes downstream the treatment with DTE, western blot analysis were performed. In particular, after reconstitution, proteoliposomes were separated from empty liposomes by ultracentrifugation (see Materials and Methods section 2.2.4.) and run on SDS-PAGE under oxidizing conditions to not alter the oligomerization states of the proteins. After that, immunoblot analysis was performed using both anti-4F2hc and anti-LAT1 antibodies (Fig. 12). As shown in the figure, both antibodies identified a band of 120 kDa in liposome reconstituted with cell extracts not treated with DTE before reconstitution (lane 1 of both A and B). These results confirm that 4F2hc/LAT1 heterodimer was present in the proteoliposome membrane. Whereas, in liposome reconstituted with cell extracts treated with DTE before reconstitution, the apparent molecular mass of the proteins

diminished to about 80 kDa (Fig. 12 A lane 2) when immuno-detected with anti-4F2hc and to about 35 kDa when immuno-detected with anti-LAT1 (Fig. 12 B lane 2), confirming the presence of each single protein under reducing conditions.

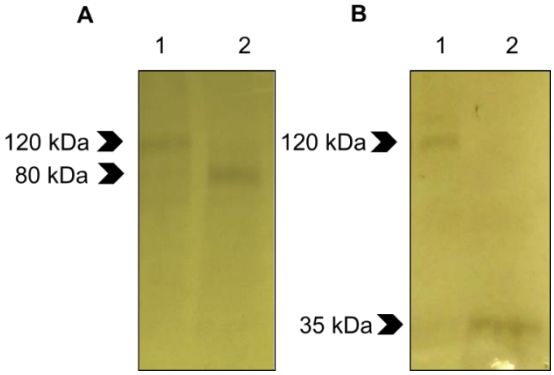

Fig. 12: Western blot analysis of 4F2hc/LAT1 in proteoliposomes. 4F2hc/LAT1 was solubilized from cells and not treated with DTE (*lanes 1*) or treated with 10 mM DTE (*lanes 2*). Proteoliposomes were separated as described in Section 2.2.4. and then subjected on SDS-PAGE under non-reducing conditions. Western blot analyses were conducted using anti-4F2hc (A) and anti-hLAT1 (B) antibodies. The images (A-B) are representative of at least two independent experiments.

The emerging conclusion from reconstitution of native proteins in liposomes is that the pre-treatment with DTE breaks the disulphide. Even though we can not exclude that a fraction of 4F2hc and LAT1 remains associated to the liposomal membrane, data on proteoliposomes (Fig.12), suggested that either 4F2hc was independently reconstituted in proteoliposomes or it was co-reconstituted together with LAT1 in the same vesicles. Thus, this result highlighted capacity of LAT1 to mediate transport activity *per se*.

3.1.4. Transport assay of purified hLAT1 and h4F2hc in proteoliposomes

To definitively gain insights on this issue, recombinant proteins were adopted for reconstitution into liposomes and [^{3}H]His/His antiport was measured in time course . As shown in Fig. 13 reconstituted 4F2hc did not mediate transport activity, whereas the reconstituted LAT1 alone was sufficient to mediate amino acid transport. In this reaction, the equilibrium was reached after 30 min with an initial transport rate of 0.70±0.03 nmol·min^{-1}·mg protein^{-1}. The difference with respect the transport rate exerted by reconstitution of native protein (Fig. 11) could be attributed to the presence of other amino acids transporters probably present in SiHa cells extract, which, even though have lower affinity for His could affect transport activity (e.g. causing the efflux of His from proteoliposomes).

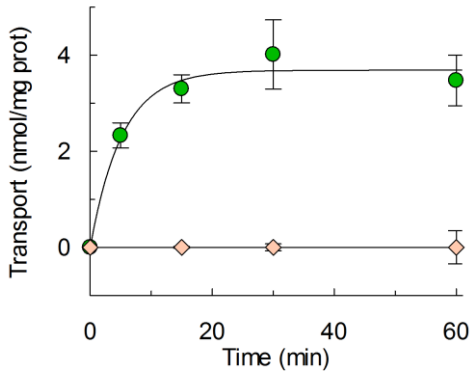

Fig. 13: Time course of [^{3}H]His uptake in liposomes reconstituted with purified hLAT1 (●) or h4F2hc (◆). Transport reaction was stopped at indicated times as described in Section 2.8.1. Results are mean ± S.D. from three experiments.

Data obtained with reconstitution in liposomes of the recombinant LAT1 confirmed the observation made with endogenous protein: LAT1 is the sole competent transport unit of the heterodimer.

3.1.5. Involvement of 4F2hc in transport specificity

Besides the ability of LAT1 to mediate transport activity in absence of 4F2hc, another important aspect was the possible role of 4F2hc in the specificity of LAT1 towards amino acids. This aspect could not be easily investigated in intact cells due to the impossibility to control the internal compartment. Proteoliposomes are indeed suitable for this type of investigation that was carried out with the native proteins as well as the recombinant hLAT1. In particular, two kind of experiments were performed to shed light on the functional property of LAT1 and on 4F2hc involvement, inhibition and counter substrates analyses.

Inhibition analyses were performed by adding 5 mM of different amino acids in the external space of proteoliposomes obtained with proteins extracted from SiHa cells untreated or treated with 10 mM DTE before reconstitution, and with recombinant hLAT1 (Fig. 14 A-B-C respectively).

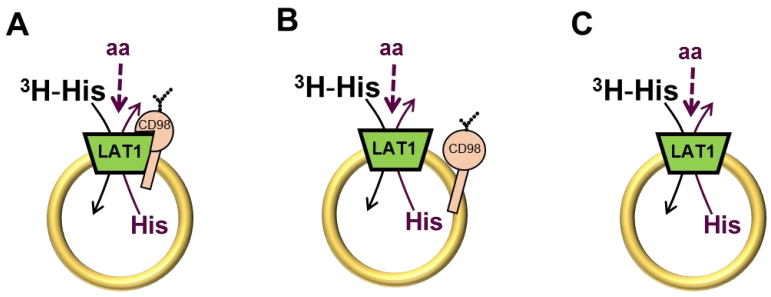

Fig. 14: Sketch of experimental design for inhibition analysis. Reconstitution of SiHa cells extracted proteins not treated (A) or treated with 10 mM DTE (B), (C) reconstitution of recombinant hLAT1.

The externally added amino acids were used to evaluate their ability to inhibit [^{3}H]His$_{ex}$/His$_{in}$ antiport. Transport was performed in 30 minutes for both native and recombinant proteins. Results obtained are shown as percentage of residual activity with respect to the control, i.e. in absence of externally added amino acids,

to highlight differences in substrate specificity and to normalize the actual differences of absolute transport activities between the analysed conditions (Fig. 15).

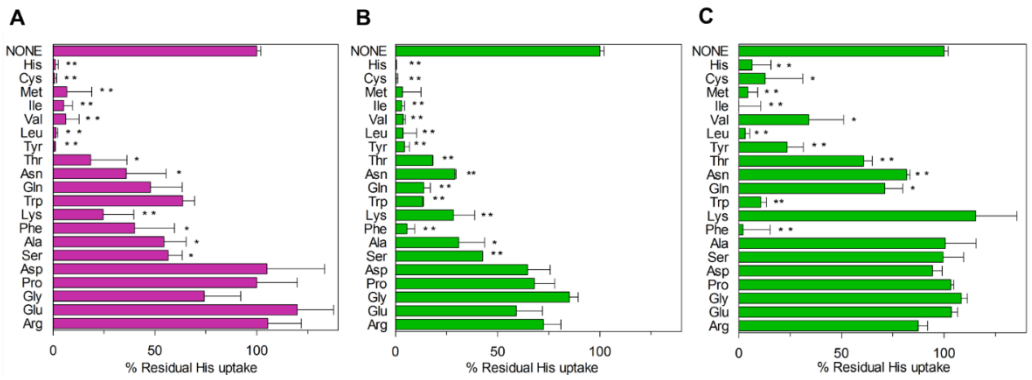

Fig. 15: Effect of amino acids on [^{3}H]His uptake in liposomes reconstituted with SiHa cells extracted proteins (A) not treated or (B) treated with 10 mM DTE and (C) in liposomes reconstituted with recombinant hLAT1. 5 mM of the indicated amino acids were added together with [^{3}H]His. Transport was performed in 30 min and stopped as described in Section 2.8.1. Percentage of residual His uptake was calculated with respect to controls (without added amino acids). Results are mean ± S.D. from three experiments. Student's two tailed unpaired t-test was performed on the control; p values were symbolized as follows: $^{*}p < 0.05$; $^{**}p < 0.01$ (A–C).

As shown in Fig. 15 inhibition ranged from 80 to 90%, by hydrophobic amino acids such as Ile, Val, Leu, Cys, Met and by more hydrophilic amino acids such as His as well as Tyr and Thr. Instead, inhibition exerted by Ala, Ser, Trp and Asn appeared to be lower, ranging between 70 and 50%. The other tested amino acids led to a very slight, if any inhibition. However, inhibition profiles for most of the amino acids were very similar under oxidizing or reducing conditions of native proteins (Fig. 15 A-B) and these overlapped almost completely that obtained with recombinant hLAT1 (Fig. 15 C). These data suggest that the specificity on the external side of LAT1 is different for the diverse amino acids and does not depend on the presence of 4F2hc. To shed light on transport specificity of hLAT1 and on the involvement of 4F2hc, counter substrates analyses were also performed. In this type of experiments, 10 mM of different amino acids were inserted in the intraliposomal space during reconstitution as represented in the sketches in Fig. 16 (see Materials and Methods section 2.6., 2.7.). In this way, counter-substrate were identified for their capacity to induce [^{3}H]His uptake (Fig. 17).

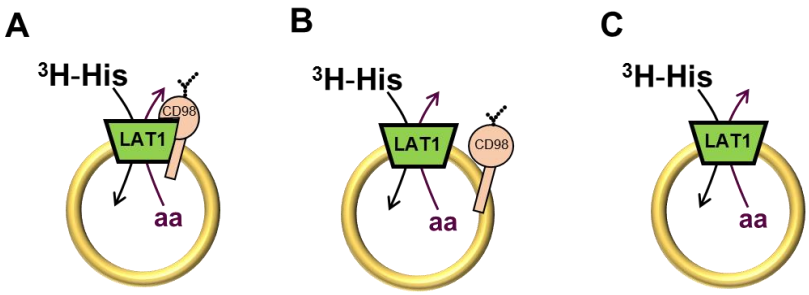

Fig. 16: Sketch of experimental design for counter substrates analysis. Reconstitution of SiHa cells extracted proteins not treated (A) or treated with 10 mM DTE (B), (C) reconstitution of recombinant hLAT1.

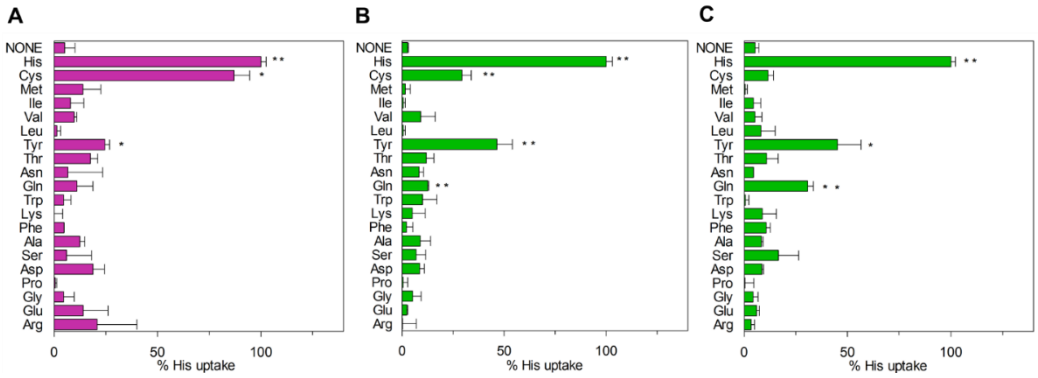

Fig. 17: Counter substrates for [^{3}H]His in liposomes reconstituted with SiHa cells extracted proteins (A) not treated or (B) treated with10 mM DTE and (C) in liposomes reconstituted with recombinant hLAT1. Transport was performed in 30 min by adding [^{3}H]His to proteoliposomes containing 10 mM of the indicated amino acids. Transport reaction was stopped as described in Section 2.8.1. Percentage of His uptake was calculated with respect to proteoliposomes containing 10 mM internal His (control). Results are mean ± S.D. from three experiments. Student's two tailed unpaired t-test was performed on the control; p values were symbolized as follows: $^*p < 0.05$; $^{**}p < 0.01$ (A–C).

In particular, as shown in Fig. 17, besides His also Tyr and Gln appeared to stimulate [^{3}H]His accumulation in proteoliposomes both in the case of native proteins (Fig. 17 A-B) and of recombinant hLAT1 (Fig. 17 C), whereas a discrepancy was observed in the case of Cys as counter substrate in all analysed conditions. Moreover, in spite of their ability to inhibit LAT1 from external side, internal Ile and Leu did not induce [^{3}H]His accumulation both in the case of native proteins and in the case of recombinant hLAT1, so, also in this case the results obtained with native proteins (Fig. 17 A-B) and recombinant protein (Fig. 17 C) overlapped almost completely.

Taken together, transport assays, inhibition analysis and counter substrates analysis performed in proteoliposomes of both native and recombinant hLAT1 demonstrate that neither the covalent interaction, nor the presence of 4F2hc is necessary for both transport competence and specificity of hLAT1.

3.1.6. hLAT1 functional asimmetry

The described results have drawn attention to another interesting aspect of hLAT1: its possible functional asymmetry. Indeed, as observed in inhibition and in counter-substrate analyses, the specificity on the external and internal sides of LAT1 appeared to be peculiar for different amino acids, with some substrates such as Ile able to inhibit [^{3}H]His uptake if added on the extraliposomal space, but unable to induce [^{3}H]His accumulation

when used as counter substrate. Thus, to gain further insight on this issue, reconstitution of recombinant protein was adopted to measure the uptake of other radiolabelled amino acids and for efflux analysis (Fig. 18). Only recombinant hLAT1 was used for these experiments. Indeed, even though the results obtained with native proteins and recombinant hLAT1 overlapped each other almost completely, small differences were observed, possibly due to the presence of other amino acid transporters in SiHa cell extract.

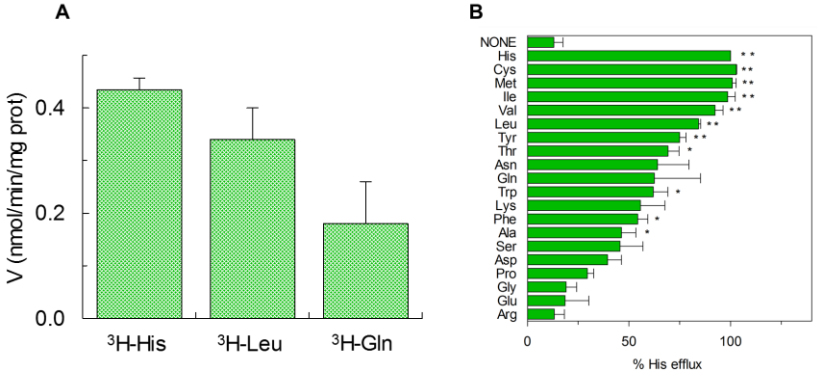

Fig. 18: [^{3}H]His uptake and efflux in proteoliposomes reconstituted with recombinant hLAT1. (A) Uptake of different radiolabelled amino acids. Transport reaction was performed in 30 min and stopped as described in Section 2.8.1. Results are mean ± S.D. from three experiments. (B) Efflux of [^{3}H]His from proteoliposomes in presence of 5 mM of indicated amino acids as counter substrates. Transport reaction was stopped after 10 min as described in Section 2.8.1. Percentage is referred to proteoliposomes with externally His (control). Results are mean ± S.D. from three experiments. Student's two tailed unpaired t-test was performed on the control; p values were symbolized as follows: $^{*}p < 0.05$; $^{**}p < 0.01$ (B).

As shown in figure 18, uptake of [^{3}H]His, [^{3}H]Leu and [^{3}H]Gln occurs in 30 minutes at different extent.

Efflux analysis was also performed to identify which amino acids were able to induce [^{3}H]His efflux from proteoliposomes, i.e., were able to be transported from the external to the internal side of the membrane. In these experiments, 5 mM of different amino acids were added to the extraliposomal space of proteoliposomes preloaded with [^{3}H]His (see Materials and Methods section 2.8.2.) and the efflux of [^{3}H]His was measured in 10 minutes. Data were expressed as percentage of [^{3}H]His efflux in presence of each amino acids and with respect to proteoliposomes with externally His (Fig. 18 B). As shown in figure, in line with the antiport activity, only a slow efflux of His was observed in absence of external substrate, whereas besides His also Cys, Met, Ile, Val, Leu, Tyr and Thr strongly induced [^{3}H]His efflux. Other amino acids, such as Gln, Ser or Lys were much less efficient in inducing [^{3}H]His efflux.

In all the analysed conditions, transport activity was stopped using the known inhibitor BCH (Materials and Methods section 2.8.1.). Its IC50 value of 6.8±2.0 µM was calculated from dose-response analyses (Fig. 19).

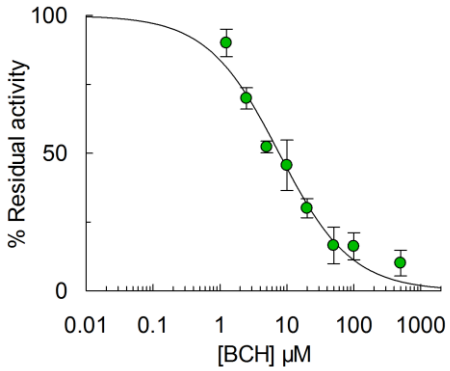

Fig. 19: Dose-response curve for BCH. Transport was measured in 15 min and stopped as described in Section 2.8.1. Percent residual activity with respect to the control is reported. Results are mean ± S.D. from three experiments.

Taken together, the described results allowed to confirm the suitability of proteoliposomes model to study LAT1 mediated transport. Indeed, the described data deriving from different experimental approaches, i.e. inhibition, counter substrates and efflux analyses, indicate that amino acids showed different specificity on the two sides of the protein. His and Tyr were recognized by both sides of the transporter, Leu or Ile were only inwardly transported, while Gln appeared to be preferentially outwardly transported (Fig. 20). This feature has physiological relevance and explains the link between the transport activity of LAT1 and that of ASCT2 another neutral amino acids transporter. Indeed, this correlation allows Gln, which is transported in a Na^+-dependent manner by ASCT2, to be used by LAT1 as counter (efflux) substrate for the entry of Leu by the LAT1 mediated antiport (Leu/Gln). Taken up Leu modulates the mTOR pathway. This function is important in pathological conditions as well being involved in triggering cell survival and/or death (see Introduction section 1.10. and Fig 20).

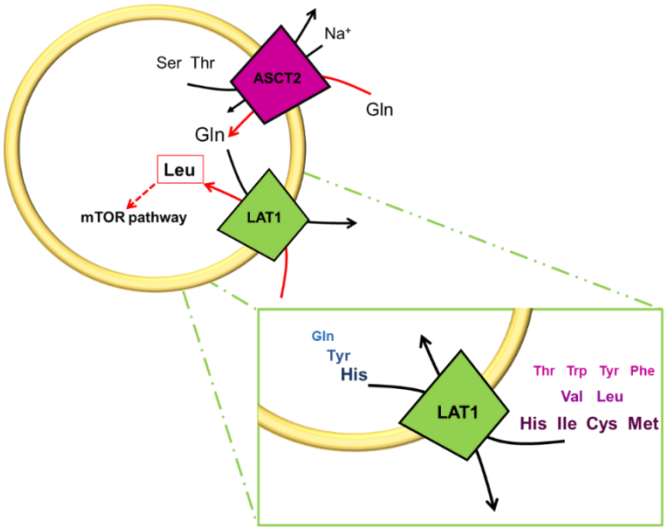

Fig. 20: Correlation between LAT1 and ASCT2 amino acids transporters in cell membranes. The sketch represents the cell membrane with the two transporters inserted and the arrows indicate the flux of the amino acids. The enlargement focus on the functional asymmetry exerted by LAT1, with amino acids efficiency transport highlighted by growing characters size and different shade of colours.

3.1.7. Effect of cations on LAT1 transport activity

By means of the proteoliposome model, the possible influence of physiological ions on transport was investigated. Indeed, as shown in Fig. 21 A, the presence of K^+, at 100 mM a concentration close to that present inside cells, stimulated His antiport with respect to the control containing sucrose. To the same extent, Na^+ showed a similar effect, whereas the Cl^- was not involved in stimulation as suggested by using both K-gluconate and KCl. The effect of K^+ was further investigated as dependence of His uptake on intraliposomal K^+ concentrations. As shown in Fig. 21 B, the activity increased along with the internal K^+ concentration, reaching a plateau at 80 mM, i.e., a concentration not far from the physiological one.

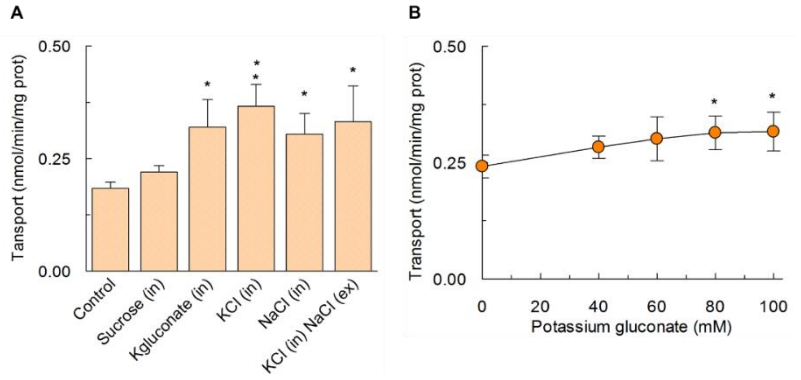

Fig. 21: Effects of intraliposomal salts on His_{ex}/His_{int} transport in proteliposomes. (A) Transport was started adding 5 µM [^{3}H]His to proteoliposomes containing 10 mM His and 100 mM of indicated salts. Sucrose at 200 mM was used as control of osmotic stress. Effect of 100 mM NaCl added to the extraliposomal compartment was also evaluated. Transport was performed in 30 min and stopped as described in section 2.8.1. (B) Transport was started adding 5 µM [^{3}H]His to proteoliposomes containing 10 mM His and indicated concentrations of Potassium gluconate and stopped at 30 min as described in section 2.8.1. Results are mean ± S.D. from three experiments. Student's two tailed unpaired t-test was performed on the sample without internal compounds (control); p values were symbolized as follows: $^*p < 0.05$; $^{**}p < 0.01$ (A–B).

3.2. Kinetic characterization of hLAT1

After completion of the functional characterization, reconstitution of recombinant protein was adopted for kinetic analysis. External and internal Km values for His were calculated (Fig. 22) showing that the external Km value (Fig. 22 A) was 24.6±5.6 µM, whereas the internal Km was 2.8±1.7 mM (Fig 22 B). External Km was investigated also in presence of K^+, showing an increase of V_{max} from 2.1±0.16 to 3.1±0.28 $nmol \cdot mg^{-1} \cdot min^{-1}$, in the presence of internal K^+, while the Km was not significantly influenced.

In summary, the strong differences between external and internal Km values demonstrated that LAT1 shows, besides a functional asymmetry, also a kinetic asymmetry.

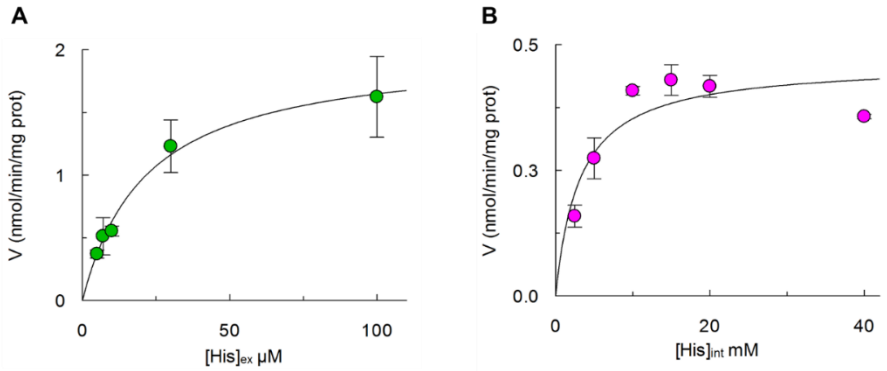

Fig. 22: Kinetics analysis of His transport in proteoliposomes reconstituted with over-expressed hLAT1. Transport rate was measured in 10 min by adding [^{3}H]His at the indicated concentration (A) to proteoliposomes containing 10 mM of internal His or (B) 5 µM [^{3}H]His to proteoliposomes containing internal His at the indicated concentrations. Transport reaction was stopped as described in section 2.8.1. Data were plotted according to Michaelis-Menten equation. Results are mean ± S.D. from three experiments.

Moreover, external Km was calculated for Leu (25±13 µM), Met (31±11 µM), Val (57±20 µM), Gln (0.7±0.4 mM) and Ala (>1 mM). All these values corresponded to that measured in intact cells with the only exception of Ala for which no Km values were reported in literature [27, 28].

The correspondence among data obtained with recombinant protein and intact cells confirmed that the protein was inserted in proteoliposomes with the same orientation as in cell membranes. This important feature was confirmed by an experimental set up in which an anti-His antibody was used to target the His tag located at the N-terminus of the protein. In this experiment, the transporter was incubated with the antibody before or after incorporation in proteoliposomes to evaluate the position of the N-terminus of the protein as function of the inhibition of transport activity (Fig. 23).

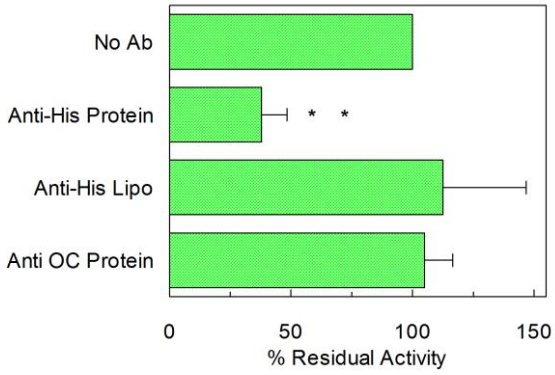

Fig. 23: Inhibition of His transport by antibody. The anti-His antiserum was added to protein before reconstitution (Anti-His Protein), or after reconstitution (Anti-His Lipo) during transport assay. Anti-OCTN1 antiserum was added to protein before reconstitution as for Anti-His protein (Anti OC Protein). Percentage is referred to proteoliposomes without added antibody (control). Transport reaction was performed in 30 min and stopped as described in section 2.8.1. Results are mean ± S.D. from three experiments. Student's two tailed unpaired t-test was performed on the sample without added antibody (control); p values were symbolized as follows: $^{*}p < 0.05$; $^{**}p < 0.01$.

As shown in Fig. 23, incubation of the protein before reconstitution (Anti-His protein) strongly inhibited hLAT1 with respect to the untreated control (No-Ab). This inhibition is due to the steric hindrance caused by the binding of the anti-His antibody to the N-terminal of LAT1 confirming its intraliposomal localization. On the contrary, the antibody externally added to proteoliposomes (Anti-His Lipo) did not inhibit at all. As control the protein was incubated with an antibody raised against a different protein, OCTN1, under the same

condition leading to inhibition by anti-His (Anti OC Protein); in this case, no effect was observed indicating that inhibition was specifically due to N-terminal His tag recognition. Thus, these data demonstrated an intraliposomal localization of the N-terminus of the protein corresponding to the same orientation as in cell membrane [20]. Furthermore, the complete absence of inhibition by externally added anti-His antibody indicated that the virtually 100% of LAT1 was right-side out oriented in proteoliposomes.

Taken together, all the data confirmed the reliability of results obtained with recombinant protein and proteoliposome tool. For this reason, the suitability of reconstitution into liposomes was adopted for studying the mechanism of His_{int}/His_{ex} antiport through bi-reactant analyses; these experiments required that both the external and the internal His concentrations were changed in the same experiment. To discriminate between ping-pong and simultaneous mechanisms, transport rate of [^{3}H]His uptake was then plotted as function of external or internal His concentrations according to Lineweaver-Burk (Fig. 24 A and B respectively). Indeed, as shown in Fig. 24, the straight lines showed non-parallel patterns intersecting in proximity of the X-axis, and this was indicative of a simultaneous mechanism.

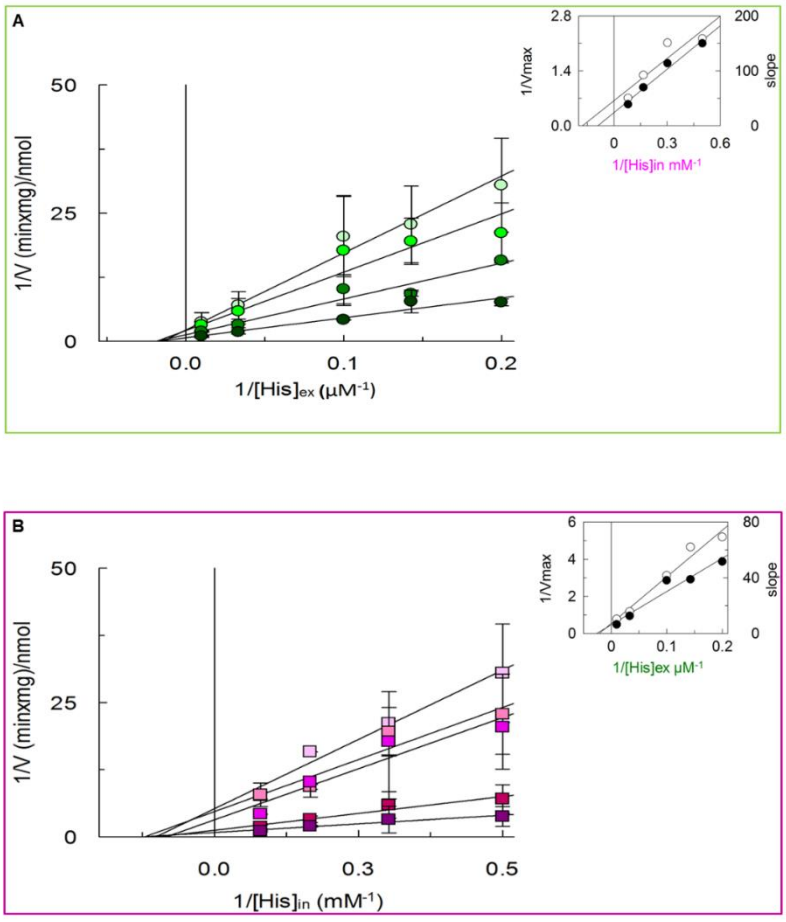

Fig. 24: Kinetics and Transport mechanism of the recombinant hLAT1. Data were analysed by Lineweaver–Burk plots showing the dependence of reciprocal transport rate on reciprocal external (A) or internal (B) His concentrations. Transport reaction was stopped at 15 min as described in section 2.8.1. In (A), the concentrations of intraliposomal His were 2.0 (○), 3.3 (○), 6.0 (○), 12.5 (●) mM; the concentrations of external [^{3}H]His were 5.0, 7.0, 10, 30, 100 μM. In (B) the same data of (A) were plotted as function of the internal His concentration at external [^{3}H]His 5.0 (□), 7.0 (□), 10 (□), 30 (□), 100 (□) μM. In A–B the insets show the re-plots of the intercepts on the Y-axis (1/Vmax - ○) or the slopes (Km/Vmax - ●) from the primary plots as a function of internal (A) or external (B) His. Results are mean ± S.D. from three independent experiments (A-B).

The simultaneous mechanism can be random or ordered, thus, to completely clarify the His_{ex}/His_{in} transport reaction the dissociation constant of the ternary (His_{ex}-transporter-His_{in}) and binary transporter His complexes were analysed. These constants were calculated by re-plotting the values of the intercepts on the Y-axis or the slopes of the straight lines, as function of the reciprocal substrate concentrations (insets of Fig. 24 A and B). In this way, concentration independent (K_S) values obtained were 47.5 μM for external His and 5.6 mM for internal His, whereas the calculated Ki_S values were 73 μM for external His and 9.5 mM for internal His. The same constants fulfilled the relation $Ki_S \cdot K_{S2} = Ki_{S2} \cdot K_{S1}$ which is typical of a random simultaneous mechanism implying that the two substrates bind at the same time to the external and internal sites.

3.2.1. Oligomeric structure of hLAT1

The random simultaneous mechanism described is an unexpected observation for a transport protein. Indeed, considering that membrane transporters work through an alternating-access model, this implies conformational transition of the transporter between states in which the substrate-binding site is exposed to opposite sides of the membrane in an alternating manner. This means that the access from both sides of the membrane to the substrate-binding site cannot be simultaneous [68]. In fact, our observation of a random simultaneous mechanism was supported by an oligomeric structure of the transporter, which was observed through western blot analyses and predicted by bioinformatics (Fig. 25 A-D).

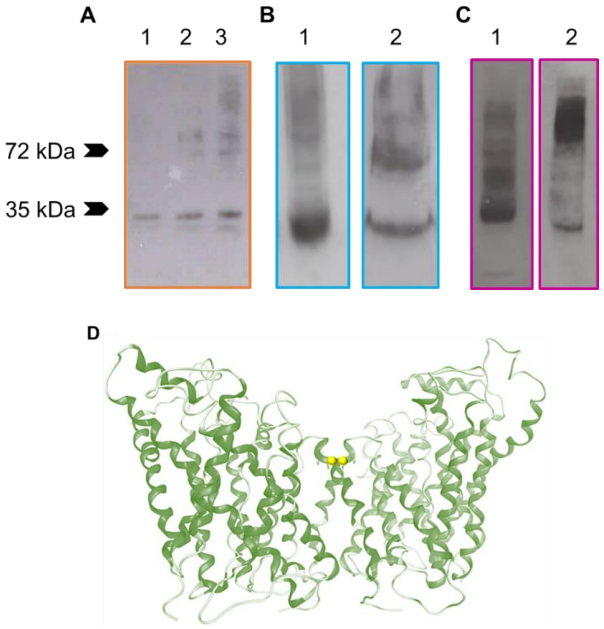

Fig. 25: Oligomeric state of recombinant and native hLAT1. In (A) purified and functional hLAT1 has been treated with 1 mM (*lane 2*) and 2 mM (*lane 3*) Cu^{++}-phenanthroline compared to untreated control (*lane 1*). After stopping cross-linking reaction, samples were ran on a SDS-PAGE 10% without reducing agents in sample buffer. In (B) purified and functional hLAT1 (*lane 1*) or hLAT1 inserted in proteoliposomes (*lane 2*) was subjected to electrophoresis under mild denaturing conditions, using sarkosyl (0.1%) instead of SDS in all run buffers without reducing agents in sample buffer. Protein monomers and oligomers were detected by immunoblotting analysis using anti-His antiserum 1:1000 dilution as described in Section 2.2.7. (A–B). In (C) native hLAT1 was extracted from SiHa cell membrane and subjected to electrophoresis under mild denaturing conditions (as in A) treated (*lane 1*) or not (*lane 2*) with 100 mM DTE before running. Protein monomers and oligomers were detected by immunoblotting analysis using anti-LAT1 antiserum 1:2000 dilution as described in Section 2.2.7. The images (A-C) are representative of at least two independent experiments. (D) hLAT1 homology models. hLAT1 is shown as ribbon representation in its dimeric conformation. Cys (C458) at the interface of LAT1 dimer were shown in stick representation and thiol groups were indicated as yellow spheres.

Western blot analyses were performed in different conditions. To appreciate the formation of an oligomeric structure of the protein on SDS-PAGE, recombinant purified protein was subjected to a cross-link strategies using Cu^{++}-phenantroline that catalysed the formation of disulphides through closes Cys residues of the protein (see Materials and Methods section 2.2.5.). The incubation of the protein with 1 or 2 mM of the catalyst (Fig. 25 A, lanes 2 and 3 respectively), was performed for ten minutes and the same samples were then subjected to SDS-PAGE under oxidizing conditions and stained with Anti-His. As shown in Fig 25, after treatment with the reagent most of the protein migrated at a double molecular mass with respect to the untreated monomer (Fig. 25 A, lane 1) due to formation of disulphide(s) and suggesting the possible the existence of dimeric form of hLAT. Then, the possible existence of a dimeric structure was investigated by electrophoresis under mild denaturing conditions on Sarkosyl-PAGE on both purified hLAT1 and after insertion of the same protein in liposomal membranes (Fig. 25 B). As shown in the case of purified protein (Fig. 25 B, lane 1), the presence of aggregates at higher molecular masses was observed, besides hLAT1 monomer, suggesting that functional hLAT1 may have an oligomeric composition, a feature confirmed by the results obtained after insertion of the protein into liposomes (Fig. 25 B, lane 2). Furthermore, the existence of a dimeric structure of LAT1 was investigated in SiHa cell extracts both under reducing and oxidizing conditions (Fig. 25 C) using anti-LAT1 antibody. In particular, samples were treated with 10 mM DTE to separate LAT1 from 4F2hc and under this condition two major bands were observed one at about 35 kDa and the other at about doubled molecular mass (Fig. 25 C, lane 1). On the contrary, under oxidizing conditions a large higher band was detected, which can include both hLAT1 homodimer and/or LAT1/4F2hc heterodimer (Fig. 25 C, lane 2). Thus, in all the analysed conditions an oligomeric form of hLAT1 was observed. However, the possible existence of a dimeric structure was also predicted by bioinformatics. Indeed, the structural model of hLAT1 was built by homology, using as template the bacterial AdiC, whose crystallographic structure is currently available in different conformational states and in analogy to AdiC also hLAT1 could form a homodimer (Fig. 25 D).

3.3. Characterization of substrate-binding site of hLAT1

3.3.1. Identification of critical amino acid residues

The choice of using AdiC (L-Arginine/agmantine antiporter) as template for building hLAT1 homology model, derives from the growing knowledge on the crystallographic structure of this transporter in different conformational states, i.e. the open-to-out apo form (PDB ID 3LRB and 3NCY) [56, 57], the substrate-bound open-to-out form (PDB ID 3OB6) [29], and the outward-facing Arg^{+}-bound occluded (PDB ID 3L1L) [21] conformation. This knowledge is important to clarify the conformational changes that occur during each transport cycle even though this is only a step forward in the elucidation of the transport mechanism, which requires also the knowledge of the substrate-binding site. In this regard, comparison of the crystal structures of amino acids transporter with the LeuT-fold (see Introduction section 1.14.) highlighted the conservation of

the substrate binding site location as well as the key residues involved in both substrate recognition and translocation [56-60]. Then, moving from this basis we decided to investigate the actual role of the corresponding residues in LAT1, even though in line with their substrate specificity, the composition of the key residues coordinating the substrates in the binding sites varied significantly between different members of the APC superfamily.

Thus, to satisfy our purpose of shedding light on the transport mechanism and on the substrate translocation of the human amino acid transporter LAT1, a multi alignment including different member of the APC superfamily was performed. Considering this alignment and current literature data, the amino acids which appeared to be critical for recognition and translocation of Arg/agmantine in AdiC, were predicted. The residues of AdiC W202, W293 and S357 [59, 60, 69] important for substrates (agmatine/Arg) binding and translocation, corresponded to LAT1 F252, S342 and, C407, respectively, as also reported in Geier et al. [70]. These residues were considered for docking simulation shown in Fig. 26.

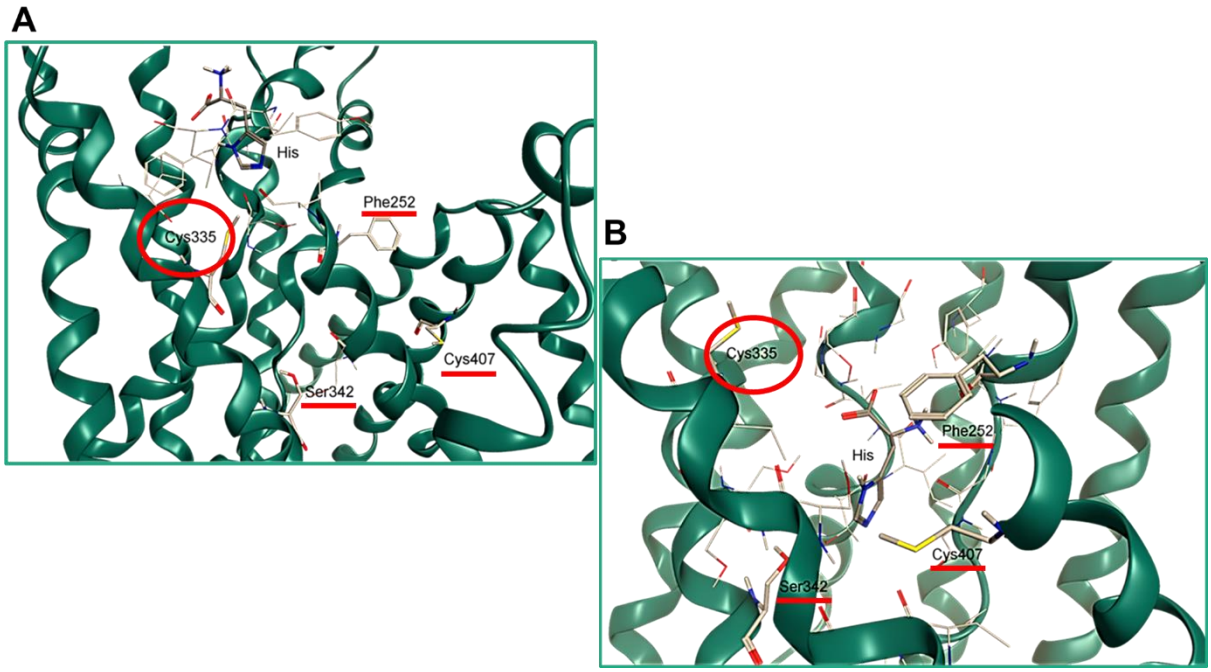

Fig. 26: hLAT1 Substrate binding site. Representative docking poses for His in LAT1 outward-open form (A) and outward-closed form (B). hLAT1 is shown in ribbon representation; His and residues of the binding site are shown as stick representation. Critical residues are highlighted in red, whereas the novel one residue identify, Cys335, is encircled in red.

All the mentioned residues corresponding to AdiC were highlighted in Fig. 26 (A), i.e. hLAT1 in outward-open conformation. Moreover, the same docking simulation identified another Cys residue never predicted before, C335, closed to the substrate-binding residue F252. Moreover, docking simulations performed also on the outward-closed conformation (Fig. 26 B), showed that all the poses, obtained for His, well fitted with the position of the Arg in AdiC, and that the residues surrounding the binding site included F252, S342 and C407. Thus, these residues were considered to shed light in substrate recognition, and, to investigate the effective role of these residues in substrate recognition, mutants were constructed and corresponding recombinant

proteins were over-expressed in *E. coli* and purified as described for wild type protein (see Materials and Methods section 2.5.).

3.3.2. Characterization of hLAT1 mutants

Concerning Cys residues, C335, C407 or both were substituted with Ala (C355A, C407A and C3355A/C407A respectively), S342 was substituted with Gly (S342G), whereas for F252 two different mutants were constructed. F252 was substituted either by the conservative residue Trp corresponding to the homologue AdiC (F252W), or by the non-conservative residue Ala to change the chemical/steric properties of the side chain. All these mutants were tested for transport activity measuring His_{int}/His_{ex} antiport in time course (Fig. 27).

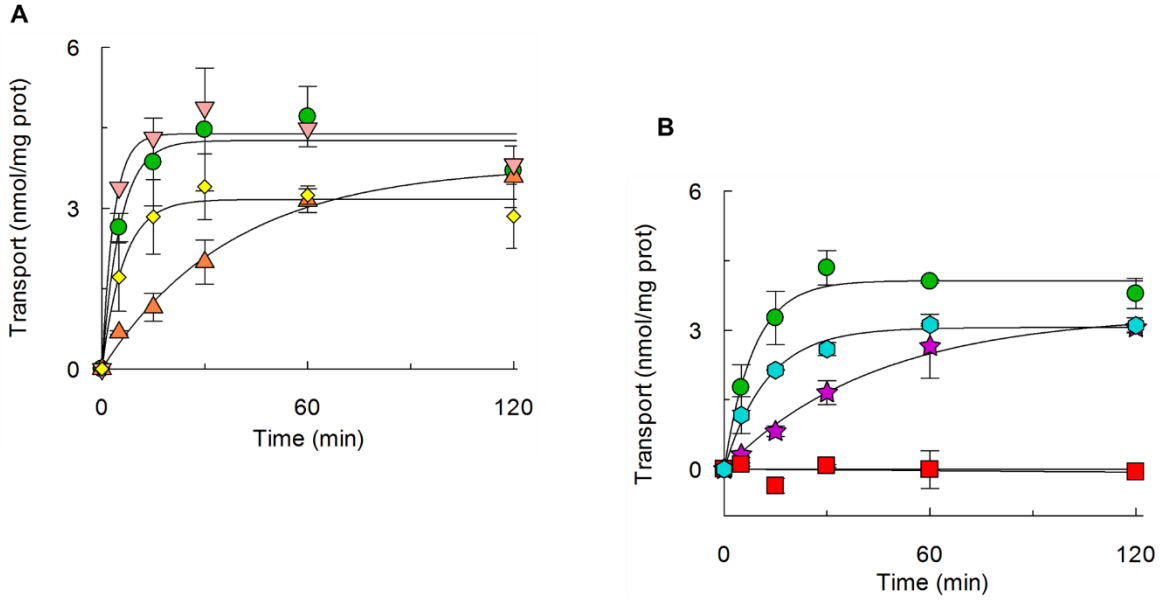

Fig. 27: Time course of [^{3}H]His uptake in proteoliposomes reconstituted with over-expressed hLAT1 wild type and mutants. (A) Transport was started adding 5 µM [^{3}H]His to proteoliposomes reconstituted with LAT1 WT (●), C335A (▲), C407A (▽) or double mutant C335A/C407A (◇) and in (B) to proteoliposomes reconstituted with LAT1 WT (●), F252W (★), F252A (■) or S342G (⬢). Proteoliposomes contained 10 mM His. Transport reaction was stopped at the indicated times as described in section 2.8.1. Data were plotted according to first rate equation. Results are mean ± S.D. from three independent experiments (A-B).

As shown in Fig. 27 (A-B), only F252A mutant completely lost transport activity (Fig. 27 B), whereas all other mutants were active even though less than wild type. Thus, to shed light on the differences observed with respect to the wild type, kinetics analyses were performed (Fig. 28-29).

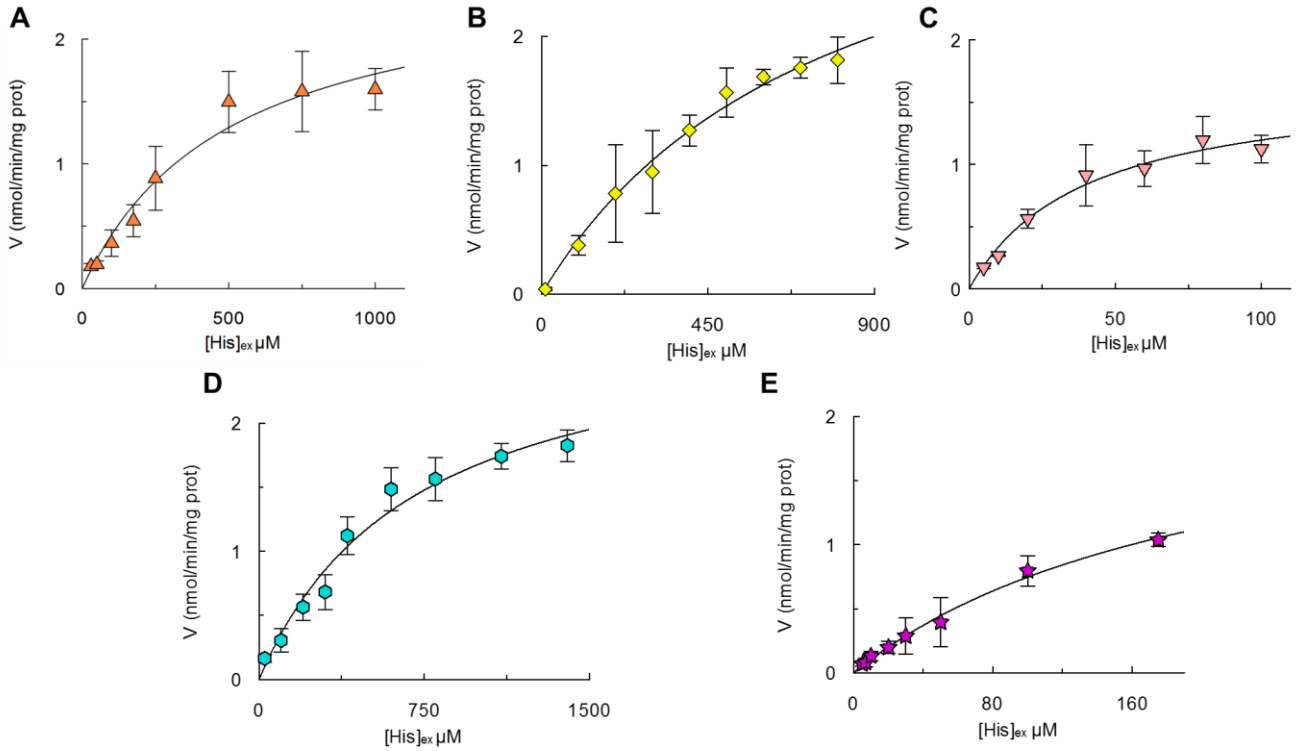

Fig. 28: Kinetics analysis of His transport in proteoliposomes reconstituted with hLAT1 mutants. Transport rate was measured in 30 min by adding [^{3}H]His at the indicated concentration to proteoliposomes containing 10 mM of internal His. (A) C335A mutant, (B) Double mutant C335A/C407A, (C) C407A mutant, (D) S342G mutant and (E) F252W mutant. Transport reaction was stopped as described in section 2.8.1. Data were plotted according to Michaelis-Menten equation. Results are mean ± S.D. from at least three independent experiments (A-E).

External Km values were measured (Fig. 28 A-E). Concerning Cys mutants, it was observed that substitution of C335 strongly increased the external Km, which was 582±234 µM, indicating that this residue was important for His binding. The same applies to double substitution of C335A/C407A, which showed an external Km value of 775±127 µM. On the contrary, C407A mutant showed an external Km similar to that of WT, i.e. 37±11 µM (Fig. 28 A-B-C respectively). As in the case of C335A and C335A/C407A, also the S342G and F252W mutants had and external Km value of 784±139 µM and 184±40 µM, respectively (Fig. 28 D-E respectively).

Then, internal Km values for His were measured (Fig. 29). In this case, C407 showed a slight increase of this value with respect to the wild type, i.e. 5.9±1.4 mM (Fig. 29 A). For all the other mutants, measured internal Km values were similar to that of wild type, i.e. 2.5±0.67 mM for C335A, 3.2±0.49 mM for S342G and 2.0±0.45 mM for F252W (Fig 29 B, C and D respectively).

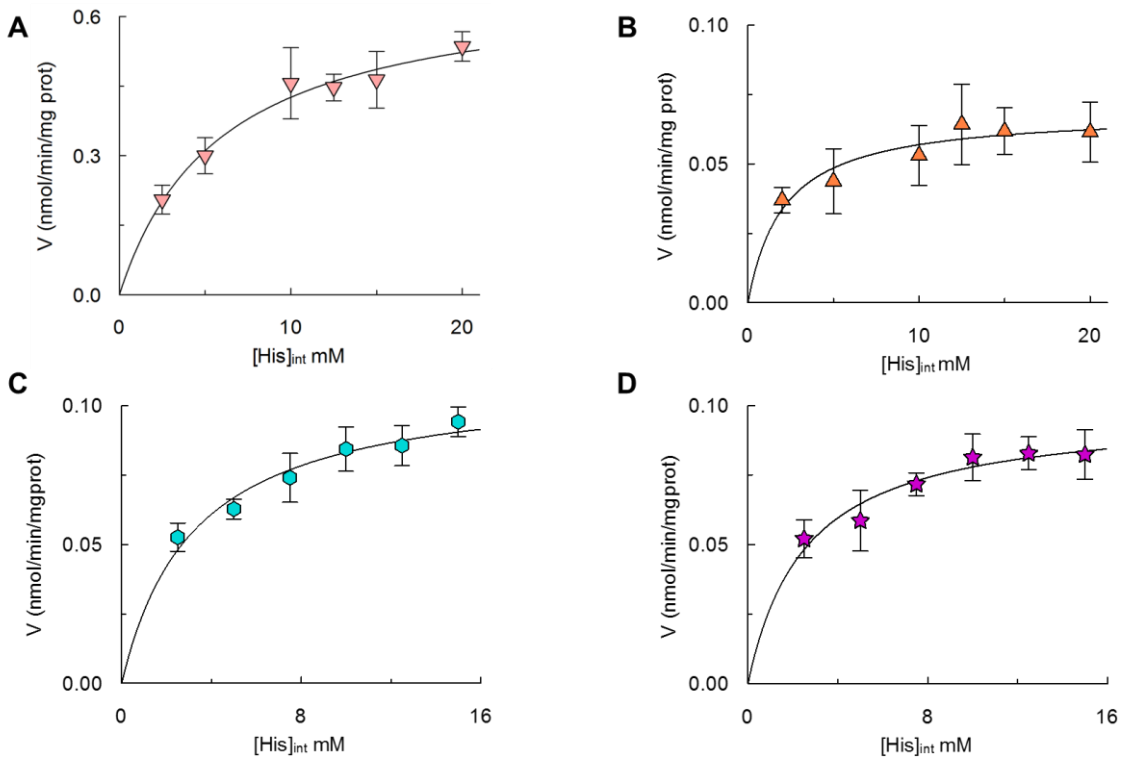

Fig. 29: Dependence of the rate of His antiport in proteoliposomes reconstituted with hLAT1 mutants. The transport rate was measured adding 5 μM [^{3}H]His to proteoliposomes containing indicated concentrations of internal His. Transport was measured in 15 min for C407A mutant (A) and in 30 min for C335A mutant (B), S342G mutant (C) and F252W (D). Transport reaction was stopped as described in section 2.8.1. Data were plotted according to Michaelis-Menten equation. Results are mean ± S.D. from at least three independent experiments (A-D).

Kinetic analyses confirmed the involvement of C335, C407, S342 and F252 residues in substrate recognition as predicted by bioinformatics but never experimentally proven, so far. F252 and S342 residues appeared to be involved in substrate translocation. F252 revealed to be essential as a gate of LAT1 as testified by disruptive effect of Ala substitution compared to F252W mutation and in analogy with structural data on AdiC, even though the conservative substitution with Trp is not sufficient to maintain proper affinity for substrate, but this feature is not unexpected. Indeed, differences between AdiC and LAT1 in terms of molecular mechanism of substrate recognition correlate with the substrate's specificity. Indeed, since LAT1 accepts aromatic or aliphatic amino acids, while AdiC is mainly involved in interactions with the charged, Arg and Agmatine [56], W202 and W293 of AdiC are replaced in LAT1, respectively, by the more hydrophobic F252 according to Kyte-Doolittle [71] and by S342. Moreover, C335, which showed an increased external Km value, can be involved in substrate binding. Indeed, the effect deriving from the substitution of Cys with Ala suggested that the thiol was the critical chemical group for His binding being a forefront residue. While, concerning C407 residue, predicted as part of the substrate binding site, kinetic analyses suggested that it had a marginal role in substrate recognition since only the internal Km showed small variation upon mutation. This feature is in line with data reported for AdiC; indeed, in this bacterial homologue C407 corresponds to S357 for which the substitution with Ala showed an affinity for substrate similar to that of WT, as we observed in LAT1. Thus,

taken together, the illustrated data showed that besides a switch from hydrophilic to neutral/hydrophobic substrate recognition between AdiC and LAT1, F252 is a gate element, allowing substrate entry in the translocation site playing, possibly, the same function as W202 in AdiC as well as other residues, i.e., S342 and C335 are responsible of substrate docking prior to translocation.

Therefore, the use of combined approaches of bioinformatics, site-directed mutagenesis and transport assay in proteoliposomes, satisfied our purpose in advancing the molecular knowledge of transport mechanism, allowing to identify experimentally for the first time amino acid residues critical for substrate recognition and translocation, with some of these previously reported and a novel one identified.

3.4. Role of Cys residues in protein stability and reactivity

Another important aspect of hLAT1 protein was investigated, concerning the role of Cys residues. Indeed, hLAT1 harbours in its primary structure twelve Cys residues, which could have a role both in the stability of the protein structure and in the reactivity to SH xenobiotics reagents such as environmental contaminants and drugs.

Relatively to the role of Cys residues on the stability of the protein, the structural model of hLAT1 (Fig. 30) showed that at least three Cys couples lie at proper distances to form disulphide bridges. Experiments conducted in SiHa intact cells, in proteoliposomes reconstituted with proteins extracted from SiHa cells and in proteoliposomes reconstituted with recombinant protein, confirmed this possibility showing that reducing conditions had a role in intrinsic activation of hLAT1 protein.

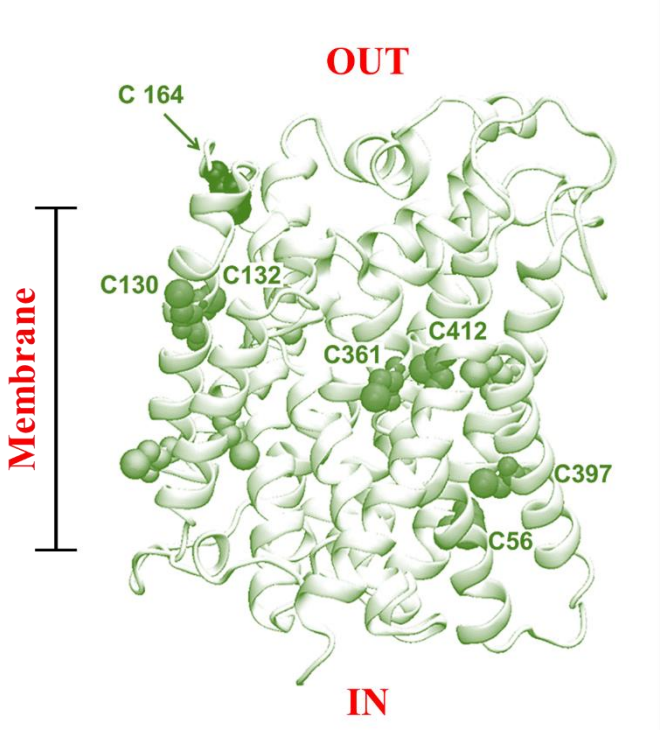

Fig. 30: Homology model of human LAT1. The model is depicted by VMD1.9.1. Cys residues are highlighted. C164 forming the disulfide with 4F2hc is indicated by arrow. Cys residues predicted to form disulphides are numbered and in dark green. Remaining Cys residues are in light green.

Indeed, activation by the S–S reducing agent DTE (and vice versa inhibition by SH oxidation) was observed for hLAT1 obtained from cell extracts (Fig. 31 A) and, more evidently, for the recombinant protein purified in presence of DTE (Fig. 31 B) while, this effect was not observed in intact cells (Fig. 31 C).

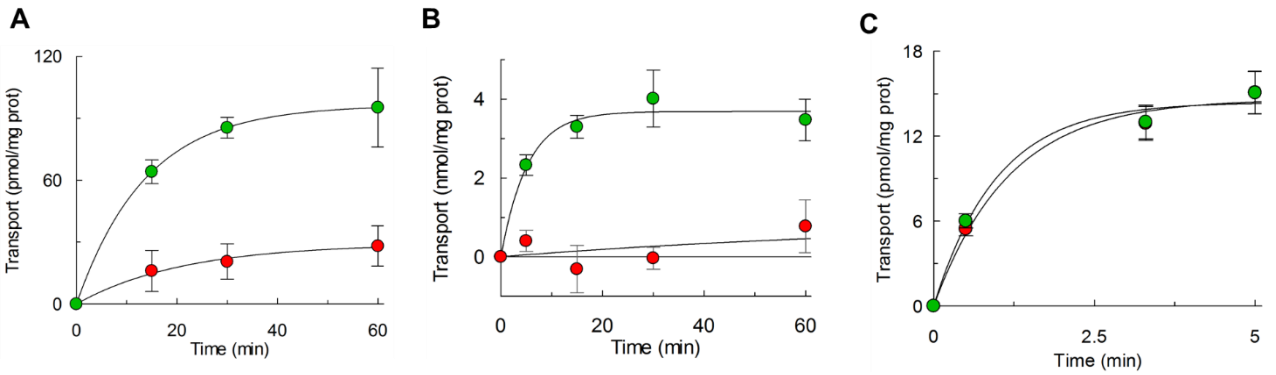

Fig. 31: Time course of [^{3}H]His uptake. (A) Transport in liposomes reconstituted with SiHa cells extract treated (●) or not (●) with 10 mM DTE. (B) Transport in liposomes reconstituted with hLAT1 purified (●) or not (●) with 2 mM DTE. Proteoliposomes contained 10 mM His. (C) Transport in SiHa intact cells with (●) or without (●) 2 mM DTE in transport buffer. Transport reactions were stopped at indicated times as described in section 2.8.1. and data were plotted according to first rate equation. Results are mean ± S.D. from three independent experiments (A-C).

The most likely explanation for this phenomena, relies on a strong influence of the redox state of SH residues of LAT1 on the correct folding and/or transport function. It is plausible that when disulphides were formed between Cys couples showed in Fig. 30, the protein lost mobility, becoming inactive. Indeed, in intact cells, where redox control systems were fully functioning, LAT1 was not sensitive to further addition of reducing agents (DTE). Whereas, during extraction from cells, the same redox control was lost causing the oxidation of a significant fraction of the protein and the consequent inactivation which justified the slow transport activity observed in absence of DTE with respect to presence of DTE. The recombinant protein, being expressed in bacterial cells, was not subjected to proper redox control systems; therefore, it was virtually completely oxidized, i.e., very sensitive to activation by reducing agent added during purification step. The redox control, exerted on hLAT1 protein was also in line with western blot analyses showing that a small fraction of endogenous LAT1 or 4F2hc protein was reduced also under oxidizing conditions, i.e. a protein bands migrating at 35 kDa or at 80 kDa were evident together with the heterodimer at 120 kDa (Fig. 8).

Besides the role exerted by Cys residues on the correct folding and/or transport function of proteins, a lot of literature data support the notion that toxic compounds (such as heavy metal cations) and drugs share a common property, i.e., the reactivity towards thiol groups of Cys residues [1]. Thus, studies were conducted on hLAT1 wild type and Cys mutants to ascertain both the reactivity to SH reagents and the possible involvement of C335 and C407 in this reactivity.

As reported in literature, LAT1 interacts with mercury compounds [72, 73], for this reason, dose response experiments for $HgCl_2$ were conducted on wild type and Cys mutants (Fig. 32).

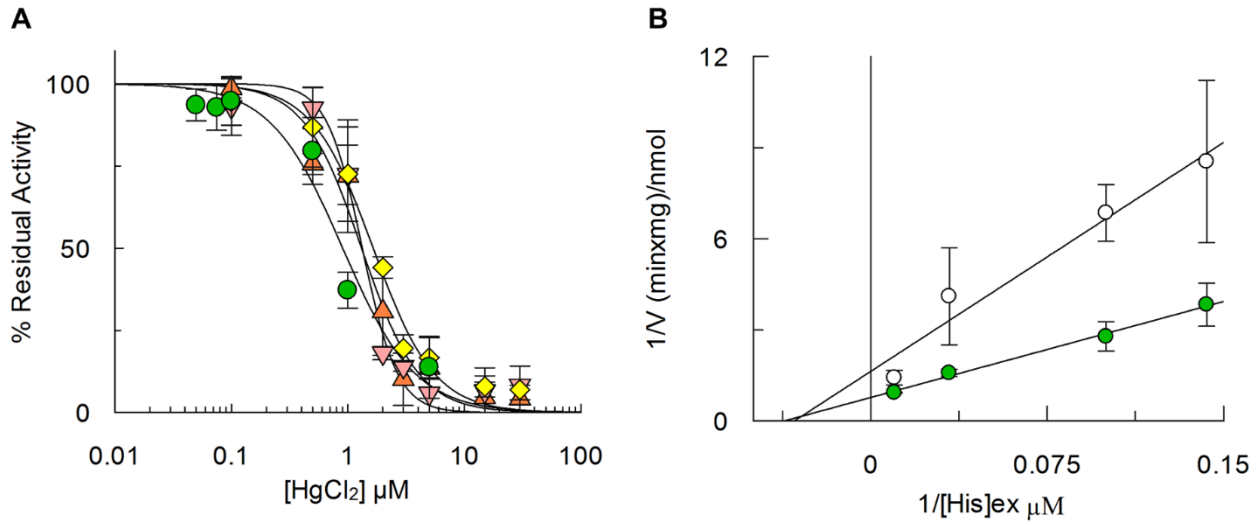

Fig. 32: Inhibition by $HgCl_2$ of the hLAT1 wild type and Cys mutants in proteoliposomes. (A) Dose response curves for the inhibition by $HgCl_2$. Transport was measured adding 5 µM [^{3}H]His to proteoliposomes containing 10 mM His reconstituted with LAT1 WT (●), C335A (▲), C407A (▽) or double mutant C335A/C407A (◆) in the presence of indicated concentrations of $HgCl_2$. Transport was measured in 30 min and stopped as described in section 2.8.1. Percentage of residual activity with respect to the control (without additions) is reported. Results are mean ± S.D. from three independent experiments. (B) Kinetic analysis of the inhibition according to Lineweaver–Burk as reciprocal transport rate vs reciprocal His concentration; transport rate was measured adding 5 µM [^{3}H]His at the indicated concentrations to proteoliposomes containing 10 mM His and stopping the reaction after 15 min as described in section 2.8.1. In (○) 0.8 µM $HgCl_2$ was added as inhibitor in comparison to samples without inhibitor (●). Results are mean ± S.D. from three independent experiments.

As shown in Fig. 32 (A), very similar patterns were observed for all wild type and mutants proteins with comparable IC50 values: 0.90±0.14 µM, 1.3±0.13 µM, 1.3± 0.10 µM or 1.7±0.12 µM for WT, C335A, C407A or C335/407A, respectively.

Moreover, the kinetic of inhibition of His transport by $HgCl_2$ (Fig. 32 B) showed a non-competitive pattern demonstrating that the interaction of the mercury compound occured via residues far from the substrate binding site. Then, other hydrophilic or hydrophobic SH reagents were tested; also in this case, it was observed that Methyl-Hg, Ethyl-Hg, MTSEA and NEM inhibited approximately at the same extent wild type and the Cys mutants (Fig. 33). Thus, the obtained results indicate that the two Cys residues were not involved in interaction with SH reagents either small, large, hydrophobic or hydrophilic, as shown by the unvaried sensitivity of C335A, C407A and C335/407A mutants to all the tested reagents.

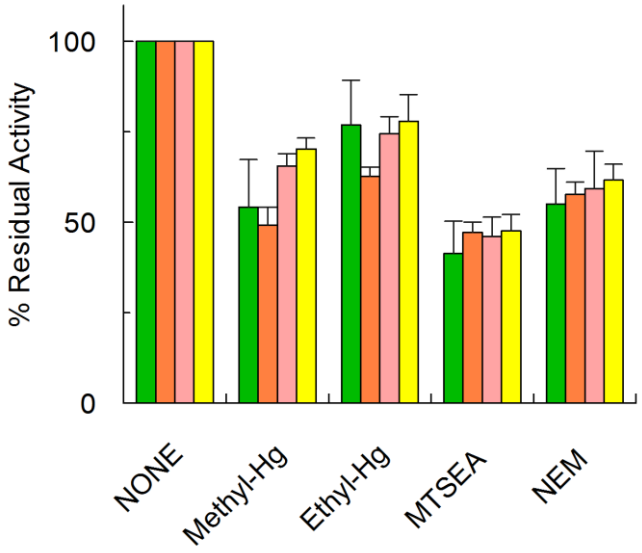

Fig. 33: Effect of Methyl-Hg, Ethyl-Hg, MTSEA and NEM on the LAT1 WT and Cys mutants. Transport was measured adding 5 µM [^{3}H]His to proteoliposomes containing 10 mM His reconstituted with LAT1 WT (green bar), C335A (orange bar), C407A (pink bar) or C335A/C407A (yellow bar) in the presence of 5 µM Methyl-Hg, 12 µM Ethyl-Hg, 50 µM MTSEA or 500 µM NEM. Transport was measured in 30 min and stopped as described in section 2.8.1. Percent residual activity with respect to the control (without additions) is reported. Results are mean ± S.D. from three independent experiments. Student's two tailed unpaired t-test was performed on the sample without external compounds (control) and no differences respect control have been observed within the p value < 0.05.

.

Chapter IV

Conclusions

The relevant role of amino acids transporters in cell physiology and pathology is now well acknowledged. Due to their hydrophobicity, transport protein studies were delayed with respect to soluble proteins. Therefore, few structural data of mammalian transporters are available, so far. Moreover, results obtained from transport assays in intact cells were insufficient for extensive characterization of transport systems. The most recent studies on transporters rely, when possible, on multidisciplinary approaches that guarantee more suitable data on structure/function relationships. Using in silico predictions, over-expression in heterologous system and in vitro methods, such as proteoliposome tool to measure transport activity, it is possible to obtain more complete information for deciphering molecular mechanisms of transport. In this work, such multiple approaches were used for the LAT1 amino acids transporter. Indeed, in spite of the growing number of literature data, most of the structures were predictive. In this work, dark sides of LAT1 were solved combining functional and kinetic data with site-directed mutagenesis and homology structural modelling. Different open questions concerning LAT1 transport function were solved and new information were obtained. The suitability of proteoliposome tool and the use of recombinant purified hLAT1 unravelled that LAT1 is the only transport competent unit of the heterodimer 4F2hc/LAT1. To the same extent using recombinant protein produced in *E. coli*, site-directed mutagenesis and transport assay in proteoliposomes the molecular knowledge on the human LAT1 transporter was improved shedding light in the complex mosaic of the structure/function relationship of LAT1. Thus, since LAT1 is a valuable target for chemotherapy, the scenario emerging from the collected data represents the optimal starting point for studies direct to the design and identification of specific inhibitor useful as potential drugs in cancer therapy.

Different molecules were tested as possible inhibitor of LAT1 protein. These studies are still in progress and will represent another important step forward in advancing the knowledge on this important target. In particular, some dithiazole derivatives showed a reactivity towards Cys residues and appeared to be able to potently inhibit LAT1 transport activity hopefully with affinity higher than that of LAT1 inhibitors previously described [74] or predicted by Virtual High Throughput Screening of drug libraries [70]. The specificity of these molecules and the affinity towards LAT1 are object of incoming studies.

Thus, the proteoliposome tool, which allowed the functional characterization and the advancement in the knowledge of LAT1 kinetics, was also useful to set up a screening tool for chemicals with the aim of identifying new potent and specific inhibitors.

References

[1] M. Scalise, L. Pochini, N. Giangregorio, A. Tonazzi, C. Indiveri, Proteoliposomes as tool for assaying membrane transporter functions and interactions with xenobiotics, Pharmaceutics, 5 (2013) 472-497.

[2] Nelson D.L., Cox M.M., Lehninger Principles of Biochemistry, Fourth Edition

[3] M.H. Saier, Jr., A functional-phylogenetic classification system for transmembrane solute transporters, Microbiol Mol Biol Rev, 64 (2000) 354-411.

[4] M.A. Hediger, Structure, function and evolution of solute transporters in prokaryotes and eukaryotes, J Exp Biol, 196 (1994) 15-49.

[5] S. Broer, Amino acid transport across mammalian intestinal and renal epithelia, Physiol Rev, 88 (2008) 249-286.

[6] H.N. Christensen, Role of amino acid transport and countertransport in nutrition and metabolism, Physiol Rev, 70 (1990) 43-77.

[7] B.P. Bode, Recent molecular advances in mammalian glutamine transport, J Nutr, 131 (2001) 2475S-2485S; discussion 2486S-2477S.

[8] C. Colas, P.M. Ung, A. Schlessinger, SLC Transporters: Structure, Function, and Drug Discovery, Medchemcomm, 7 (2016) 1069-1081.

[9] F. Casagrande, M. Ratera, A.D. Schenk, M. Chami, E. Valencia, J.M. Lopez, D. Torrents, A. Engel, M. Palacin, D. Fotiadis, Projection structure of a member of the amino acid/polyamine/organocation transporter superfamily, J Biol Chem, 283 (2008) 33240-33248.

[10] D.L. Jack, I.T. Paulsen, M.H. Saier, The amino acid/polyamine/organocation (APC) superfamily of transporters specific for amino acids, polyamines and organocations, Microbiology, 146 (Pt 8) (2000) 1797-1814.

[11] F. Verrey, D.L. Jack, I.T. Paulsen, M.H. Saier, Jr., R. Pfeiffer, New glycoprotein-associated amino acid transporters, J Membr Biol, 172 (1999) 181-192.

[12] D. Fotiadis, Y. Kanai, M. Palacin, The SLC3 and SLC7 families of amino acid transporters, Mol Aspects Med, 34 (2013) 139-158.

[13] I.A. Hansen, D.Y. Boudko, S.H. Shiao, D.A. Voronov, E.A. Meleshkevitch, L.L. Drake, S.E. Aguirre, J.M. Fox, G.M. Attardo, A.S. Raikhel, AaCAT1 of the yellow fever mosquito, Aedes aegypti: a novel histidine-specific amino acid transporter from the SLC7 family, J Biol Chem, 286 (2011) 10803-10813.

[14] N. Reig, C. del Rio, F. Casagrande, M. Ratera, J.L. Gelpi, D. Torrents, P.J. Henderson, H. Xie, S.A. Baldwin, A. Zorzano, D. Fotiadis, M. Palacin, Functional and structural characterization of the first prokaryotic member of the L-amino acid transporter (LAT) family: a model for APC transporters, J Biol Chem, 282 (2007) 13270-13281.

[15] Gabrisko M, Janecek S. Looking for the ancestry of the heavy-chain subunits of heteromeric amino acid transporters rBAT and 4F2hc within the GH13 alpha-amylase family. FEBS J. 2009 Dec; 276(24):7265-78.

[16] J. Fort, L.R. de la Ballina, H.E. Burghardt, C. Ferrer-Costa, J. Turnay, C. Ferrer-Orta, I. Uson, A. Zorzano, J. Fernandez-Recio, M. Orozco, M.A. Lizarbe, I. Fita, M. Palacin, The structure of human 4F2hc ectodomain provides a model for homodimerization and electrostatic interaction with plasma membrane, J Biol Chem, 282 (2007) 31444-31452.

[17] M. Palacin, Y. Kanai, The ancillary proteins of HATs: SLC3 family of amino acid transporters, Pflugers Arch, 447 (2004) 490-494.

[18] S. Broer, M. Palacin, The role of amino acid transporters in inherited and acquired diseases, Biochem J, 436 (2011) 193-211.

[19] M. Pineda, E. Fernandez, D. Torrents, R. Estevez, C. Lopez, M. Camps, J. Lloberas, A. Zorzano, M. Palacin, Identification of a membrane protein, LAT-2, that Co-expresses with 4F2 heavy chain, an L-type amino acid transport activity with broad specificity for small and large zwitterionic amino acids, J Biol Chem, 274 (1999) 19738-19744.

[20] F. Verrey, C. Meier, G. Rossier, L.C. Kuhn, Glycoprotein-associated amino acid exchangers: broadening the range of transport specificity, Pflugers Arch, 440 (2000) 503-512.

[21] F. Verrey, E.I. Closs, C.A. Wagner, M. Palacin, H. Endou, Y. Kanai, CATs and HATs: the SLC7 family of amino acid transporters, Pflugers Arch, 447 (2004) 532-542.

[22] N. Reig, J. Chillaron, P. Bartoccioni, E. Fernandez, A. Bendahan, A. Zorzano, B. Kanner, M. Palacin, J. Bertran, The light subunit of system $b^{o,+}$ is fully functional in the absence of the heavy subunit, EMBO J, 21 (2002) 4906-4914.

[23] B.F. Haynes, M.E. Hemler, D.L. Mann, G.S. Eisenbarth, J. Shelhamer, H.S. Mostowski, C.A. Thomas, J.L. Strominger, A.S. Fauci, Characterization of a monoclonal antibody (4F2) that binds to human monocytes and to a subset of activated lymphocytes, J Immunol, 126 (1981) 1409-1414.

[24] E. Quackenbush, M. Clabby, K.M. Gottesdiener, J. Barbosa, N.H. Jones, J.L. Strominger, S. Speck, J.M. Leiden, Molecular cloning of complementary DNAs encoding the heavy chain of the human 4F2 cell-surface antigen: a type II membrane glycoprotein involved in normal and neoplastic cell growth, Proc Natl Acad Sci U S A, 84 (1987) 6526-6530.

[25] M. Galluccio, P. Pingitore, M. Scalise, C. Indiveri, Cloning, large scale over-expression in E. coli and purification of the components of the human LAT 1 (SLC7A5) amino acid transporter, Protein J, 32 (2013) 442-448.

[26] L. Mastroberardino, B. Spindler, R. Pfeiffer, P.J. Skelly, J. Loffing, C.B. Shoemaker, F. Verrey, Amino-acid transport by heterodimers of 4F2hc/CD98 and members of a permease family, Nature, 395 (1998) 288-291.

[27] Y. Kanai, H. Segawa, K. Miyamoto, H. Uchino, E. Takeda, H. Endou, Expression cloning and characterization of a transporter for large neutral amino acids activated by the heavy chain of 4F2 antigen (CD98), J Biol Chem, 273 (1998) 23629-23632.

[28] O. Yanagida, Y. Kanai, A. Chairoungdua, D.K. Kim, H. Segawa, T. Nii, S.H. Cha, H. Matsuo, J. Fukushima, Y. Fukasawa, Y. Tani, Y. Taketani, H. Uchino, J.Y. Kim, J. Inatomi, I. Okayasu, K. Miyamoto,

E. Takeda, T. Goya, H. Endou, Human L-type amino acid transporter 1 (LAT1): characterization of function and expression in tumor cell lines, Biochim Biophys Acta, 1514 (2001) 291-302.

[29] E.M. del Amo, A. Urtti, M. Yliperttula, Pharmacokinetic role of L-type amino acid transporters LAT1 and LAT2, Eur J Pharm Sci, 35 (2008) 161-174.

[30] T. Kageyama, M. Nakamura, A. Matsuo, Y. Yamasaki, Y. Takakura, M. Hashida, Y. Kanai, M. Naito, T. Tsuruo, N. Minato, S. Shimohama, The 4F2hc/LAT1 complex transports L-DOPA across the blood-brain barrier, Brain Res, 879 (2000) 115-121.

[31] D.K. Kim, Y. Kanai, H.W. Choi, S. Tangtrongsup, A. Chairoungdua, E. Babu, K. Tachampa, N. Anzai, Y. Iribe, H. Endou, Characterization of the system L amino acid transporter in T24 human bladder carcinoma cells, Biochim Biophys Acta, 1565 (2002) 112-121.

[32] S. Broer, C.A. Wagner, Structure-function relationships of heterodimeric amino acid transporters, Cell Biochem Biophys, 36 (2002) 155-168.

[33] M. Tomi, M. Mori, M. Tachikawa, K. Katayama, T. Terasaki, K. Hosoya, L-type amino acid transporter 1-mediated L-leucine transport at the inner blood-retinal barrier, Invest Ophthalmol Vis Sci, 46 (2005) 2522-2530.

[34] R. Milkereit, A. Persaud, L. Vanoaica, A. Guetg, F. Verrey, D. Rotin, LAPTM4b recruits the LAT1-4F2hc Leu transporter to lysosomes and promotes mTORC1 activation, Nat Commun, 6 (2015) 7250.

[35] V. Ganapathy, M. Thangaraju, P.D. Prasad, Nutrient transporters in cancer: relevance to Warburg hypothesis and beyond, Pharmacol Ther, 121 (2009) 29-40.

[36] Y.D. Bhutia, E. Babu, S. Ramachandran, V. Ganapathy, Amino Acid transporters in cancer and their relevance to "glutamine addiction": novel targets for the design of a new class of anticancer drugs, Cancer Res, 75 (2015) 1782-1788.

[37] P.M. Taylor, Amino acid transporters: eminences grises of nutrient signalling mechanisms?, Biochem Soc Trans, 37 (2009) 237-241.

[38] M. Laplante, D.M. Sabatini, mTOR signaling in growth control and disease, Cell, 149 (2012) 274-293.

[39] M. Laplante, D.M. Sabatini, Regulation of mTORC1 and its impact on gene expression at a glance, J Cell Sci, 126 (2013) 1713-1719.

[40] Y. Cormerais, S. Giuliano, R. LeFloch, B. Front, J. Durivault, E. Tambutte, P.A. Massard, L.R. de la Ballina, H. Endou, M.F. Wempe, M. Palacin, S.K. Parks, J. Pouyssegur, Genetic Disruption of the Multifunctional CD98/LAT1 Complex Demonstrates the Key Role of Essential Amino Acid Transport in the Control of mTORC1 and Tumor Growth, Cancer Res, 76 (2016) 4481-4492.

[41] M. Rebsamen, L. Pochini, T. Stasyk, M.E. de Araujo, M. Galluccio, R.K. Kandasamy, B. Snijder, A. Fauster, E.L. Rudashevskaya, M. Bruckner, S. Scorzoni, P.A. Filipek, K.V. Huber, J.W. Bigenzahn, L.X. Heinz, C. Kraft, K.L. Bennett, C. Indiveri, L.A. Huber, G. Superti-Furga, SLC38A9 is a component of the lysosomal amino acid sensing machinery that controls mTORC1, Nature, 519 (2015) 477-481.

[42] D.C. Tarlungeanu, E. Deliu, C.P. Dotter, M. Kara, P.C. Janiesch, M. Scalise, M. Galluccio, M. Tesulov, E. Morelli, F.M. Sonmez, K. Bilguvar, R. Ohgaki, Y. Kanai, A. Johansen, S. Esharif, T. Ben-Omran, M. Topcu, A. Schlessinger, C. Indiveri, K.E. Duncan, A.O. Caglayan, M. Gunel, J.G. Gleeson, G. Novarino, Impaired Amino Acid Transport at the Blood Brain Barrier Is a Cause of Autism Spectrum Disorder, Cell, 167 (2016) 1481-1494 e1418.

[43] R. Pfeiffer, B. Spindler, J. Loffing, P.J. Skelly, C.B. Shoemaker, F. Verrey, Functional heterodimeric amino acid transporters lacking cysteine residues involved in disulfide bond, FEBS Lett, 439 (1998) 157-162.

[44] J. Chillaron, R. Roca, A. Valencia, A. Zorzano, M. Palacin, Heteromeric amino acid transporters: biochemistry, genetics, and physiology, Am J Physiol Renal Physiol, 281 (2001) F995-1018.

[45] A. Broer, B. Friedrich, C.A. Wagner, S. Fillon, V. Ganapathy, F. Lang, S. Broer, Association of 4F2hc with light chains LAT1, LAT2 or y^+LAT2 requires different domains, Biochem J, 355 (2001) 725-731.

[46] C.A. Fenczik, R. Zent, M. Dellos, D.A. Calderwood, J. Satriano, C. Kelly, M.H. Ginsberg, Distinct domains of CD98hc regulate integrins and amino acid transport, J Biol Chem, 276 (2001) 8746-8752.

[47] R. Franca, E. Veljkovic, S. Walter, C.A. Wagner, F. Verrey, Heterodimeric amino acid transporter glycoprotein domains determining functional subunit association, Biochem J, 388 (2005) 435-443.

[48] P.D. Prasad, H. Wang, W. Huang, R. Kekuda, D.P. Rajan, F.H. Leibach, V. Ganapathy, Human LAT1, a subunit of system L amino acid transporter: molecular cloning and transport function, Biochem Biophys Res Commun, 255 (1999) 283-288.

[49] E. Nakamura, M. Sato, H. Yang, F. Miyagawa, M. Harasaki, K. Tomita, S. Matsuoka, A. Noma, K. Iwai, N. Minato, 4F2 (CD98) heavy chain is associated covalently with an amino acid transporter and controls intracellular trafficking and membrane topology of 4F2 heterodimer, J Biol Chem, 274 (1999) 3009-3016.

[50] C.A. Wagner, F. Lang, S. Broer, Function and structure of heterodimeric amino acid transporters, Am J Physiol Cell Physiol, 281 (2001) C1077-1093.

[51] W.A. Campbell, N.L. Thompson, Overexpression of LAT1/CD98 light chain is sufficient to increase system L-amino acid transport activity in mouse hepatocytes but not fibroblasts, J Biol Chem, 276 (2001) 16877-16884.

[52] X. Fan, D.D. Ross, H. Arakawa, V. Ganapathy, I. Tamai, T. Nakanishi, Impact of system L amino acid transporter 1 (LAT1) on proliferation of human ovarian cancer cells: a possible target for combination therapy with anti-proliferative aminopeptidase inhibitors, Biochem Pharmacol, 80 (2010) 811-818.

[53] D.B. Shennan, J. Thomson, Inhibition of system L (LAT1/CD98hc) reduces the growth of cultured human breast cancer cells, Oncol Rep, 20 (2008) 885-889.

[54] S. Baniasadi, A. Chairoungdua, Y. Iribe, Y. Kanai, H. Endou, K. Aisaki, K. Igarashi, J. Kanno, Gene expression profiles in T24 human bladder carcinoma cells by inhibiting an L-type amino acid transporter, LAT1, Arch Pharm Res, 30 (2007) 444-452.

[55] M. Palacin, E. Errasti-Murugarren, A. Rosell, Heteromeric amino acid transporters. In search of the molecular bases of transport cycle mechanisms, Biochem Soc Trans, 44 (2016) 745-752.

[56] X. Gao, F. Lu, L. Zhou, S. Dang, L. Sun, X. Li, J. Wang, Y. Shi, Structure and mechanism of an amino acid antiporter, Science, 324 (2009) 1565-1568.

[57] Y. Fang, H. Jayaram, T. Shane, L. Kolmakova-Partensky, F. Wu, C. Williams, Y. Xiong, C. Miller, Structure of a prokaryotic virtual proton pump at 3.2 A resolution, Nature, 460 (2009) 1040-1043.

[58] P.L. Shaffer, A. Goehring, A. Shankaranarayanan, E. Gouaux, Structure and mechanism of a Na^+-independent amino acid transporter, Science, 325 (2009) 1010-1014.

[59] X. Gao, L. Zhou, X. Jiao, F. Lu, C. Yan, X. Zeng, J. Wang, Y. Shi, Mechanism of substrate recognition and transport by an amino acid antiporter, Nature, 463 (2010) 828-832.

[60] L. Kowalczyk, M. Ratera, A. Paladino, P. Bartoccioni, E. Errasti-Murugarren, E. Valencia, G. Portella, S. Bial, A. Zorzano, I. Fita, M. Orozco, X. Carpena, J.L. Vazquez-Ibar, M. Palacin, Molecular basis of substrate-induced permeation by an amino acid antiporter, Proc Natl Acad Sci U S A, 108 (2011) 3935-3940.

[61] G. Gregoriadis, The carrier potential of liposomes in biology and medicine (first of two parts), N Engl J Med, 295 (1976) 704-710.

[62] G. Gregoriadis, The carrier potential of liposomes in biology and medicine (second of two parts), N Engl J Med, 295 (1976) 765-770.

[63] S.V. Boddapati, G.G. D'Souza, V. Weissig, Liposomes for drug delivery to mitochondria, Methods Mol Biol, 605 (2010) 295-303.

[64] M. Kasahara, P.C. Hinkle, Reconstitution of D-glucose transport catalyzed by a protein fraction from human erythrocytes in sonicated liposomes, Proc Natl Acad Sci U S A, 73 (1976) 396-400.

[65] M.J. Newman, D.L. Foster, T.H. Wilson, H.R. Kaback, Purification and reconstitution of functional lactose carrier from Escherichia coli, J Biol Chem, 256 (1981) 11804-11808.

[66] F. Palmieri, C. Indiveri, F. Bisaccia, V. Iacobazzi, Mitochondrial metabolite carrier proteins: purification, reconstitution, and transport studies, Methods Enzymol. 260 (1995) 349–369.

[67] Pochini, L., Scalise, M., Galluccio, M., Indiveri, C., Regulation by physiological cations of acetylcholine transport mediated by human OCTN1 (SLC22A4). Implications in the non-neuronal cholinergic system, Life Sci. 91 (2012) 1013–1016.

[68] D. Drew, O. Boudker, Shared molecular mechanisms of membrane transporters, Annu. Rev. Biochem. 85 (2016) 543–572.

[69] H. Ilgu, J.M. Jeckelmann, V. Gapsys, Z. Ucurum, B.L. de Groot, D. Fotiadis, Insights into the molecular basis for substrate binding and specificity of the wild-type Larginine/agmatine antiporter AdiC, Proc. Natl. Acad. Sci. U. S. A. 113 (2016) 10358–10363.

[70] E.G. Geier, A. Schlessinger, H. Fan, J.E. Gable, J.J. Irwin, A. Sali, K.M. Giacomini, Structure-based ligand discovery for the large-neutral amino acid transporter 1, LAT-1, Proc. Natl. Acad. Sci. U. S. A. 110 (2013) 5480–5485.

[71] J. Kyte, R.F. Doolittle, A simple method for displaying the hydropathic character of a protein, J. Mol. Biol. 157 (1982) 105–132.

[72] R.J. Boado, J.Y. Li, C. Chu, F. Ogoshi, P.Wise, W.M. Pardridge, Site-directed mutagenesis of cysteine residues of large neutral amino acid transporter LAT1, Biochim. Biophys. Acta 1715 (2005) 104–110.

[73] Z. Yin, H. Jiang, T. Syversen, J.B. Rocha, M. Farina, M. Aschner, The methylmercury-L-cysteine conjugate is a substrate for the L-type large neutral amino acid transporter, J. Neurochem. 107 (2008) 1083–1090.

[74] E. Augustyn, K. Finke, A.A. Zur, L. Hansen, N. Heeren, H.C. Chien, L. Lin, K.M. Giacomini, C. Colas, A. Schlessinger, A.A. Thomas, LAT-1 activity of meta-substituted phenylalanine and tyrosine analogs, Bioorg Med Chem Lett, 26 (2016) 2616-2621.

Publications

The International Journal of Biochemistry & Cell Biology 67 (2015) 25–33

Contents lists available at ScienceDirect

The International Journal of Biochemistry & Cell Biology

journal homepage: www.elsevier.com/locate/biocel

LAT1 is the transport competent unit of the LAT1/CD98 heterodimeric amino acid transporter

Lara Napolitano [1], Mariafrancesca Scalise [1], Michele Galluccio, Lorena Pochini, Leticia Maria Albanese, Cesare Indiveri *

Department DiBEST (Biologia, Ecologia, Scienze della Terra) Unit of Biochemistry and Molecular Biotechnology, University of Calabria, Via Bucci 4C, 87036 Arcavacata di Rende, Italy

ARTICLE INFO

Article history:
Received 20 March 2015
Received in revised form 10 June 2015
Accepted 4 August 2015
Available online 6 August 2015

Keywords:
LAT1
CD98
Transport
Histidine
Heterodimer
Proteoliposomes

ABSTRACT

LAT1 (SLC7A5) and CD98 (SLC3A2) constitute a heterodimeric transmembrane protein complex that catalyzes amino acid transport. Whether one or both subunits are competent for transport is still unclear. The present work aims to solve this question using different experimental strategies. Firstly, LAT1 and CD98 were immuno-detected in protein extracts from SiHa cells. Under oxidizing conditions, i.e., without addition of SH (thiol) reducing agent DTE, both proteins were revealed as a 120 kDa major band. Upon DTE treatment separated bands, corresponding to LAT1(35 kDa) or CD98(80 kDa), were detected. LAT1 function was evaluated in intact cells as BCH sensitive [^{3}H]His transport inhibited by hydrophobic amino acids. Antiport of [^{3}H]His was measured in proteoliposomes reconstituted with SiHa cell extract in presence of internal His. Transport was increased by DTE. Hydrophobic amino acids were best inhibitors in addition to hydrophilic Tyr, Gln, Asn and Lys. Cys, Tyr and Gln, included in the intraliposomal space, were transported in antiport with external [^{3}H]His. Similar experiments were performed in proteoliposomes reconstituted with the recombinant purified hLAT1. Results overlapping those obtained with native protein were achieved. Lower transport of [^{3}H]Leu and [^{3}H]Gln with respect to [^{3}H]His was detected. Kinetic asymmetry was found with external Km for His lower than internal one. No transport was detected in proteoliposomes reconstituted with recombinant hCD98. The experimental data demonstrate that LAT1 is the sole transport competent subunit of the heterodimer. This conclusion has important outcome for following studies on functional characterization and identification of specific inhibitors with potential application in human therapy.

1. Introduction

SLC7A5 is a neutral amino acid transporter also known as LAT1 (Christensen, 1990; Pochini et al., 2014). It belongs to the SLC7 family, accounting for 13 members divided in cationic amino acid transporters (CATs) and light subunits of amino acid transporters (LATs). The peculiar property of the latter group of proteins consists in forming covalent heterodimer with larger polypeptides belonging to the SLC3 family, a small group of type II membrane glycoproteins (Palacin and Kanai, 2004; Verrey et al., 2004). In particular, SLC7A5 interacts with SLC3A2, known as CD98 or 4F2hc, via a conserved disulfide between residues C164 of hLAT1 and C109 of hCD98, forming a heterodimer (Fort et al., 2007; Wagner et al., 2001).

LAT1 is a polypeptide of 507 amino acids, corresponding to a molecular mass of 55 kDa, with 12α-helical transmembrane segments (Prasad et al., 1999); it is broadly expressed and mainly localized in basolateral membranes of polarized epithelia (Bode, 2001; Broer, 2002; Yanagida et al., 2001). Important exceptions are the luminal and abluminal membranes of BBB (blood–brain barrier) and the brush border membranes of placenta, i.e. maternal side (del Amo et al., 2008). CD98 is a 630 amino acid polypeptide with an apparent molecular mass of 68 kDa on SDS-PAGE (Galluccio et al., 2013). The role of LAT1/CD98 heterodimer in mediating amino acid transport across the plasma membrane has been assessed in cell systems, so far. However, the precise role of CD98 in the intrinsic transport function of LAT1 is still controversial

Abbreviations: CATs, cationic amino acid transporters; LATs, light subunits of amino acid transporters; CD98, cluster of differentiation 98; BBB, blood brain barrier; BCH, 2-amino-2-norbornanecarboxylic acid; $C_{12}E_8$, octaethylene glycol monododecyl ether; DTE, dithioerythritol; TX-100, Triton X-100.

* Corresponding author.
E-mail address: cesare.indiveri@unical.it (C. Indiveri).
[1] These authors contributed equally to this work.

http://dx.doi.org/10.1016/j.biocel.2015.08.004
1357-2725/

(Kanai et al., 1998; Palacin and Kanai, 2004). On the one hand, CD98 has been considered crucial for LAT1 transport activity (Kanai et al., 1998; Prasad et al., 1999). On the other hand, some authors claimed that involvement of CD98 in transport is linked to maturation and trafficking of LAT1 protein in plasma membrane (Franca et al., 2005; Mastroberardino et al., 1998; Nakamura et al., 1999; Wagner et al., 2001). Moreover, in mouse hepatocarcinoma cells, over-expressed LAT1 has been showed to mediate leucine transport without involvement of CD98 (Campbell and Thompson, 2001). Thus, the contribute of CD98 to transport function represents still an open issue. LAT1/CD98 heterodimer mediates a sodium independent amino acid antiport with preference for large amino acids such as Trp, Phe, Tyr and His even though smaller amino acids such as Met, Val, Leu, Ile are also transported (Kanai et al., 1998; Yanagida et al., 2001). Moreover, LAT1/CD98 has been suggested also as a transporter of non amino acid substrates, such as L-dopamine, gabapentin and thyroid hormones (del Amo et al., 2008; Kageyama et al., 2000). It is specifically inhibited by BCH that has been used to discriminate its activity from that of other amino acid transporters in cells (Kim et al., 2002). The three dimensional structure of CD98 has been recently solved (Fort et al., 2007), while crystals of LAT1 are not available, as for all the mammalian amino acid transporters. Some homology structural models have been built on the basis of the arginine/agmatine transporter, AdiC, from *Escherichia coli* and the ApcT from *Methanococcus jannaschii*, whose structures have been solved by X-ray crystallography (Gao et al., 2010). The interest in shedding light on the functional and regulatory properties of LAT1 is strengthened by its well documented over-expression in many tumors, together with the glutamine transporter ASCT2 (SLC1A5). Indeed, tumor survival is characterized by increased absorption of amino acids, used both as oxidative fuel and signaling molecules (Fuchs and Bode, 2005; Ganapathy et al., 2009; Wang et al., 2013). Therefore, LAT1 represents an important novel target for chemotherapy since inhibitors of this transporter are potential anticancer drugs (Baniasadi et al., 2007; Fan et al., 2010; Shennan and Thomson, 2008). Recently, an elegant approach of Virtual High Throughput Screening of drug libraries has been described (Geier et al., 2013). To unravel dark sides of this transporter on both functional and structural point of views, heterologous over-expression of the human proteins LAT1 and CD98 have been performed. Abundant expression was obtained by cloning hLAT1 and hCD98 in the plasmids pH6EX3 (Brizio et al., 2000) and pGEX4T1 (Galluccio et al., 2013). In the present work, hLAT1 mediated transport has been investigated in intact cells as well as in proteoliposomes reconstituted with protein extracted from SiHa cells or recombinant hLAT1 protein. Using these combined strategies, it was shown that hLAT1 is the only competent transport unit of the heterodimer.

2. Materials and methods

2.1. Materials

His Trap HP columns, thrombin, PD-10 columns, ECL plus and Hybond ECL membranes were purchased from GE Healthcare; SiHa cell line was kindly provided by Dr. Massimo Tommasino (IARC/CIRC WHO, Lyon France); culture media and Fetal Bovine Serum were purchased from Life Technologies; radiolabeled amino acids were purchased from ARC (American Radiolabeled Chemicals); anti-hLAT1, anti-hCD98 and anti-rabbit IgG HRP conjugate from Cell Signaling; all the other reagents are from Sigma–Aldrich.

2.2. Cell culture

SiHa cells were maintained in Dulbecco's Modified Eagle Medium (DMEM) supplemented with 10% (v/v) fetal bovine serum (FBS), 1 mM glutamine, 1 mM sodium pyruvate and Pen/strep as antibiotics. Cells were grown on 10 cm^2 plates at 37 °C in a humidified incubator and a 5% CO_2 atmosphere.

2.3. Extraction of LAT1/CD98 complex from SiHa cells

LAT1/CD98 complex was solubilized, from SiHa pellets, with RIPA buffer and incubated for 30 min on ice. After centrifugation (12,000 × *g*, 15 min, 4 °C) proteins were quantified using Lowry method, analyzed on SDS-PAGE 10% and transferred onto nitrocellulose membranes for western blot.

2.4. Western blot analysis

hCD98 and hLAT1 were immuno-detected incubating membranes with anti-LAT1 antibody 1:2000 or anti-CD98 1:1000 over night at 4 °C. The reaction was detected by Electro Chemi Luminescence (ECL) assay after 1 h incubation with secondary antibody anti-rabbit 1:5000.

2.5. Transport measurement in cells

SiHa cells were seeded onto 12 well plates up to 80% confluence. For transport assay, cells were rinsed twice with transport buffer: 20 mM Tris–HCl pH 7.4, 200 mM glucose and 2 mM DTE where indicated. Radiolabeled 5 μM [^{3}H]His was added and the transport reaction terminated at the indicated times by discarding the uptake buffer and rinsing the cells with the same ice-cold buffer (0.5 ml) plus 1 mM BCH. Cells from each well were solubilized in 500 μl of 1% TX-100. Cell extracts were counted for radioactivity.

2.6. Purification of hCD98 and hLAT1

hCD98 was over-expressed with a GST tag in *E. coli* and purified as previously described (Galluccio et al., 2013). hLAT1 was over-expressed in *E. coli* and purified as previously described (Galluccio et al., 2013) with the following modifications: after cell lysate solubilization and centrifugation (12,000 × g, 10 min, 4 °C) the supernatant was applied on a His Trap HP column (5 ml Ni Sepharose) equilibrated with 10 mL buffer (20 mM Tris–HCl pH 8.0, 10% glycerol, 200 mM NaCl, 0.1% sarkosyl, and DTE 2 mM) using ÄKTA start. Column was washed with 10 mL of buffer (20 mM Tris–HCl pH 8, 10% glycerol, 200 mM NaCl, 0.1% n-dodecyl β-D-maltoside and 2 mM DTE). Protein was eluted with the same buffer plus 400 mM imidazole; 2.5 mL were pooled and desalted on a PD-10 column.

2.7. Reconstitution of the hCD98–hLAT1 complex extracted from SiHa cells into liposomes

The hCD98/hLAT1 complex was extracted from SiHa cells membrane with RIPA buffer and reconstituted in liposomes by removing the detergent using the batch-wise method. Mixed micelles containing detergent, protein and phospholipids were incubated with 0.5 g Amberlite XAD-4 at room temperature for 40 min (Scalise et al., 2012). The initial mixture contained: 150 μg of cell extract, 100 μL of 10% $C_{12}E_8$, 100 μL of 10% egg yolk phospholipids (w/v) in the form of liposomes prepared as previously described (Indiveri et al., 1994), 20 mM Tris–HCl pH 7.5 and 10 mM L-His, except were differently indicated, in a final volume of 700 μL. Cell extracts were treated or not with 10 mM DTE.

2.8. Reconstitution of the purified hLAT1 or hCD98 into liposomes

The purified hLAT1 or hCD98 were reconstituted as above described using 4 μg protein for both the over-expressed proteins.

2.9. Transport measurements

For uptake experiments, to remove the external substrate, 600 μL of proteoliposomes were passed through a Sephadex G-75 column (0.7 cm diameter × 15 cm height) pre-equilibrated with 20 mM Tris–HCl pH 7.5 and sucrose at an appropriate concentration to balance internal osmolarity; transport was started by 5 μM [^{3}H]His. For efflux measurements, proteoliposomes containing 10 mM His were preloaded by incubation with 5 μM [^{3}H]His (1 μCi/ml) for 60 min (Pochini et al., 2012). External compounds were removed by another passage through Sephadex G-75. Efflux was started by adding 5 mM amino acids to the preloaded proteoliposomes. In both uptake and efflux, transport was stopped by 100 μM BCH. In controls, inhibitor was added at time zero according to the inhibitor stop method (Palmieri et al., 1995). At the end of the transport assay, 100 μL proteoliposomes was passed through a Sephadex G-75 column (0.6 cm diameter × 8 cm height) to separate the external from the internal radioactivity. Liposomes were eluted with 1 mL 50 mM NaCl in 4 mL scintillation mixture and counted. For [^{3}H]His uptake, experimental values were corrected by subtracting controls. For [^{3}H]His efflux experimental values at 10 min were subtracted from the radioactivity present in the proteoliposomes at time zero. Initial transport rate was measured by stopping the reaction after 10 min, i.e., within the initial linear range of [^{3}H]His uptake or efflux in proteoliposomes. To calculate kinetic parameters or IC_{50}, experimental data were fitted in Michaelis–Menten or dose–response equation, using Grafit software. To measure the hLAT1 specific activity, protein concentration was estimated by Chemidoc imaging system (Giancaspero et al., 2013).

2.10. Ultracentrifugation of proteoliposomes

To separate hCD98 and/or hLAT1 reconstituted proteoliposomes from liposomes without incorporated proteins, 500 μl of samples after passage through Sephadex G-75 column, were ultracentrifuged (110,000 × *g*, 1 h 30 min, 4 °C). After washing with saline buffer, samples were ultracentrifuged again and pellet solubilized with 3% SDS and subjected to western blot analysis.

2.11. Homology modeling of hLAT1

The homology structural model of the hLAT1 was built using as template the structure of the arginine/agmatine antiporter AdiC from *E. coli* (PDB 3L1L). The amino acid sequence of the human LAT1 (NP_003477.4) and the AdiC (P60063) were aligned using ClustalW and manually adjusted. The optimized alignment was used to run the program Modeller 9.14.

3. Results

3.1. LAT1 and CD98 are linked by disulfide in native membrane

LAT1/CD98 heterodimer was immuno-detected in SiHa cell extracts using both anti-LAT1 and anti-CD98 antibodies. Under oxidizing conditions, i.e., in absence of DTE during gel run, both antibodies identified a protein band of 120 kDa, resulting from the sum of the molecular mass of LAT1 plus CD98 (Fig. 1A and B, lines −DTE). When the gel was run under reducing condition, i.e. in the presence of the S–S reducing agent DTE, the apparent molecular mass of the proteins diminished to approximately 35 kDa

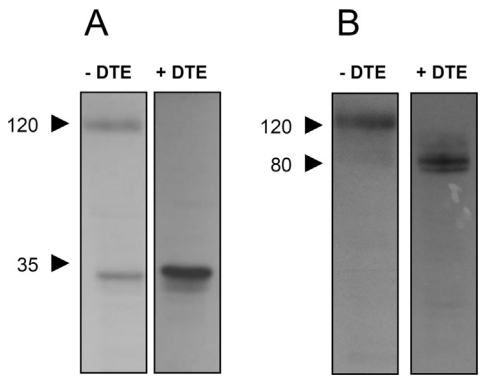

Fig. 1. Western blot analysis of hCD98–hLAT1 complex from SiHa cells membrane. Cell membranes were solubilized with buffer without (−DTE) or with DTE (+DTE) and analyzed by WB using anti-hLAT1 (A) or anti-hCD98 (B). The image is representative of at least two independent experiments.

when detected with anti-LAT1 antibody (Fig. 1A, line +DTE) or to about 80 kDa when detected with anti-CD98 antibody (Fig. 1B, line +DTE). These were approximately the molecular masses of the single polypeptides LAT1 or CD98, respectively. It has to be stressed that the apparent molecular mass of LAT1 is lower than the theoretical one, due to the hydrophobicity of this polypeptide (Galluccio et al., 2013). Smaller amount of the unlinked LAT1 or CD98 was also detected under non-reducing condition (Fig. 1, lines −DTE). These results indicate that most of LAT1 and CD98 proteins are cross-linked in the cell membrane.

3.2. Transport assay of native LAT1(CD98) in intact SiHa cells

Intact SiHa cells were assayed for transport activity of LAT1 under oxidizing or reducing condition, i.e., in absence or presence of DTE in the transport buffer. Among LAT1 substrates, [^{3}H]His was chosen. As shown by Fig. 2A, time dependent uptake of [^{3}H]His was detected in intact SiHa cells reaching the equilibrium after 5 min with an initial transport rate of 12.2 ± 3.5 pmol min^{-1} mg protein^{-1} and 14.5 ± 3.8 pmol min^{-1} mg protein^{-1} in presence or absence of DTE in transport buffer. Thus, no differences were observed in cells with LAT1/CD98 heterodimer (absence of DTE) or with LAT1 separated from CD98 (presence of DTE). The same samples were subjected to SDS-PAGE under oxidizing conditions, i.e. absence of reducing agent, to not alter the holigomerization state of the proteins after extraction from intact cells. LAT1 and CD98 were immuno-detected as a band of 120 kDa (Fig. 2B and C, lines −DTE) in Western blot analysis. When transport buffer contained DTE, LAT1 and CD98 migrated at 35 and 80 kDa, respectively (Fig. 2B and C, lines +DTE), confirming that DTE caused reduction of S–S disulfide in cell membranes. The specificity of transport was evaluated by adding amino acids together with [^{3}H]His (Fig. 2D). Overlapping results were obtained under oxidizing and reducing conditions. Branched chain Ile, Leu and other hydrophobic amino acids, Phe and Cys inhibited [^{3}H]His uptake, while Ala and Gln had much lower inhibitory effect. Specificity of LAT1 activity was demonstrated by the abrogation of transport activity observed in the presence of BCH, which is a specific inhibitor commonly used in cells (see Section 1). These results suggested that LAT1 transport function and specificity are not influenced by covalent interaction with CD98.

3.3. Transport function of native LAT1(CD98) in proteoliposomes

To gain further insight on this issue, the proteoliposome experimental model was adopted given its suitability in finely

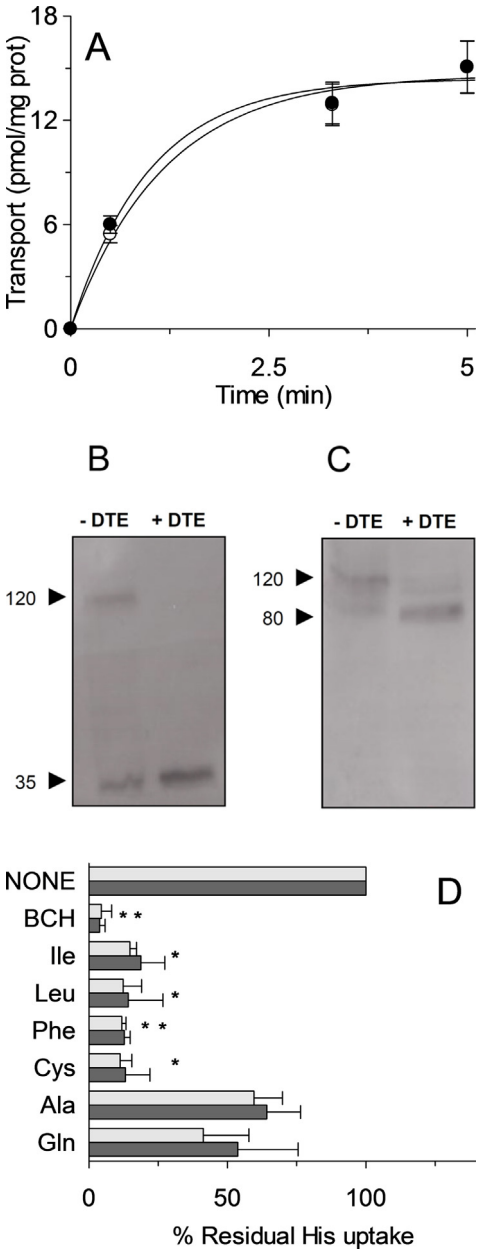

Fig. 2. [^{3}H]His uptake in SiHa cells and western blot analysis. (A) Cells were cultured and used for transport measurement as described in Section 2.5. Results are mean ± S.D. of three experiments. (B, C) WB analysis of hCD98–hLAT1 in SiHa treated or not with 2 mM DTE. Samples for WB were solubilized with buffer without DTE, hLAT1 (B) or hCD98 (C) antibody were used. The image is representative of at least two independent experiments. (D) Cells were used for transport adding 5 μM [^{3}H]His and the indicated 1 mM substrates. Percentage of residual His uptake was calculated with respect to controls (sample without added external substrate). Results are mean ± S.D. from three experiments. Significantly different from controls as estimated by 1Way ANOVA test (*$P < 0.05$; **$P < 0.01$).

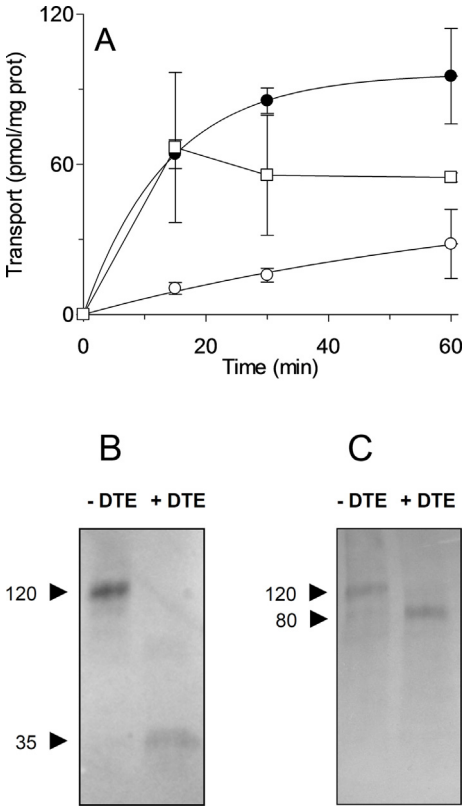

Fig. 3. Reconstitution of SiHa extract in proteoliposomes. (A) Time course of [^{3}H]His uptake. Reconstitution was performed in the absence (○) or presence (●, □) of 10 mM DTE. In (□),50 mM Na-gluconate was added during transport, performed as described in Section 2.9. Results are mean ± S.D. of three experiments. (B, C) WB of CD98/LAT1 in proteoliposomes. CD98/LAT1 was solubilized from cells and reconstituted in absence (−DTE) or presence of 10 mM DTE. Proteoliposomes were separated as described in Section 2.10. After SDS-PAGE under non-reducing conditions WB was performed by anti-hLAT1 (B) or anti-hCD98 (C). The image is representative of at least two independent experiments.

controlling experimental conditions in both internal and external compartments (Rebsamen et al., 2015; Scalise et al., 2013). Cell extracts were subjected to oxidizing or reducing treatment, i.e. in the absence or presence of DTE, and then reconstituted in liposomes for transport assay (Fig. 3A). The reducing treatment, which cleaved LAT1/CD98 disulfide (see Fig. 1), led to strong activation of [^{3}H]His transport. The time course showed that the equilibrium was reached after 30 min with an initial transport rate of 0.68 ± 0.03 pmol min^{-1} mg protein^{-1} or 7.02 ± 2.86 pmol min^{-1} mg protein^{-1} under oxidizing or reducing conditions, respectively. Nearly no transport was detected in proteoliposomes with no internal substrate (not shown but next figs). No significant effect by external Na^+ was observed (Fig. 3A). The delayed equilibration with respect to cells was due to the presence of single transporter molecules per each liposome vesicle differently from cells in which many transporter molecules per cell are present (Scalise et al., 2013).

To verify whether the SiHa cell heterodimer was cleaved and inserted into liposomes, cell extracts subjected to oxidizing or reducing treatment were reconstituted. To eliminate liposomes without incorporated proteins, proteoliposomes were separated by ultracentrifugation. Immunoblot analysis was performed running the gel under oxidizing conditions, i.e., absence of reducing agents (Fig. 3B and C). A band of 120 kDa was detected in proteoliposomes reconstituted with proteins subjected to oxidizing conditions (lines −DTE). In the case of cell extract pre-incubated under reducing conditions, bands of apparent molecular mass of 35 kDa with anti-LAT1 (Fig. 3B, line +DTE) or 80 kDa with anti-CD98 (Fig. 3C, line +DTE) were detected. This data confirmed the presence of the covalent LAT1/CD98 heterodimer in proteoliposomal membrane under oxidizing conditions. Transport specificity was assayed adding amino acids to the extraliposomal compartment and measuring the residual activity of reconstituted protein both under oxidizing (Fig. 4A) and reducing (Fig. 4B) conditions. Among hydrophobic amino acids, Ile, Val, Leu, Cys and Met exerted more than 90% inhibition; while Phe and Ala inhibited at a lower extent. Among hydrophilic amino acids, besides His, also Tyr and Thr strongly (more than 80%)

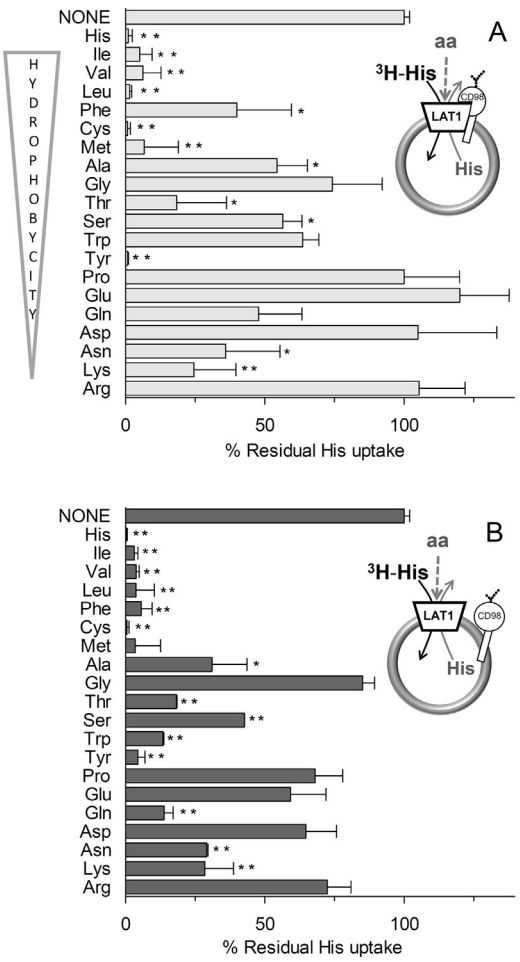

Fig. 4. Effect of external amino acids on [^{3}H]His transport in proteoliposomes reconstituted with SiHa extract. Reconstitution was performed in absence (A, light gray) or presence (B, dark gray) of 10 mM DTE. Transport was performed in 30 min. 5 mM of the indicated amino acids were added together with [^{3}H]His. Percentage of residual His uptake was calculated with respect to controls (without added amino acids). Transport activity of control was 80 pmol mg protein^{-1} 30 min^{-1} or 15 pmol mg protein^{-1} 30 min^{-1} in the presence or absence of DTE, respectively. Results are mean ± S.D. from three experiments. Significantly different from controls as estimated by 1Way ANOVA test (*P < 0.05; **P < 0.01). Proteoliposomes sketch describes experimental design in all histogram figures.

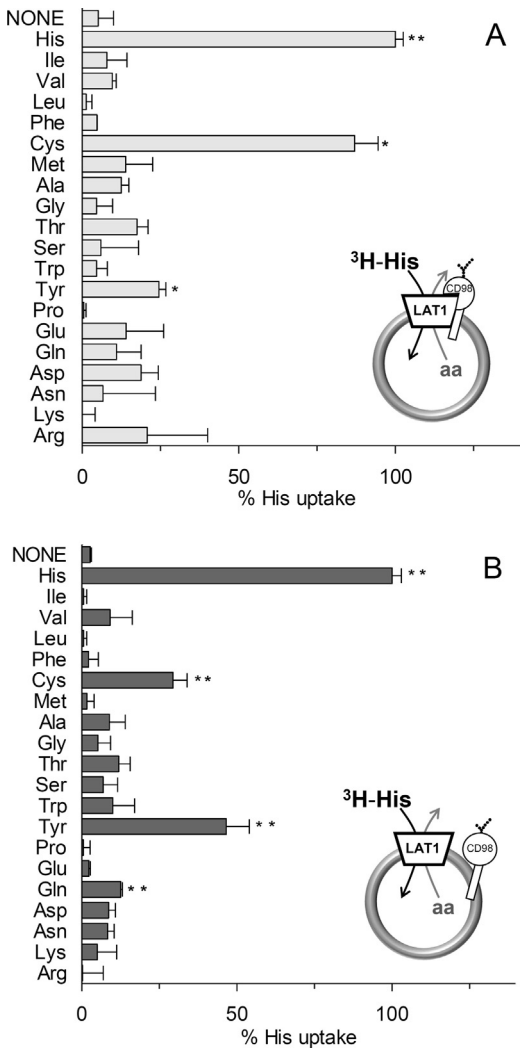

Fig. 5. Counter substrates for [^{3}H]His in proteoliposomes reconstituted with SiHa cell extract. Reconstitution was performed in absence (A, light gray) or presence (B, dark gray) of 10 mM DTE. Transport was started as in Fig. 4 in proteoliposomes containing 10 mM of the indicated amino acids. Percentage His uptake was calculated with respect to proteoliposomes containing 10 mM internal His. Transport activity of control was 92 pmol mg protein^{-1} 30 min^{-1} or 19 pmol mg protein^{-1} 30 min^{-1} in the presence or absence of DTE, respectively. Results are mean ± S.D. from three experiments. *Significantly different from sample without intraliposomal amino acids as estimated by 1Way ANOVA test (*P < 0.05; **P < 0.01).

inhibited transport. Ser, Trp, Gln, Asn and Lys inhibited by about 50%. Other amino acids led to a very slight, if any inhibition. Inhibition profile was very similar under oxidizing or reducing conditions for most of the amino acids. Only in case of Phe, Trp, Glu and Gln a slightly higher degree of inhibition was observed under reducing conditions (Fig. 4B). Counter-substrates were identified (Fig. 5): under oxidizing conditions, Cys allowed accumulation of [^{3}H]His in the intraliposomal compartment comparable to the control, i.e. internal His. Hydrophilic amino acids such as Tyr led to lower but significant accumulation of [^{3}H]His. In spite of their ability to strongly inhibit LAT1 from external side, internal Ile and Leu did not stimulate [^{3}H]His accumulation (Fig. 5A). Only a slight difference was observed under reducing conditions regarding the lower efficiency of Cys as counter-substrate (Fig. 5B). These results indicated that the presence of CD98 did not influence function and specificity of LAT1 mediated transport. To highlight differences in substrate specificity between oxidizing and reducing conditions, results are expressed as percent respect to controls. This hides the actual difference of absolute transport activities in absence or presence of DTE (see legend to Figs. 4 and 5 and Fig. 3A for comparison).

3.4. Transport function of recombinant hLAT1 or hCD98 in proteoliposomes

To definitively prove the major role of LAT1 in transport function, a single component experimental model was used. This system consists in reconstitution in liposomes of a single protein obtained by over-expression in *E. coli* (Galluccio et al., 2013) exploiting the property of liposomes in studying unique features of transport proteins (Rebsamen et al., 2015). The recombinant hLAT1 was reconstituted following conditions set up for the endogenous transporter measuring [^{3}H]His uptake in antiport with internal His. This definitively demonstrated that hLAT1 is the sole transport competent unit of LAT1/CD98 heterodimer (Fig. 6). According to literature data and, differently from LAT2, transport was independent of pH in the range from pH 6.5 to pH 8.0 (not shown). The reconstitution of hCD98 over-expressed in *E. coli* and purified, did not allow amino acid uptake (Fig. 6A). In line with data shown in Fig. 3A, reducing conditions, i.e. hLAT1 purified in the presence of DTE, strongly activated [^{3}H]His time course, with respect to oxidizing

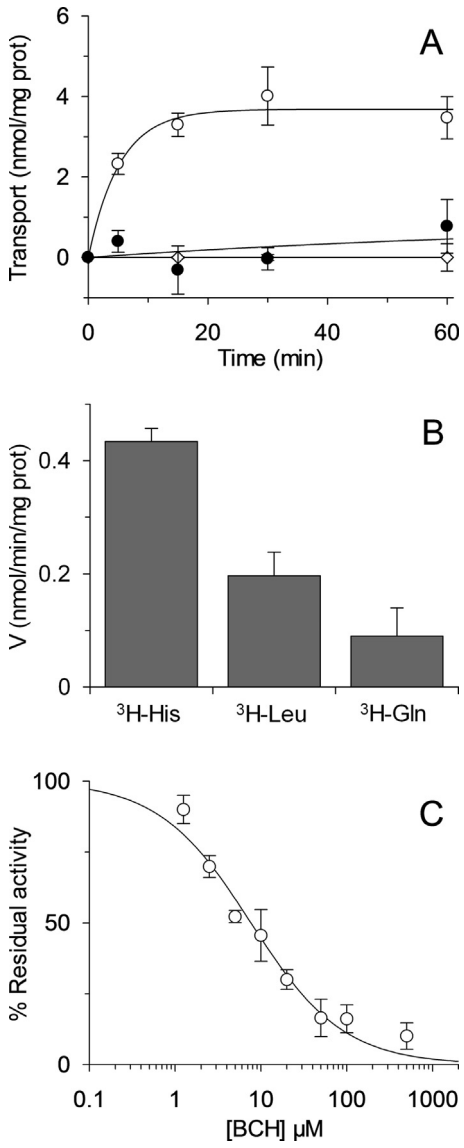

Fig. 6. [^{3}H]His uptake in proteoliposomes reconstituted with over-expressed hLAT1 or hCD98. (A) hLAT1 or hCD98 were purified in the presence (○, ◊) or absence (●) of DTE. Transport was started as in Section 2.10 with hLAT1(●, ○) or hCD98 (◊) proteoliposomes. (B) Uptake of various radiolabeled amino acids in proteoliposomes reconstituted with over-expressed hLAT1. Transport was measured in 30 min by adding 5 μM [^{3}H]His or [^{3}H]Leu or [^{3}H]Gln. (C) Dose–response curve for BCH. Transport was measured in 15 min as described in Section 2.9. Percent residual activity with respect to the control is reported. Results are mean ± S.D. from three experiments.

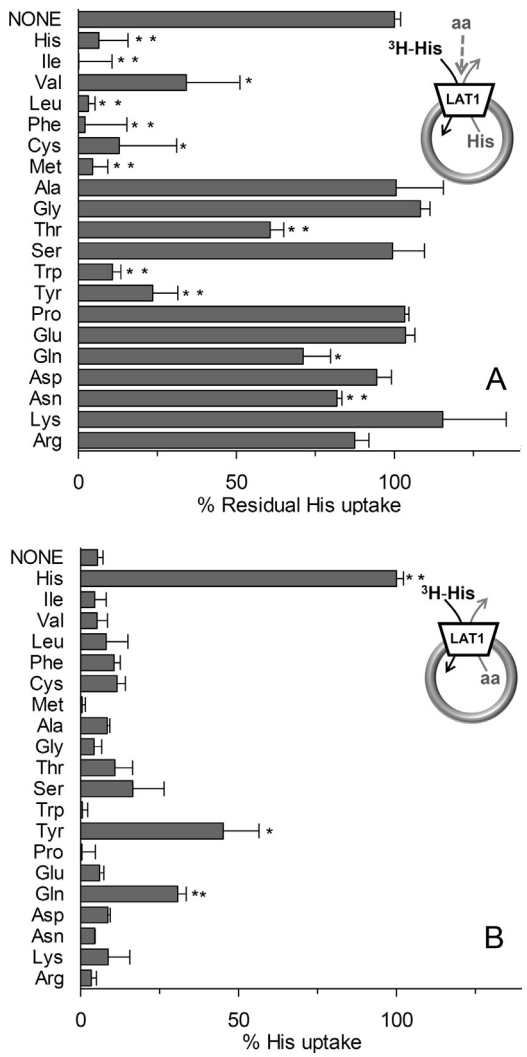

Fig. 7. Effect of amino acids on [^{3}H]His transport in proteoliposomes reconstituted with over-expressed hLAT1. (A) Inhibition by external amino acids. Transport was measured as described in Section 2.9. 1 mM of indicated amino acids were added. Percentage of residual activity was calculated with respect to the control. Significantly different from sample without added external amino acids as estimated by 1Way ANOVA test (*P < 0.05; **P < 0.01) (B) Amino acid as counter substrates for [^{3}H]His uptake. Transport was started as Section 2.9 in proteoliposomes containing 10 mM of the indicated amino acids. Percentage His uptake was calculated with respect to proteoliposomes containing 10 mM internal His. Results are mean ± S.D. from three experiments. *Significantly different from sample without intraliposomal amino acids as estimated by 1Way ANOVA test (*P < 0.05; **P < 0.01).

conditions, i.e. hLAT1 purified in the absence of DTE (Fig. 6A). The equilibrium was reached after 30 min with an initial transport rate of 0.70 ± 0.03 nmol min^{-1} mg protein^{-1} under reducing condition. These results, on the one hand, confirmed those obtained with endogenous protein (Fig. 3A), on the other hand, suggested that reducing conditions have a role in intrinsic activation of hLAT1 protein. Thus, all the following experiments were performed using protein purified in presence of DTE. In the same experiment it was demonstrated that external Na^+ is not required for transport function (not shown). Different radiolabeled amino acids were used; His was the best substrate also for reconstituted hLAT1 (Fig. 6B), correlating well with previous work (Mastroberardino et al., 1998). IC_{50} for the amino acid analog BCH was calculated from dose-response analysis; its value was 6.8 ± 2.0 μM (Fig. 6C). Inhibition analysis was finally conducted (Fig. 7A): the profile overlapped almost completely that obtained with the endogenous protein, with the exception of Lys. Then, counter-substrates have been detected including the amino acids in the intraliposomal compartment and measuring [^{3}H]His uptake which was slightly stimulated by hydrophilic Gln, Ser and Tyr (Fig. 7B). Hydrophobic Ile and Leu, which were strong inhibitors of [^{3}H]His uptake, did not stimulate accumulation, reproducing the discrepancies observed with the protein extracted from SiHa cells.

Thus, efflux experiments were conducted: according to the antiport mechanism, no or very slow efflux of [^{3}H]His from preloaded proteoliposomes was observed (Fig. 8) in absence of external amino acid. Ile, Leu, Cys, Met, Thr, Tyr and the control His, strongly stimulated [^{3}H]His efflux. Phe, Ala as well as hydrophilic Ser, Gln, Asn and Lys, induced efflux at a much lower extent. These results suggest a functional asymmetry for hLAT1, with some of the substrates only inwardly transported.

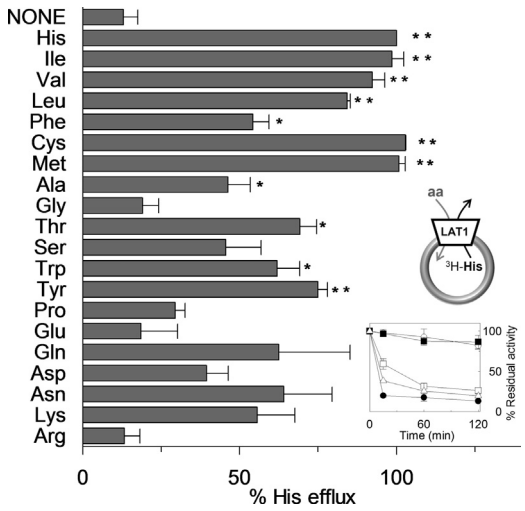

Fig. 8. Amino acids as counter substrates for [^{3}H]His efflux in proteoliposomes reconstituted with over-expressed hLAT1. Efflux was measured in the presence of 5 mM of the indicated external amino acid (Section 2.9). Percentage is referred to proteoliposomes with externally His. Inset, represents a typical efflux time course in absence (○) or in the presence of external His (●), Lys (□), Glu (■), Leu (△). Results are mean ± S.D. from three experiments. *Significantly different from sample without added substrates was estimated by 1Way ANOVA test (*$P < 0.05$; **$P < 0.01$).

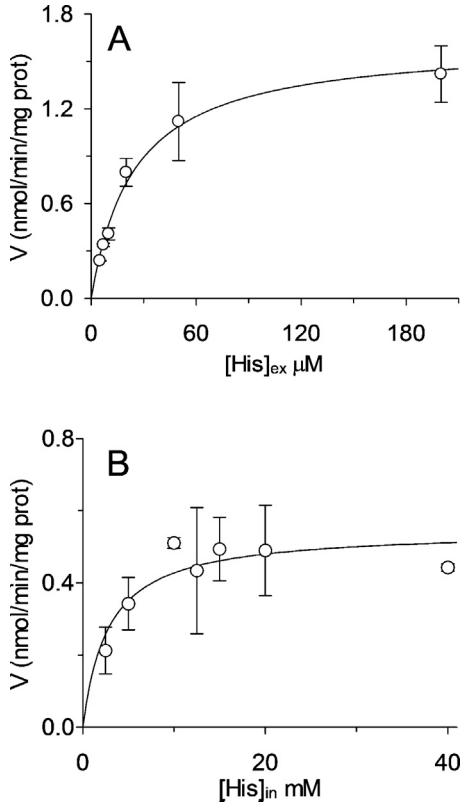

Fig. 9. His transport kinetics in proteoliposomes reconstituted with over-expressed hLAT1. Transport rate was measured in 10 min adding [^{3}H]His at the indicated concentration (A) to proteoliposomes containing 10 mM internal His or 5 μM [^{3}H]His to proteoliposomes containing internal His at the indicated concentrations (B). Results are mean ± S.D. from three experiments.

Finally, kinetic analysis was performed (Fig. 9). The external Km for His was 24.6 ± 5.6 μM (Fig. 9A); the internal Km for His was 2.8 ± 1.7 mM (Fig. 9B). The two values are dramatically different, demonstrating, besides a functional, also a kinetic asymmetry. The external Km corresponds to that reported in cells indicating that the orientation in proteoliposomes and in cells is the same.

The homology structural model of the hLAT1 protein was constructed on the basis of the arginine/agmatine transporter, whose structure has been solved by X-ray crystallography (Gao et al., 2010). As stated in Section 1, LAT1 contains 12 transmembrane α-helices connected by hydrophilic stretches with random coil structures and few α-helical segments. LAT1 harbors twelve Cys residues; however, the residue C496 is not visible in the model because is located in the missing 74C-terminal amino acids, which cannot be modeled. C164 is involved in the dimerization with CD98 and is exposed toward the extracellular side. Six Cys residues are close enough to form pair wise disulfides as indicated in the figure, namely C176-C178; C102-C397; C407-C458 with predicted distances of 6.5 Å, 5.4 Å and 5.5 Å, respectively.

4. Discussion

LAT1 is the sole transport competent unit of the LAT1/CD98 heterodimer as disclosed, for the first time, by transport assays in intact SiHa cells, proteoliposomes reconstituted with SiHa cell extracts and proteoliposomes reconstituted with the recombinant transporter. Congruence of results obtained with the three experimental models allowed us to conclude that CD98 has no role in transport function clarifying the long lasting controversy concerning this issue (see Section 1). The lack of CD98 competence in transport is expected, given the presence of a single transmembrane segment in its structure (Fort et al., 2007). Therefore, the accessory CD98 subunit, linked to LAT1 in cells (Fig. 1), would play different roles, such as trafficking of the heterodimer to the membrane as previously described for mouse LAT1 (Nakamura et al., 1999). This, however, does not deny previously reported data obtained in intact cells, indicating an essential role of CD98 for transport function (Kanai et al., 1998; Mastroberardino et al., 1998; Prasad et al., 1999). Indeed, in those experimental conditions, CD98 would be required to route LAT1 to membrane, being apparently essential for amino acid transport. It has to be highlighted that LAT1 is not a glycosylated protein, in line with the detection of a 35 kDa band with no higher bands (Figs. 2 and 3). On the contrary, CD98 is a glycoprotein as demonstrated by the presence of multiple bands at molecular mass higher than 80 kDa (Fig. 1) (Fotiadis et al., 2013). Very recently, some elegant data have defined the interaction of CD98 with another protein belonging to the SLC7 family, SLC7A8 or LAT2 which shares 52% identity with LAT1 and is an amino acid transporter specific for Gln, Ile and Leu. In that case, it was demonstrated that interaction occurs with covalent disulfide formation and with hydrophobic interactions. In the proposed model, CD98 played a role in stabilizing LAT2 but not in its folding and function (Rosell et al., 2014). This phenomenon is not unusual, since also in the case of the heterodimeric transporter $b^{0,+}$, which is very distant from LAT1 and LAT2 (Verrey et al., 2004), the ancillary protein rBAT was not involved in transport function (Reig et al., 2002). In the present work, the proteoliposome tool allowed to gain new insights on structure/function relationships of LAT1. First, the influence of different redox conditions was described. Activation by the S–S reducing agent DTE (and vice versa inhibition by SH oxidation) was observed for LAT1 obtained from cell extracts (Fig. 3A) and, more evidently, for the recombinant protein (Fig. 6A). While this effect was not observed in intact cells (Fig. 2A). The most likely explanation for these phenomena relies on a strong influence of the redox state of SH residues of LAT1 on the correct folding and/or transport function. In intact cells, where redox control systems are fully functioning, LAT1 is not sensitive to further addition of reducing agents (DTE). On the contrary, during extraction from cells the redox control is lost and, hence, a significant fraction of the protein is oxidized,

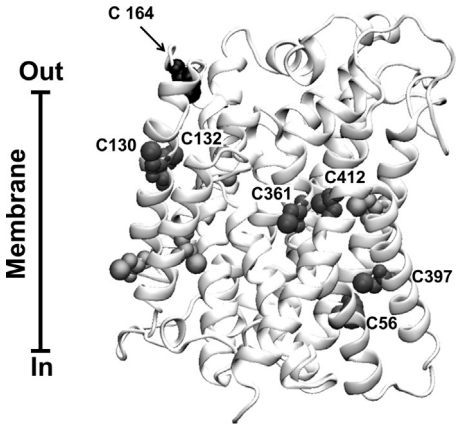

Fig. 10. Homology model of human LAT1. The model is depicted by VMD1.9.1. Cys residues are highlighted. C164 forming the disulfide with CD98 is in black and indicated by arrow. Cys residues predicted to form disulfides are numbered and in dark gray. Remaining Cys residues are in light gray.

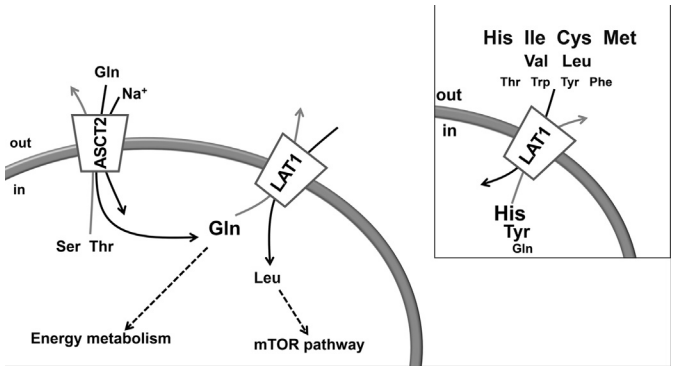

Fig. 11. Interplay between LAT1 and ASCT2 amino acid transporters. Transporters are depicted in the cell membrane. Arrows indicate amino acid fluxes. Dotted arrows indicate Gln or Leu intracellular pathways. In the inset, substrates outwardly or inwardly transported by LAT1 are indicated. Character sizes indicate efficiency of amino acids transport.

becoming inactive; this condition, however, is not irreversible since addition of DTE allows recovery of transport activity. The recombinant protein, since expressed in bacterial cells, is not subjected to proper redox controlling systems; therefore, it is virtually completely oxidized, i.e., very sensitive to activation by reducing agent. Therefore, all experiments with the recombinant hLAT1 were performed in the presence of DTE. That oxidation (S–S formation) will have negative effect on transport is well explained by the structural model of LAT1 from which it is evident that at least three Cys couples lie at proper distances to form S–S (Fig. 10). It is plausible that when disulfides are formed between these Cys couples the protein looses mobility, being inactive. This is in line with western blot analysis showing that a small fraction of endogenous LAT1 or CD98 protein is reduced also in oxidizing conditions, i.e. a protein band migrating at 35 kDa or at 80 kDa is evident together with the heterodimer at 120 kDa (Figs. 1, 2B and C). A further observation coming from data on proteoliposomes is that endogenous LAT1 and CD98, even after DTE treatment of SiHa cell extracts, remain associated to the liposomal membrane. This finding suggested that either CD98 is independently reconstituted in proteoliposomes or it is co-reconstituted together with LAT1 in the same vesicles (Fig. 3B and C).

In the present work, all the transport assays have been performed using His as substrate to better discriminate LAT1 from other transporters present in intact cells or in cell extracts. Indeed, SNAT3-5-8, y+LAT1 and CAT1-2 which are known plasma membrane transporters for His are strictly Na^+-dependent (Broer, 2008; Palacin et al., 1998; Verrey et al., 2000). Moreover LAT2, even though shares some substrate preferences with LAT1, has lower affinity toward His (del Amo et al., 2008). Thus, using His avoided the overlap of transport signals coming from the two proteins if both present in cell membranes. Noteworthy, functional characterization performed in this work revealed that the association of CD98 with LAT1 does not influence transporter specificity. Extracellular and extraliposomal sides of proteins are very similar as confirmed by the overlapping inhibition profiles obtained (Figs. 4 and 7A). Small differences have been observed between Fig. 4A and B (oxidizing and reducing conditions), concerning Phe, Trp, Glu and Gln inhibition. These are due to some changes in exposure of hydrophobic/hydrophilic residues following reduction of protein Cys residues by DTE and/or to interferences exerted by similar amino acid transporters possibly present in cell membrane and in cell extract. The most suitable results are, indeed, those obtained with the purified recombinant protein. The suitability of this model for transport studies allowed to reveal a novel property of recombinant hLAT1, i.e. its functional asymmetry (Figs. 7B, 8 and inset of 11). In line with previous literature data, external Km is nearly 100 fold lower than internal one (Fig. 9) (Mastroberardino et al., 1998; Meier et al., 2002; Wagner et al., 2001; Yanagida et al., 2001), being in the range of plasmatic His concentration (Cynober, 2002). Under a physiological point of view, His transport via LAT1 accomplishes the function of providing cells with this essential amino acid in those tissue, such as retina, where His plays the important role of flush sensitivity regulation (Usui et al., 2013). Given the sub cellular localization of LAT1, this protein would allow the accumulation of His and other neutral amino acids representing a tertiary-active mechanism of transport when coupled with sodium-dependent transporters. Interestingly, no OMIM (Online Mendelian Inherited in Man) records are linked to LAT1 and/or CD98 inherited mutations. This may be due to the need of Leu, recognized as substrate by LAT1 (Figs. 6B and 8), during mammalian embryo development for mTOR pathway regulation; thus, absence of Leu transporter(s) is incompatible with life (Taylor, 2014). An intensive research area of investigation is represented by the transport of different drugs mediated by LAT1 (del Amo et al., 2008; Geier et al., 2013). This interest relies on LAT1 localization at the BBB which is a critical barrier for delivery of pharmacological and xenobiotic compounds to nervous tissue (Boado et al., 2005; Ylikangas et al., 2013; Zimmermann et al., 2013). The pointed out proteoliposome model will be useful in easy screening for transport competence of virtually every compound. The above described functional asymmetry is shared with the “companion” transporter hASCT2 (Pingitore et al., 2013; Scalise et al., 2014). As mentioned in Section 1, LAT1 is greatly over-expressed in cancers, where altered amino acid metabolism occurs. In this scenario, LAT1 functional and kinetic asymmetry, refine the model proposed by Nicklin et al. (2009). Indeed Gln is taken up by ASCT2 in a Na^+-dependent manner in antiport with smaller amino acids, such as Ser (Fig. 11). Then, the same Gln is used for both energetic purposes and for allowing Leu uptake via LAT1. Leu, Gln and other amino acids are well known to modulate mTOR pathway (Laplante and Sabatini, 2013).

The described findings, open interesting perspectives on the study of LAT1 in proteoliposomes as a powerful tool for direct large scale screening of inhibitors, useful in anticancer therapy. Further investigation on the still unknown transport mechanism and on the actual function of the glycoprotein CD98 will be carried out to definitively establish its role in the human heterodimer.

Conflict of interest

The authors declare no conflict of interest.

Acknowledgements

The authors are grateful to Dr. Jiping Yue for valuable discussion of previous literature. This work was supported by grant from Italian MIUR, Ministero dell'Istruzione, dell'Università e della Ricerca [PON01_00937].

References

Baniasadi, S., Chairoungdua, A., Iribe, Y., Kanai, Y., Endou, H., Aisaki, K., et al., 2007. Gene expression profiles in T24 human bladder carcinoma cells by inhibiting an L-type amino acid transporter, LAT1. Arch. Pharm. Res. 30, 444–452.

Boado, R.J., Li, J.Y., Chu, C., Ogoshi, F., Wise, P., Pardridge, W.M., 2005. Site-directed mutagenesis of cysteine residues of large neutral amino acid transporter LAT1. Biochim. Biophys. Acta 1715, 104–110.

Bode, B.P., 2001. Recent molecular advances in mammalian glutamine transport. J. Nutr. 131, 2475S–2485S, discussion 86S–87S.

Brizio, C., Otto, A., Brandsch, R., Passarella, S., Barile, M., 2000. A protein factor of rat liver mitochondrial matrix involved in flavinylation of dimethylglycine dehydrogenase. Eur. J. Biochem. 267, 4346–4354.

Broer, S., 2002. Adaptation of plasma membrane amino acid transport mechanisms to physiological demands. Pflug. Arch. 444, 457–466.

Broer, S., 2008. Amino acid transport across mammalian intestinal and renal epithelia. Physiol. Rev. 88, 249–286.

Campbell, W.A., Thompson, N.L., 2001. Overexpression of LAT1/CD98 light chain is sufficient to increase system L-amino acid transport activity in mouse hepatocytes but not fibroblasts. J. Biol. Chem. 276, 16877–16884.

Christensen, H.N., 1990. Role of amino acid transport and countertransport in nutrition and metabolism. Physiol. Rev. 70, 43–77.

Cynober, L.A., 2002. Plasma amino acid levels with a note on membrane transport: characteristics, regulation, and metabolic significance. Nutrition 18, 761–766.

del Amo, E.M., Urtti, A., Yliperttula, M., 2008. Pharmacokinetic role of L-type amino acid transporters LAT1 and LAT2. Eur. J. Pharm. Sci. 35, 161–174.

Fan, X., Ross, D.D., Arakawa, H., Ganapathy, V., Tamai, I., Nakanishi, T., 2010. Impact of system L amino acid transporter 1 (LAT1) on proliferation of human ovarian cancer cells: a possible target for combination therapy with anti-proliferative aminopeptidase inhibitors. Biochem. Pharmacol. 80, 811–818.

Fort, J., de la Ballina, L.R., Burghardt, H.E., Ferrer-Costa, C., Turnay, J., Ferrer-Orta, C., et al., 2007. The structure of human 4F2hc ectodomain provides a model for homodimerization and electrostatic interaction with plasma membrane. J. Biol. Chem. 282, 31444–31452.

Fotiadis, D., Kanai, Y., Palacin, M., 2013. The SLC3 and SLC7 families of amino acid transporters. Mol. Aspects Med. 34, 139–158.

Franca, R., Veljkovic, E., Walter, S., Wagner, C.A., Verrey, F., 2005. Heterodimeric amino acid transporter glycoprotein domains determining functional subunit association. Biochem. J. 388, 435–443.

Fuchs, B.C., Bode, B.P., 2005. Amino acid transporters ASCT2 and LAT1 in cancer: partners in crime? Semin. Cancer Biol. 15, 254–266.

Galluccio, M., Pingitore, P., Scalise, M., Indiveri, C., 2013. Cloning, large scale over-expression in *E. coli* and purification of the components of the human LAT 1 (SLC7A5) amino acid transporter. Protein J. 32, 442–448.

Ganapathy, V., Thangaraju, M., Prasad, P.D., 2009. Nutrient transporters in cancer: relevance to Warburg hypothesis and beyond. Pharmacol. Ther. 121, 29–40.

Gao, X., Zhou, L., Jiao, X., Lu, F., Yan, C., Zeng, X., et al., 2010. Mechanism of substrate recognition and transport by an amino acid antiporter. Nature 463, 828–832.

Geier, E.G., Schlessinger, A., Fan, H., Gable, J.E., Irwin, J.J., Sali, A., et al., 2013. Structure-based ligand discovery for the large-neutral amino acid transporter 1, LAT-1. Proc. Natl. Acad. Sci. U.S.A. 110, 5480–5485.

Giancaspero, T.A., Busco, G., Panebianco, C., Carmone, C., Miccolis, A., Liuzzi, G.M., et al., 2013. FAD synthesis and degradation in the nucleus create a local flavin cofactor pool. J. Biol. Chem. 288, 29069–29080.

Indiveri, C., Palmieri, L., Palmieri, F., 1994. Kinetic characterization of the reconstituted ornithine carrier from rat liver mitochondria. Biochim. Biophys. Acta 1188, 293–301.

Kageyama, T., Nakamura, M., Matsuo, A., Yamasaki, Y., Takakura, Y., Hashida, M., et al., 2000. The 4F2hc/LAT1 complex transports L-DOPA across the blood–brain barrier. Brain Res. 879, 115–121.

Kanai, Y., Segawa, H., Miyamoto, K., Uchino, H., Takeda, E., Endou, H., 1998. Expression cloning and characterization of a transporter for large neutral amino acids activated by the heavy chain of 4F2 antigen (CD98). J. Biol. Chem. 273, 23629–23632.

Kim, D.K., Kanai, Y., Choi, H.W., Tangtrongsup, S., Chairoungdua, A., Babu, E., et al., 2002. Characterization of the system L amino acid transporter in T24 human bladder carcinoma cells. Biochim. Biophys. Acta 1565, 112–121.

Laplante, M., Sabatini, D.M., 2013. Regulation of mTORC1 and its impact on gene expression at a glance. J. Cell Sci. 126, 1713–1719.

Mastroberardino, L., Spindler, B., Pfeiffer, R., Skelly, P.J., Loffing, J., Shoemaker, C.B., et al., 1998. Amino-acid transport by heterodimers of 4F2hc/CD98 and members of a permease family. Nature 395, 288–291.

Meier, C., Ristic, Z., Klauser, S., Verrey, F., 2002. Activation of system L heterodimeric amino acid exchangers by intracellular substrates. EMBO J. 21, 580–589.

Nakamura, E., Sato, M., Yang, H., Miyagawa, F., Harasaki, M., Tomita, K., et al., 1999. 4F2 (CD98) heavy chain is associated covalently with an amino acid transporter and controls intracellular trafficking and membrane topology of 4F2 heterodimer. J. Biol. Chem. 274, 3009–3016.

Nicklin, P., Bergman, P., Zhang, B., Triantafellow, E., Wang, H., Nyfeler, B., et al., 2009. Bidirectional transport of amino acids regulates mTOR and autophagy. Cell 136, 521–534.

Palacin, M., Estevez, R., Bertran, J., Zorzano, A., 1998. Molecular biology of mammalian plasma membrane amino acid transporters. Physiol. Rev. 78, 969–1054.

Palacin, M., Kanai, Y., 2004. The ancillary proteins of HATs: SLC3 family of amino acid transporters. Pflug. Arch. 447, 490–494.

Palmieri, F., Indiveri, C., Bisaccia, F., Iacobazzi, V., 1995. Mitochondrial metabolite carrier proteins: purification, reconstitution, and transport studies. Methods Enzymol. 260, 349–369.

Pingitore, P., Pochini, L., Scalise, M., Galluccio, M., Hedfalk, K., Indiveri, C., 2013. Large scale production of the active human ASCT2 (SLC1A5) transporter in Pichia pastoris – functional and kinetic asymmetry revealed in proteoliposomes. Biochim. Biophys. Acta 1828, 2238–2246.

Pochini, L., Scalise, M., Galluccio, M., Indiveri, C., 2012. Regulation by physiological cations of acetylcholine transport mediated by human OCTN1 (SLC22A4). Implications in the non-neuronal cholinergic system. Life Sci. 91, 1013–1016.

Pochini, L., Scalise, M., Galluccio, M., Indiveri, C., 2014. Membrane transporters for the special amino acid glutamine: structure/function relationships and relevance to human health. Front. Chem. 2, 61.

Prasad, P.D., Wang, H., Huang, W., Kekuda, R., Rajan, D.P., Leibach, F.H., et al., 1999. Human LAT1, a subunit of system L amino acid transporter: molecular cloning and transport function. Biochem. Biophys. Res. Commun. 255, 283–288.

Rebsamen, M., Pochini, L., Stasyk, T., de Araujo, M.E., Galluccio, M., Kandasamy, R.K., et al., 2015. SLC38A9 is a component of the lysosomal amino acid sensing machinery that controls mTORC1. Nature.

Reig, N., Chillaron, J., Bartoccioni, P., Fernandez, E., Bendahan, A., Zorzano, A., et al., 2002. The light subunit of system b(o,+) is fully functional in the absence of the heavy subunit. EMBO J. 21, 4906–4914.

Rosell, A., Meury, M., Alvarez-Marimon, E., Costa, M., Perez-Cano, L., Zorzano, A., et al., 2014. Structural bases for the interaction and stabilization of the human amino acid transporter LAT2 with its ancillary protein 4F2hc. Proc. Natl. Acad. Sci. U.S.A. 111, 2966–2971.

Scalise, M., Galluccio, M., Pochini, L., Indiveri, C., 2012. Over-expression in *Escherichia coli*, purification and reconstitution in liposomes of the third member of the OCTN sub-family: the mouse carnitine transporter OCTN3. Biochem. Biophys. Res. Commun. 422, 59–63.

Scalise, M., Pochini, L., Giangregorio, N., Tonazzi, A., Indiveri, C., 2013. Proteoliposomes as tool for assaying membrane transporter functions and interactions with xenobiotics. Pharmaceutics 5, 472–497.

Scalise, M., Pochini, L., Panni, S., Pingitore, P., Hedfalk, K., Indiveri, C., 2014. Transport mechanism and regulatory properties of the human amino acid transporter ASCT2 (SLC1A5). Amino Acids 46, 2463–2475.

Shennan, D.B., Thomson, J., 2008. Inhibition of system L (LAT1/CD98hc) reduces the growth of cultured human breast cancer cells. Oncol. Rep. 20, 885–889.

Taylor, P.M., 2014. Role of amino acid transporters in amino acid sensing. Am. J. Clin. Nutr. 99, 223S–230S.

Usui, T., Kubo, Y., Akanuma, S., Hosoya, K., 2013. Beta-alanine and L-histidine transport across the inner blood–retinal barrier: potential involvement in L-carnosine supply. Exp. Eye Res. 113, 135–142.

Verrey, F., Closs, E.I., Wagner, C.A., Palacin, M., Endou, H., Kanai, Y., 2004. CATs and HATs: the SLC7 family of amino acid transporters. Pflug. Arch. 447, 532–542.

Verrey, F., Meier, C., Rossier, G., Kuhn, L.C., 2000. Glycoprotein-associated amino acid exchangers: broadening the range of transport specificity. Pflug. Arch. 440, 503–512.

Wagner, C.A., Lang, F., Broer, S., 2001. Function and structure of heterodimeric amino acid transporters. Am. J. Physiol. Cell Physiol. 281, C1077–C1093.

Wang, Q., Tiffen, J., Bailey, C.G., Lehman, M.L., Ritchie, W., Fazli, L., et al., 2013. Targeting amino acid transport in metastatic castration-resistant prostate cancer: effects on cell cycle, cell growth, and tumor development. J. Natl. Cancer Inst. 105, 1463–1473.

Yanagida, O., Kanai, Y., Chairoungdua, A., Kim, D.K., Segawa, H., Nii, T., et al., 2001. Human L-type amino acid transporter 1 (LAT1): characterization of function and expression in tumor cell lines. Biochim. Biophys. Acta 1514, 291–302.

Ylikangas, H., Peura, L., Malmioja, K., Leppanen, J., Laine, K., Poso, A., et al., 2013. Structure–activity relationship study of compounds binding to large amino acid transporter 1 (LAT1) based on pharmacophore modeling and in situ rat brain perfusion. Eur. J. Pharm. Sci. 48, 523–531.

Zimmermann, L.T., Santos, D.B., Naime, A.A., Leal, R.B., Dorea, J.G., Barbosa Jr., F., et al., 2013. Comparative study on methyl- and ethylmercury-induced toxicity in C6 glioma cells and the potential role of LAT-1 in mediating mercurial–thiol complexes uptake. Neurotoxicology 38, 1–8.

Biochimica et Biophysica Acta 1861 (2017) 727–736

Contents lists available at ScienceDirect

Biochimica et Biophysica Acta

journal homepage: www.elsevier.com/locate/bbagen

Novel insights into the transport mechanism of the human amino acid transporter LAT1 (SLC7A5). Probing critical residues for substrate translocation

Lara Napolitano [a], Michele Galluccio [a], Mariafrancesca Scalise [a], Chiara Parravicini [b], Luca Palazzolo [c], Ivano Eberini [b], Cesare Indiveri [a,*]

[a] Department DiBEST (Biologia, Ecologia, Scienze della Terra) Unit of Biochemistry and Molecular Biotechnology, University of Calabria, Via P. Bucci 4C, 87036 Arcavacata di Rende, Italy
[b] Dipartimento di Scienze Farmacologiche e Biomolecolari, Università degli Studi di Milano, Italy
[c] Dipartimento di Scienze Farmacologiche e Biomolecolari e Dipartimento di Scienze Biomediche e Cliniche "L. Sacco", Università degli Studi di Milano, Italy

ARTICLE INFO

Article history:
Received 28 September 2016
Received in revised form 21 December 2016
Accepted 10 January 2017
Available online 11 January 2017

Keywords:
Liposome
Membrane transporter reconstitution
Docking
Recombinant protein expression
Site-directed mutagenesis

ABSTRACT

Background: LAT1 (SLC7A5) is the transport competent unit of the heterodimer formed with the glycoprotein CD98 (SLC3A2). It catalyzes antiport of His and some neutral amino acids such as Ile, Leu, Val, Cys, Met, Gln and Phe thus being involved in amino acid metabolism. Interestingly, LAT1 is over-expressed in many human cancers that are characterized by increased demand of amino acids. Therefore LAT1 was recently acknowledged as a novel target for cancer therapy. However, knowledge on molecular mechanism of LAT1 transport is still scarce.
Methods: Combined approaches of bioinformatics, site-directed mutagenesis, chemical modification, and transport assay in proteoliposomes, have been adopted to unravel dark sides of human LAT1 structure/function relationships.
Results: It has been demonstrated that residues F252, S342, C335 are crucial for substrate recognition and C407 plays a minor role. C335 and C407 cannot be targeted by SH reagents. The transporter has a preferential dimeric structure and catalyzes an antiport reaction which follows a simultaneous random mechanism.
Conclusions: Critical residues of the substrate binding site of LAT1 have been probed. This site is not freely accessible by molecules other than substrate. Similarly to LeuT, K^+ has some regulatory properties on LAT1.
General significance: The collected data represent a solid basis for deciphering molecular mechanism underlying LAT1 function.

1. Introduction

LAT1 (SLC7A5) is a Na^+ and pH-independent amino acid antiporter with 12 predicted transmembrane α-helices (TMs) (Uniprot ID: Q01650) that regulates distribution of specific amino acids across cell membranes. It was described as a branched chain amino acid transporter [1] and, more recently, it was shown that His is one of the major substrates [2]. LAT1 belongs to a special group of Heterodimeric Amino acid Transporters (HATs) structurally coupled to the glycoprotein CD98 (SLC3A2). The interaction occurs through a conserved disulfide between C164 of hLAT1 and C109 of hCD98 [1]. The interest on this peculiar transporter increased a lot in the recent years since its over-expression in many tumors has been described; therefore, LAT1 is now considered a novel pharmacological target [3,4].

However, identification or design of potent inhibitors to be proposed as potential drugs, requires a deep knowledge of the target structure and action mechanism that, in the case of LAT1, are still missing. Indeed, besides the well-known functional properties of the heterodimeric complex LAT1/CD98, information on structure/function relationships are only predicted by in silico methodologies [5].

The tissue distribution of LAT1 is quite narrow but it becomes wider in tumors [6–9]. Canonical sub-cellular localization for LAT1 is the plasma membrane where it catalyzes inwardly directed flux of His, Ile, Leu, Val, Cys, Met, Gln and some other neutral amino acids, in antiport with His, Tyr or Gln; LAT1 activity is combined to the action of other amino acid transporters whose expression is often redundant [3,10].

Due to its capacity of exchanging Gln with other amino acids, LAT1 is involved in "Glutamine addiction", a typical hallmarks of tumors. In fact, this transporter, together with its companion ASCT2 (SLC1A5) gives rise to a combined transport cycle of Gln and Leu, used for both cancer

Abbreviations: DTE, dithioerythritol; BCH, 2-amino-2-norbornanecarboxylic acid; $C_{12}E_8$, octaethylene glycol monododecyl ether; MTSEA, 2-Aminoethyl methanethiosulfonate hydrobromide; NEM, N-ethylmaleimide.

* Corresponding author.
E-mail address: cesare.indiveri@unical.it (C. Indiveri).

http://dx.doi.org/10.1016/j.bbagen.2017.01.013
0304-4165/

growth and progression [11]. Indeed it is considered a prognostic marker of malignancy [6–9]. Very recently, a role of LAT1 in cell signaling has been proposed due to an alternative localization in the lysosomal membrane [12] where it transports Leu, thus transducing amino acids sufficiency to mTORC1 together with SLC38A9 which transports Gln and Arg [13,14].

The role of CD98 in the heterodimer formation/activity has been matter of investigation for years. Only recently, it has been demonstrated that LAT1 is the sole transport competent unit while CD98 does not play any role in the intrinsic transport function [2]. This correlates well with the finding that CD98 is a multifunctional protein with other functions unrelated to transport, such as integrin signaling [15] or oxidative stress response [16]. The hypothesis is that CD98 may function mainly as molecular chaperone routing LAT1 [17] or other transporters to its definitive localization in plasma (or intracellular) membrane.

In some elegant studies the homology structural model of hLAT1 has been built using, as template, the bacterial AdiC transporter, whose structure has been solved by X-ray crystallography and hypothetical LAT1 inhibitors have been used for docking analysis [5,18–21]. In the present work, the homology model of LAT1 was constructed allowing us to predict amino acid residues critical for substrate recognition and translocation. Interestingly, some of these residues correspond to those previously suggested [18] and a novel one was identified. For the first time, the role of these residues has been demonstrated by combined approaches of site-directed mutagenesis, chemical modification, and transport assay in proteoliposomes. This novel information on LAT1 structure/function relationships may have also important outcomes in cancer drug design.

2. Materials and methods

2.1. Materials

His Trap HP columns, PD-10 columns, ECL plus and Hybond ECL membranes were purchased from GE Healthcare; anti-hLAT1 and anti-rabbit IgG HRP conjugate from Cell Signalling (5347S Lot1 and 7074S Lot 25 respectively); anti-His HRP conjugate from Sigma-Aldrich (A7058); radiolabeled amino acids were purchased from ARC (American Radiolabeled Chemicals); all the other reagents are from Sigma-Aldrich.

2.2. Construction and over-expression of recombinant hLAT1 proteins

The mutagenesis of hLAT1 has been performed by PCR overlap extension method as described in [22,23] by using primers reported in Table 1. hLAT1 WT and mutant proteins have been over-expressed in *E. coli* Rosetta(DE3)pLysS as described in [24].

2.3. Purification of hLAT1

hLAT1, over-expressed in *E. coli*, has been purified as previously described with some modifications [24]. In brief, cell lysates were solubilized, centrifuged (12,000*g*, 10 min, 4 °C) and the purification has been performed using ÄKTA start. The supernatant was applied on a His Trap HP column (5 mL Ni-Sepharose) equilibrated with 10 mL buffer (20 mM Tris HCl pH 8.0, 10% glycerol, 200 mM NaCl, 0.1% sarkosyl, and DTE 2 mM). 10 mL of buffer (20 mM Tris HCl pH 8, 10% glycerol, 200 mM NaCl, 0.05% n-Dodecyl β-D-maltoside and 2 mM DTE) was used to wash column while the protein was eluted with the same buffer plus 400 mM imidazole. Imidazole was removed using a PD-10 column by desalting 2.5 mL of the purified protein collected in 3.5 mL of desalt buffer (20 mM Tris HCl pH 8, 10% glycerol, 0.05% n-Dodecyl β-D-maltoside and 10 mM DTE).

Table 1
Sequences of primers used for mutagenesis. The modified codons are in underlined italic.

LAT1 F252A forward	ATTATACAGCGGCCTC*GCG*GCCTATGGAGGATG
LAT1 F252A reverse	CATCCTCCATAGGC*CGC*GAGGCCGCTGTATAAT
LAT1 F252W forward	ATTATACAGCGGCCT*CT*GGGCCTATGGAGGATG
LAT1 F252W reverse	CATCCTCCATAGGC*CCA*GAGGCCGCTGTATAAT
LAT1 C335A forward	TTCGTGGGCCTGTC*CGC*CTTCGGCTCCGTCAAT
LAT1 C335A reverse	ATTGACGGAGCCGAA*GGC*GGACAGGCCCACGAA
LAT1 S342G forward	CGGCTCCGTCAATGG*GGC*CTGTTCACATCCTCC
LAT1 S342G reverse	AGGATGTGAACAG*GCC*CCCATTGACGGAGC
LAT1 C407A forward	TTCTTCAACTGGCT*CGC*CGTGGCCCTGGCCATC
LAT1 C407A reverse	GATGGCCAGGGCCA*CGG*CGAGCCAGTTGAAGAA

2.4. Reconstitution of the purified hLAT1

The desalted hLAT1 was reconstituted by removing detergent from mixed micelles of detergent, protein and phospholipids using batch wise method as previously described [2] with the modification of the time of incubation with 0.5 g Amberlite XAD-4 performed at room temperature for 90 min. The initial mixture contained: 4 μg of purified protein, 100 μL of 10% $C_{12}E_8$, 100 μL of 10% egg yolk phospholipids (w/v) in the form of liposomes prepared as previously described [25], 20 mM Tris HCl pH 7.5 and 10 mM L-His, except were differently indicated, in a final volume of 700 μL.

2.5. Transport measurements

Uptake experiments were performed by removing the external substrate through the flow of 600 μL of proteoliposomes on a Sephadex G-75 column (0.7 cm diameter × 15 cm height) pre-equilibrated with 20 mM Tris HCl pH 7.5 and sucrose at an appropriate concentration to balance internal osmolarity. Transport was started by adding 5 μM [^{3}H]His to proteoliposomes containing 10 mM L-His, except were differently indicated. Transport was stopped by a mixture of 100 μM BCH and 1.5 μM $HgCl_2$ at the indicated times; for the controls samples the mixture of inhibitors was added at time zero according to the inhibitor stop method [26]. At the end of the transport assay, 100 μL proteoliposomes was passed through a Sephadex G-75 column (0.6 cm diameter × 8 cm height), to separate the external from the internal radioactivity. Liposomes were eluted with 1 mL 50 mM NaCl in 4 mL scintillation mixture and counted. Experimental values were obtained by subtracting controls: for the measurement of initial transport rate, the reaction was stopped after 15 min, i.e., within the initial linear range of [^{3}H]His uptake in proteoliposomes, except where differently indicated. To calculate transport rate, IC50 values or kinetic parameters, Grafit 5.0.13 software has been used for fitting data in first order rate, dose response or Michaelis–Menten and Lineweaver-Burk equations, respectively. Km values similar to the WT or to previous literature data, are reported in the Results section with S.D. but not shown graphs. All these data derive from three experiments. Protein concentration was estimated by Chemidoc imaging system to calculate the hLAT1 specific activity [27].

2.6. Ultracentrifugation of proteoliposomes

500 μL of samples were ultracentrifuged (110,000*g*, 1 h 30 min, 4 °C) after passage through Sephadex G-75 column to separate hLAT1 reconstituted proteoliposomes from liposomes without incorporated proteins as previously described [2]. The obtained pellet was solubilized with 3% sarkosyl for western blot analysis.

2.7. Western blot analysis

Western blot analyses were performed using anti-LAT1 antibody 1:2000 or anti-His antiserum 1:1000 to immuno-detect hLAT1. The reaction has been performed over night at 4 °C for anti-LAT1 antibody and detected by Electro Chemi Luminescence (ECL) assay after an incubation of 1 h with secondary antibody anti-rabbit 1:5000. For anti-His HRP conjugate the reaction has been performed for 1 h at room

temperature and detect by Electro Chemi Luminescence (ECL) at the end of incubation.

2.8. Comparative modelling and quality validation

A multiple alignment of some members of the amino acid-polyamine-organocation (APC) superfamily was carried out through the multiple alignment program ClustalW, including 3 amino acid/polyamine antiporters (APC), AdiC, CadB and PotE, 1 cationic amino acid transporter (CAT), CAT6, 1 amino acid/choline transporter (ACT), Uga4, 1 glutamate/GABA antiporter (GGA), GadC, the large neutral amino acid transporters LAT2, and our target protein hLAT1. This multiple alignment has been used to carry out the comparative modelling of hLAT1 via the Molecular Operating Environment (MOE) Homology Model software with default settings. Three different models for hLAT1 were generated: an outward- open holo monomeric form, 3OB6 [28]; an outward- closed holo monomeric form, 3L1L [20]; and outward- open apo dimeric form, 3LRB [29]. All the refinement procedures were based on molecular mechanics with the Amber12:EHT force field. The PSIPRED Protein Sequence Analysis Workbench (http://bioinf.cs.ucl.ac.uk/psipred/) and the TMHMM Server (http://www.cbs.dtu.dk/services/TMHMM/) were also used to predict LAT1 secondary structure and the TM helices. In order to operate a quality validation, a solvent/membrane explicit molecular dynamics (MD) simulation was carried out on the outward-closed monomeric holo form of hLAT1 by GROMACS [30]. As a first step, Desmond, a Schrodinger tool [31], was used to insert hLAT1 into a pre-equilibrated model of membrane bilayer composed by 212 POPC. hLAT1 was oriented into the membrane model keeping the longest axis of the protein perpendicular to the membrane surface. The system was solvated with 15538 TIP3P water molecules.

Then, the system was equilibrated for 100 ps at 300 K, applying pressures independently in the *x*, *y*, and *z* directions using the Berendsen coupling method [32], and 1000 ps of NPT equilibration at 1.0 Bar using Nose-Hoover thermostat [33]. At last, a 50 ns MD simulation was carried out with the following parameters: 300 K, 1 bar, Nose-Hoover temperature and Parrinello-Rahman pressure couplings, 2 fs of integration time step. The N- and C-terminal domains were capped and the Charmm36 force field was used in all MD steps.

2.9. Identification of hLAT1 binding site

hLAT1 binding site was identified through the MOE Site Finder module, which uses a geometric approach to calculate possible binding sites in a receptor starting from its 3D atomic coordinates. This method is based not on energy models but on alpha spheres, which are a generalization of convex hulls [34].

2.10. Molecular docking of His in the hLAT1 binding site

His was docked always in zwitterionic form with respect to the Cα-bound carboxylic and aminic groups. The Nδ and Nε tautomers and the protonated form of the imidazole heteroaromatic ring were generated and tested.

Molecular docking was carried out through the MOE Docking program with default settings and the Amber12:EHT force field, using both the monomeric hLAT1 models as receptors and the dummy atoms created by Site Finder as explored site. The receptor was considered as a rigid body.

2.11. Protein mutation design

C335A and C407A mutations were introduced in the hLAT1 models through the MOE Protein Design program, and the variation of His affinity (Δ affinity) of mutant hLAT1 was computed with respect to the wild-

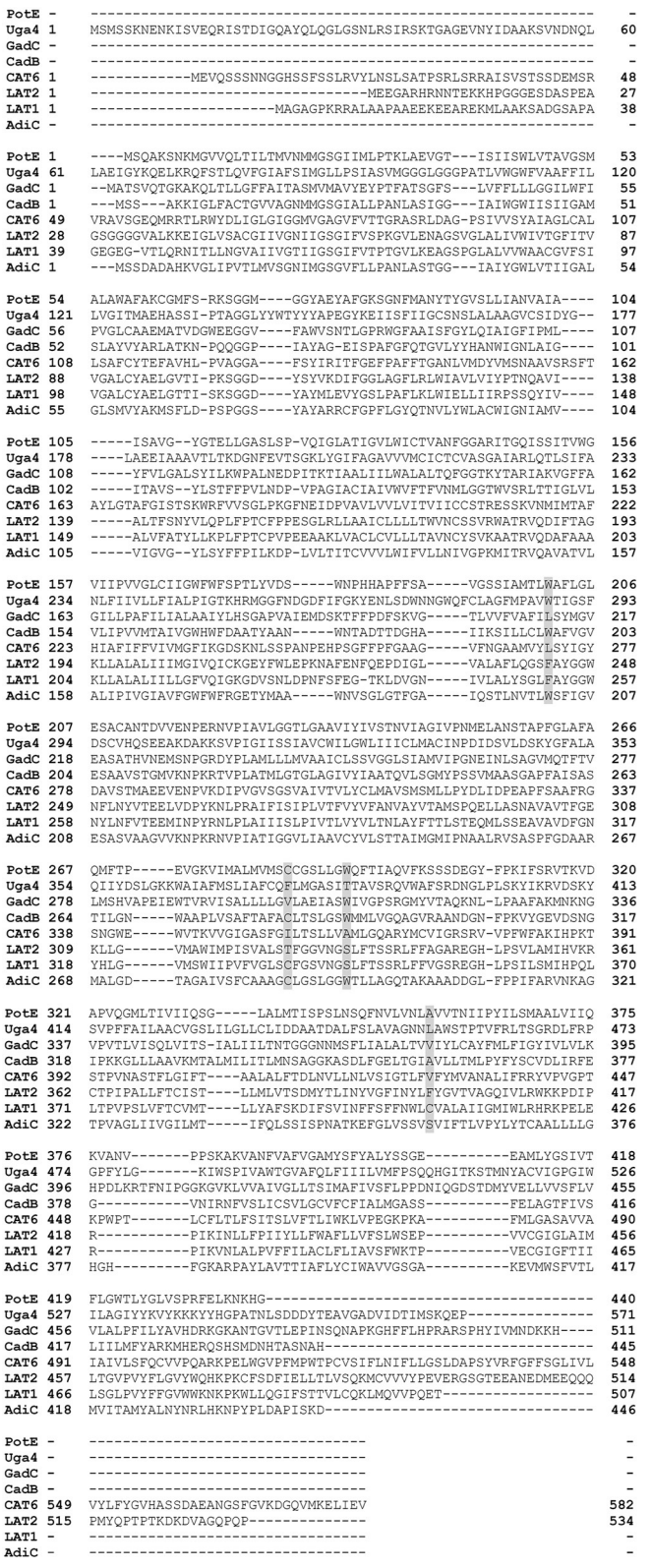

Fig. 1. Critical amino acids discovery. Complete alignment of hLAT1 with orthologous members of the APC transporter family has been performed as described in Section 2.8. The crucial amino acids identified and then mutated are shadowed in grey. AdiC: Arginine/agmatine antiporter (P60061); PotE: ornithine/putrescine antiporter (P0AAF1); Uga4: GABA-specific permease (P32837); GadC: glutamate/gamma-aminobutyrate antiporter (P63235); CadB lysine/cadaverine antiporter (P0AAE8); Cat6: cationic amino acid transporter 6 (Q9LZ20); LAT2: large neutral amino acids transporter 2 (Q9UHI5); LAT1: large neutral amino acids transporter 1 (Q01650).

type. Also the Protein Design program was run with the Amber12:EHT force field.

3. Results

3.1. Identification of crucial amino acid residues

The structural model of hLAT1 was built by homology, using as template the bacterial AdiC, whose crystallographic structure is currently available in different conformational states within the transport cycle: the open-to-out apo form (PDB ID 3LRB and 3NCY) [29,35], the substrate-bound open-to-out form (PDB ID 3OB6) [28], and the outward-facing Arg^{+}-bound occluded (PDB ID 3L1L) conformation [20]. In line with already published alignments, due to the low sequence identity shared between hLAT1 and AdiC, also other members of APC transporter family, were included in the alignment, among which the large neutral amino acids transporter 2 (LAT2), the glutamate:gamma-aminobutyrate antiporter (GadC), the lysine:cadaverine antiporter (CadB), the ornithine:putrescine antiporter (PotE), the GABA-specific permease (Uga4), and the cationic amino acid transporter 6 (Cat6) [18,29] (Fig. 1). Helices of LAT1 are highlighted in Supplemental Fig. 1 as derived from hydropathy plot of Supplemental Fig. 2 [36]. Notably, the last published structure of AdiC [21] revealed the same characteristics of that built in this work (not shown, but see Supplemental Fig. 3). In analogy to AdiC, hLAT1 could form a homodimer (Fig. 2A) in which monomers are present either in outward-open (Fig. 2B) or closed (Fig. 2C) forms. To predict some of the crucial residues for substrate binding and transport, the alignment with AdiC was considered (Fig. 1 and Supplemental Fig. 1). The residues of AdiC W202, W293 and S357 which are important for substrate (agmatine/Arg) binding and translocation [20,21,28] corresponded to LAT1 F252, S342 and, C407, respectively (Fig. 1) as also reported in Geier et al. [18]. The structural stability and the quality of the hLAT1 homology model were confirmed by the analysis of the molecular dynamics trajectory. The root means

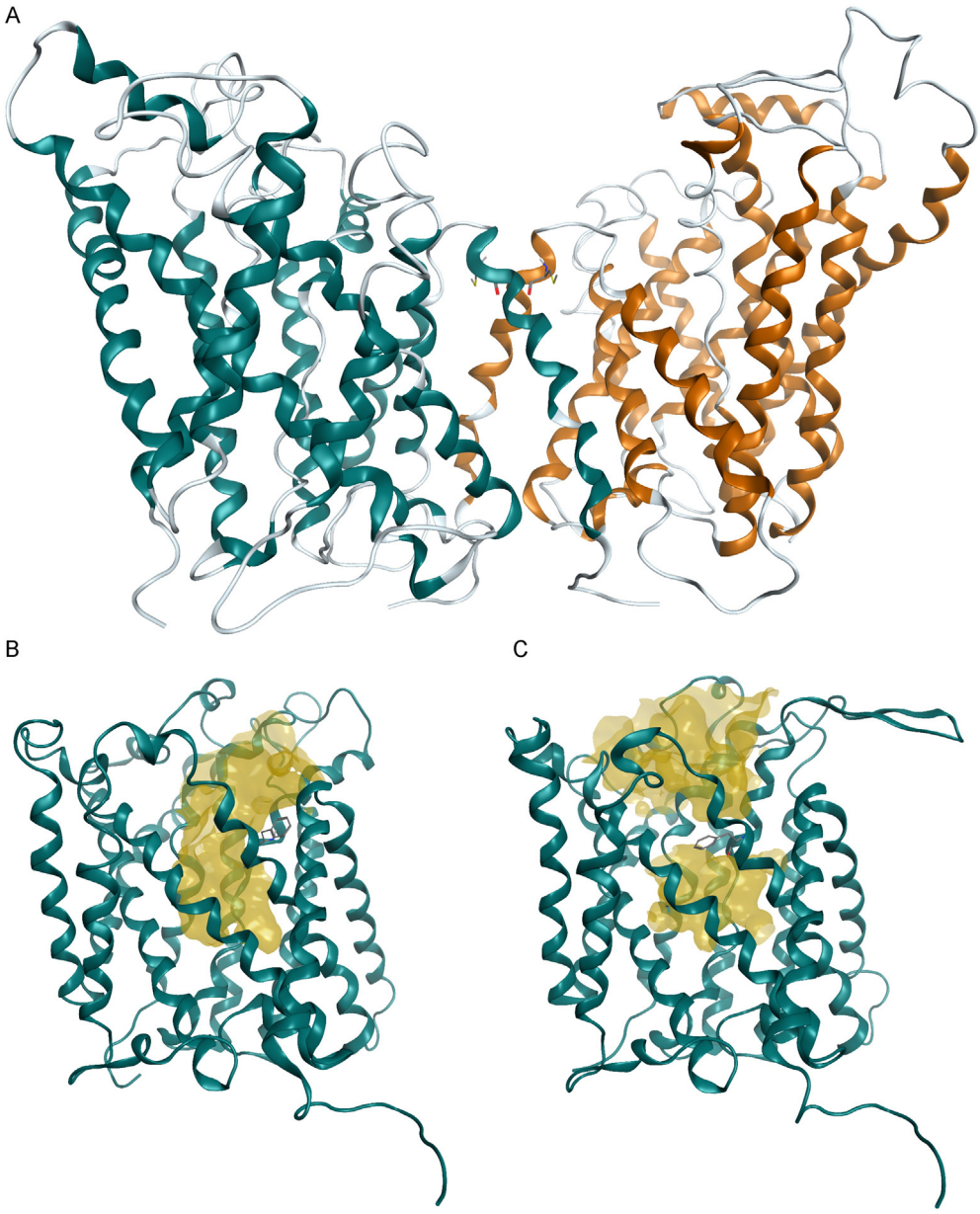

Fig. 2. hLAT1 homology models. hLAT1 is shown as ribbon representation in its dimeric, outward-open and outward-closed conformation in A), B) and C), respectively. Cys (C458) at the interface of LAT1 dimer are shown in stick representation in A). Similarly to residue W202 of AdiC, also the conserved residue F252 (stick representation), behaves like a gate in LAT1, hindering the substrate access pathway (yellow surface), as shown in B) and C).

square deviation (RMSD) for the main chain shows that the protein reaches a plateau at 0.27 nm after approx. 20 ns (Supplemental Fig. 4). A low RMSD value (0.21 nm) was also obtained when the starting protein structure and the final MD frame (Supplemental Fig. 5) were superposed. A z-section of the whole simulated system (hLAT1, membrane and solvent) is depicted in Supplemental Fig. 6.

Docking simulations on LAT1 outward- open form highlighted an additional Cys residue, besides C407, never predicted before and close to the substrate binding site F252, i.e., C335 (Fig. 3A). Docking simulations performed on the outward- closed conformation show that all the poses, obtained for the natural LAT1 substrate His, well fit with the position of the Arg substrate in AdiC, and that the residues surrounding the binding site include F252, S342 and C407 (Fig. 3B) [20]. A comparison between the hLAT1 and the AdiC binding sites is shown in Supplemental Fig. 3. As reported in Geier et al. [18], our model confirmed that the hLAT1 binding site volume is greater than the AdiC one, and this is due to the substitutions of the corresponding residues between the two primary structures, e.g. W202 is replaced by F252 and W293 by S342 (Fig. 1). To investigate the actual role of these residues, mutants were constructed and the corresponding recombinant proteins were produced in *E. coli* and purified as described in Sections 2.2 and 2.3. F252 was substituted either by a conservative residue, corresponding to the AdiC homologue (F252W), or by a non-conservative residue (F252A), changing the chemical/steric properties of the side chain. The transport activity of the mutant proteins was tested in proteoliposomes as His_{ex}/His_{in} antiport (Fig. 4A) to evaluate possible loss of function. Interestingly, the substitution F252A completely abolished transport activity; while, substitution F252W only impaired transport with respect to the WT. To gain further insights into this aspect, kinetic analysis was conducted on F252W. The measured Km (Fig. 4B) was 184 ± 40 μM, higher than that of WT [2]. The internal Km of F252W was very similar to that of WT, i.e., 2.0 ± 0.45 mM (Supplemental Fig. 7).

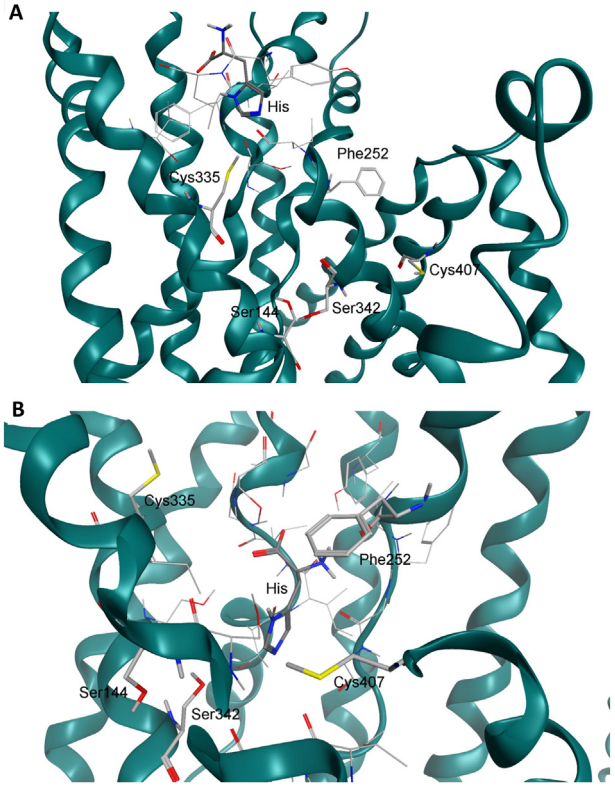

Fig. 3. hLAT1 Substrate binding site. Representative docking poses for His in LAT1 outward-open form A) and outward-closed form B). hLAT1 is shown in ribbon representation; His and residues of the binding site are shown as stick representation.

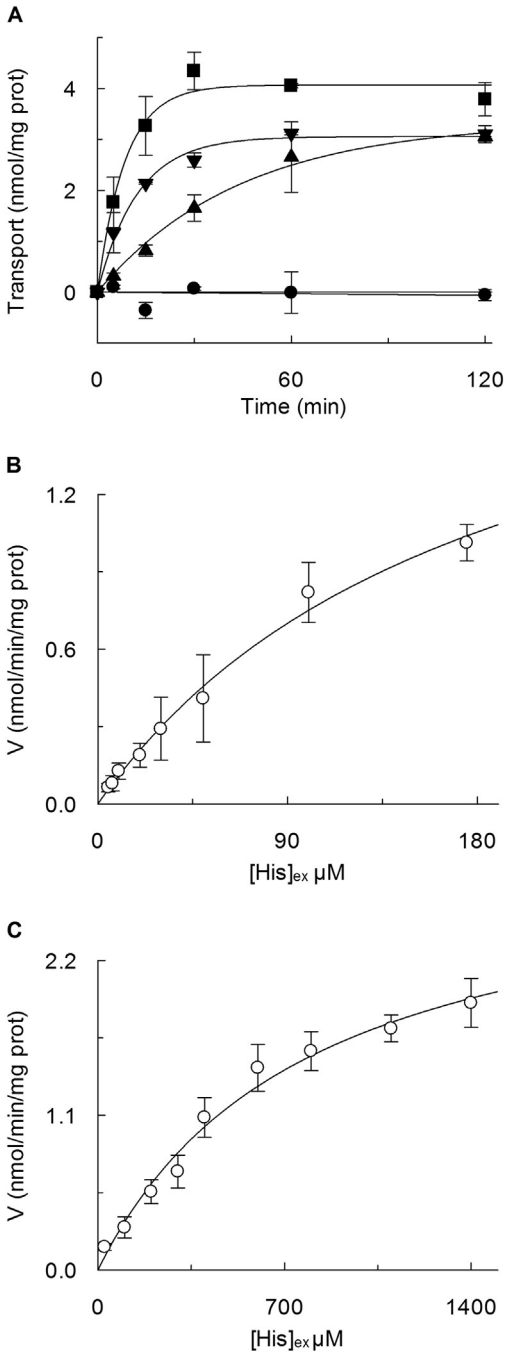

Fig. 4. [^{3}H]His uptake in proteoliposomes reconstituted with over-expressed hLAT1 WT and mutants. A) Transport was started adding 5 μM [^{3}H]His to proteoliposomes reconstituted with LAT1 WT (■), F252W (▲), F252A (●) or S342G (▼). Proteoliposomes contained 10 mM His and transport reaction was stopped at indicated times as described in Section 2.5. Data are plotted according to first rate equation. Results are mean ± S.D. from three independent experiments. B–C) Dependence of the rate of His antiport. The transport rate at 30 min was measured adding [^{3}H]His at the indicated concentrations to proteoliposomes reconstituted with LAT1 F252W B) or LAT1 S342G C) containing 10 mM internal His. Data were plotted according to Michaelis–Menten equation. Results are mean ± S.D. from five independent experiments.

The mutant S342G was also tested for activity (Fig. 4A). This protein was functional and the transport activity was similar to that of WT. The Km for His of S342G was much higher than that of WT with a value of 784 ± 139 μM (Fig. 4C); while the internal Km, i.e., 3.2 ± 0.49 mM (Supplemental Fig. 7), was similar to the WT Km. Cys mutants were generated substituting C335 or C407 or both with Ala. The time

course of the two mutants showed that they are functional, even though C335A and the double mutant were less active than the WT (Fig. 5A). Km for substrate were measured on both the external and internal membrane sides. As shown in Fig. 5B, substitution of C335 strongly increased the external Km which was 582 ± 234 μM indicating that also C335 is crucial for substrate binding. C407A mutant showed a Km (37 ± 11 μM, Supplemental Fig. 8) similar to that of WT [2]. In silico mutants strongly confirmed this experimental evidence: the mutation of C335 to A reduces the affinity for the substrate to 2.4 kcal/mol, on the contrary, the same mutation on C407 does not modify the affinity for His with respect to the WT hLAT1 (0.1 kcal/mol). Internal Km was not influenced by the substitution of C335 (2.5 ± 0.67 mM) but slightly impaired by the substitution of C407, with a value of 5.9 ± 1.4 mM (Fig. 5C). The external Km of the double mutant was strongly impaired as in the case of C335A (775 ± 127 μM, Supplemental Fig. 9) while the internal one was similar to that of C407A (not shown).

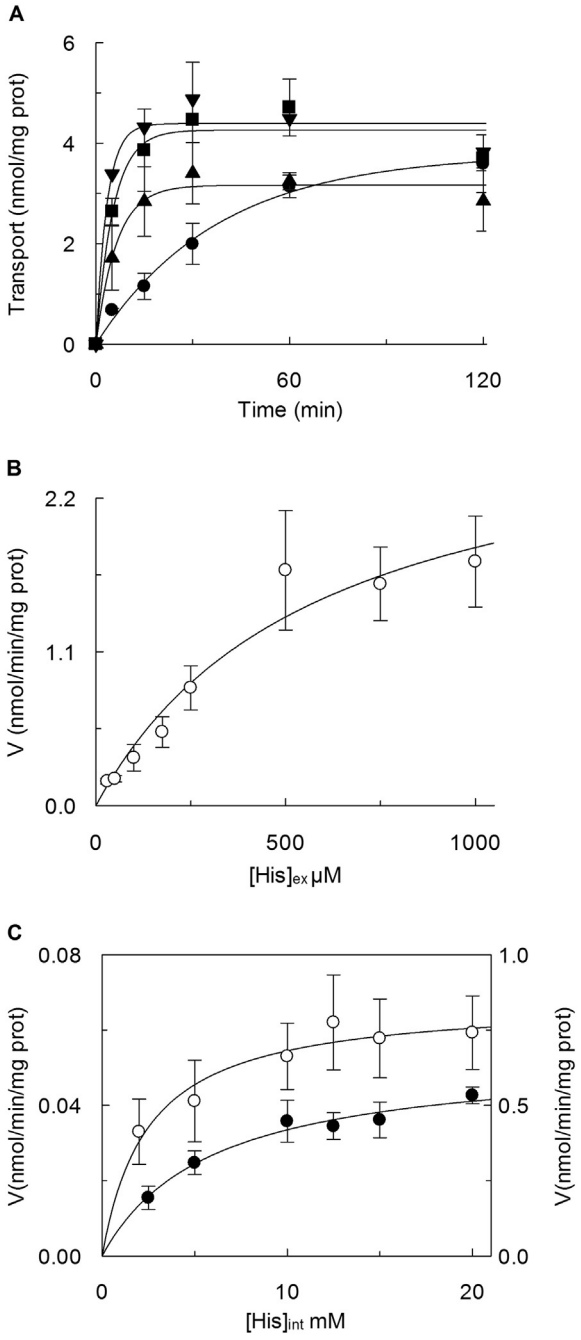

Fig. 5. [^{3}H]His uptake in proteoliposomes reconstituted with over-expressed hLAT1 WT and mutants. A) Transport was started adding 5 μM [^{3}H]His to proteoliposomes reconstituted with LAT1 WT (■), C335A (●), C407A (▼) or double mutant C335A/C407A (▲). Proteoliposomes contained 10 mM His and transport reaction was stopped at indicated times as described in Section 2.5. Data are plotted according to first rate equation. Results are mean ± S.D. from three independent experiments. B) Dependence of the rate of His antiport. The transport rate at 30 min was measured adding [^{3}H]His at the indicated concentrations to proteoliposomes reconstituted with LAT1 C335A containing 10 mM internal His. Data were plotted according to Michaelis–Menten equation. Results are mean ± S.D. from three independent experiments. C) Dependence of the rate of His antiport. The transport rate at 30 min for C335A mutant and at 15 min for C407A mutant was measured adding 5 μM [^{3}H]His to proteoliposomes reconstituted with LAT1 C335A (○) or C407 (●) containing indicated concentrations of internal His. Data were plotted according to Michaelis-Menten equation, left y-axys corresponds to C335A data and right y-axis to C407A. Results are mean ± S.D. from three independent experiments.

3.2. Inhibition by mercury compounds

To further investigate the topological relationships of the two Cys residues namely C335 and C407, the reactivity of WT and mutants towards SH reagents was tested. Indeed, it has been previously demonstrated that LAT1 interacts with mercury compounds [37,38]. Dose-response experiments for $HgCl_2$ were performed on WT, C335A, C407A and C335/407A (Fig. 6A). Very similar patterns were observed for WT and the mutants with comparable IC50 values: 0.90 ± 0.14 μM, 1.3 ± 0.13 μM, 1.3 ± 0.10 μM or 1.7 ± 0.12 μM for WT, C335A, C407A or C335/407A, respectively. These data ruled out the possible involvement of these Cys residues in the interaction with the mercury compound. The kinetic of inhibition of His transport by $HgCl_2$ (Fig. 6B) showed a non-competitive pattern demonstrating that the interaction of the mercury compound occurs via residues far from the substrate binding site. Other hydrophilic or hydrophobic SH reagents were also tested. Methyl-Hg, Ethyl-Hg, MTSEA and NEM inhibited approximately at the same extent the WT and the Cys mutants (Fig. 6C) confirming that the two Cys residues are not involved in interaction with SH reagents. The inhibition by mercury compounds was reversed by the S-S reducing agent DTE (experiments not shown), proving the involvement of thiol group(s) of Cys residue(s) other than C335 or C407, in the inhibition.

3.3. Effect of intracellular cations on LAT1 transport activity

As previously shown, His transport mediated by hLAT1 is not dependent on external Na^+ in agreement with data from intact cells [1]. By means of the proteoliposome model, the possible influence by intraliposomal (intracellular) ions on transport was investigated. Fig. 7A shows that internal K^+ stimulated His antiport with respect to the control, containing sucrose. K-gluconate and KCl exerted similar effects demonstrating that the Cl^- was not involved in stimulation. Na^+ had a similar effect of that of K^+. Fig. 7B shows the dependence of stimulation on K^+ concentration. The activity increased along with the internal K^+ level reaching a plateau at 80 mM, i.e., a concentration not far from the physiological level. To understand if intraliposomal (intracellular) K^+ could affect transporter affinity towards its substrates, kinetic analysis was performed showing an increase of Vmax from 2.1 ± 0.16 to 3.1 ± 0.28 nmol mg^{-1} min^{-1}, while the Km was not significantly influenced being 36.4 ± 6.7 μM or 36.0 ± 8.0 μM in absence or presence of internal K^+, respectively (Fig. 7C).

3.4. Kinetics and transport mechanism of LAT1

The kinetic mechanism of the His_{ex}/His_{in} antiport was investigated by a bi-reactant analysis. In this type of experiment, the concentrations of both external and internal substrates were varied in a single experiment [39,40]. The rate of [^{3}H]His uptake was plotted as function of the external (Fig. 8A) or internal His (Fig. 8B) concentrations. Data were plotted according to Lineweaver-Burk, which allows discriminating between ping-pong and simultaneous mechanisms [41]. In all the

analysed reactions, the straight lines showed non parallel patterns intersecting in proximity of the X-axis. These data demonstrated that the His_{ex}/His_{in} transport reaction follows a simultaneous mechanism that can be random or ordered. The first is characterized by no preferential binding order of the two substrates to the transporter; while in the ordered type, one of the two substrates binds first to the transporter. The two types can be discriminated by analyzing the dissociation constant of the ternary (His_{ex}-transporter-His_{in}) and binary transporter-His complexes [41,42]. These constants were calculated by re-plotting the values of the intercepts on the Y-axis or the slopes of the straight lines, as function of the reciprocal substrate concentrations (insets of Fig 8A and B). Concentration independent (Ks) values were 47.5 μM for external His and 5.6 mM for internal His. The Ki_S values were 73 μM for external His and 9.5 mM for internal His, i.e., similar to the respective Ks values and fulfilling the relation $Ki_{S1} \cdot K_{S2} = Ki_{S2} \cdot K_{S1}$ which is typical of a random simultaneous mechanism. This implies that the two substrates bind at the same time to the external and internal sites. External Km for other substrates of LAT1, namely Leu, Met, Val, Gln or Ala was 25 ± 13 μM, 31 ± 11 μM, 57 ± 20 μM, 0.7 ± 0.4 mM or >1 mM, respectively (experiments not shown). These values are in the same order of magnitude of those previously measured in intact cells, i.e., 19.7 μM, 20.2 μM, 47.2 μM, 1.6 mM for Leu, Met, Val, Gln, respectively. While no values of Km for Ala are available in intact cells [2,43,44]. This confirms that the functional properties of the recombinant protein resemble those of the native one.

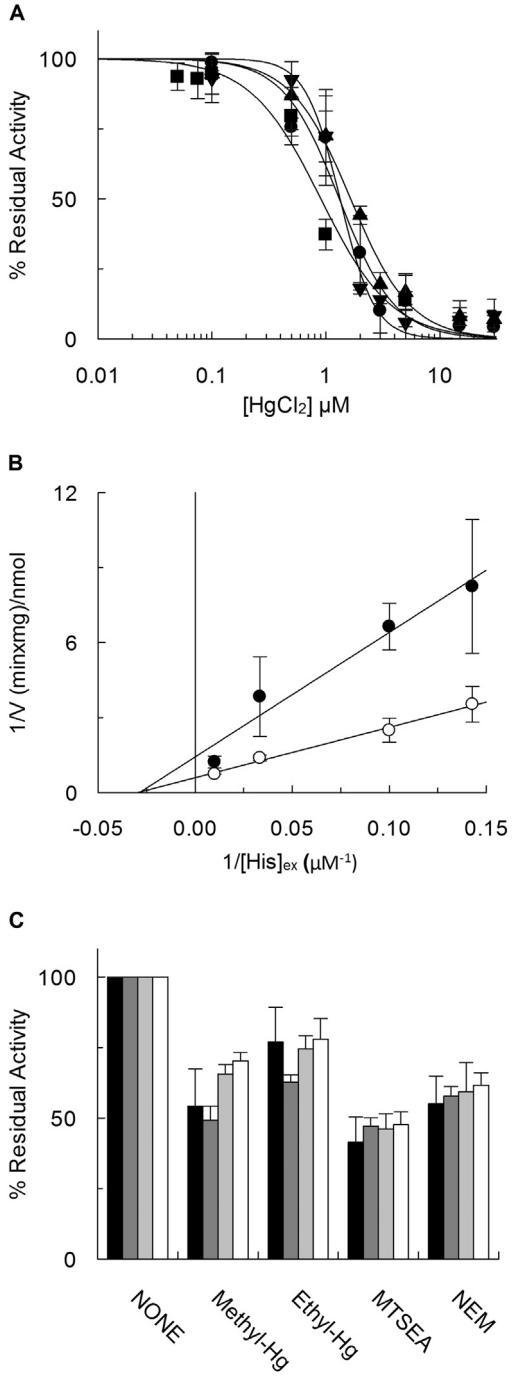

Fig. 6. Inhibition by SH-reagents of the recombinant hLAT1 in proteoliposomes. A) Dose-response curves for the inhibition by $HgCl_2$ of the hLAT1 WT and mutants. Transport was measured adding 5 μM [^{3}H]His to proteoliposomes containing 10 mM His reconstituted with LAT1 WT (■), C335A (●), C407A (▼) or double mutant C335A/C407A (▲) in the presence of indicated concentrations of $HgCl_2$. Transport was measured in 30 min as described in Section 2.5. Percent residual activity with respect to the control (without additions) is reported. Results are mean ± S.D. from three independent experiments. B) Kinetic analysis of the inhibition according to Lineweaver–Burk as reciprocal transport rate vs reciprocal His concentration; transport rate was measured adding 5 μM [^{3}H]His at the indicated concentrations to proteoliposomes containing 10 mM His and stopping the reaction after 15 min as described in Section 2.5. In (●) 0.8 μM $HgCl_2$ was added as inhibitor in comparison to samples without inhibitor (○). Results are mean ± S.D. from three independent experiments. C) Effect of Methyl-Hg, Ethyl-Hg, MTSEA and NEM on the LAT1 WT and Cys-mutants. Transport was measured adding 5 μM [^{3}H]His to proteoliposomes containing 10 mM His reconstituted with LAT1 WT (black bar), C335A (dark gray bar), C407A (light gray bar) or C335A/C407A (white bar) in the presence of 5 μM Methyl-Hg, 12 μM Ethyl-Hg, 50 μM MTSEA or 500 μM NEM. Transport was measured in 30 min as described in Section 2.5. Percent residual activity with respect to the control (without additions) is reported. Results are mean ± S.D. from three independent experiments. Student's two tailed unpaired *t*-test was performed on the sample without external compounds (control) and no differences respect control have been observed within the p value <0.05. (For interpretation of the references to color in this figure legend, the reader is referred to the web version of this article.)

3.5. Oligomeric structure of hLAT1

The possible existence of a dimeric structure as predicted by bioinformatics (Fig. 1), was investigated. Fig. 9A shows Western Blot of recombinant hLAT1 analysed by electrophoresis under mild denaturing conditions on Sarkosyl-PAGE and stained by anti-His. The presence of aggregates at higher molecular mass, in addition to the hLAT1 monomer, were observed. This indicated that the functional hLAT1 may have oligomeric composition. A similar analysis was performed on hLAT1 after insertion into proteoliposome membrane. In this case (Fig. 9A, lane 2), the oligomeric form of the protein was predominant. The apparent molecular mass of the monomeric and dimeric forms were lower than in lane 1; this was due to interference, during the run, of phospholipids deriving from proteoliposomes. To further analyze the presence of an oligomeric hLAT1 by SDS-PAGE, a cross-linking strategy was adopted. The solubilized protein was treated with Cu^{++}-phenanthroline which induces disulfide formation between vicinal Cys residues of proteins [45,46]. After treatment with the reagent, most of the protein migrated at a double molecular mass with respect to the untreated monomer (Fig. 9B, lane 2) due to formation of disulfide(s), confirming the existence of a prevalent dimeric form of hLAT1. To investigate the presence of oligomeric form of the protein in vivo, membranes from SiHa cells were solubilized and assayed with anti-LAT1 antibody (Fig. 9C). Solubilized sample was treated with DTE to separate CD98 from LAT1. Two major bands were observed under this condition, one at about 35 kDa and the other at about doubled molecular mass (Fig. 9C, lane 1). In the sample not treated with DTE (Fig. 9C, lane 2), a diffuse band was detected at an higher molecular mass which may have an heterogeneous composition including hLAT1 homodimer and/or LAT1/CD98 heterodimer.

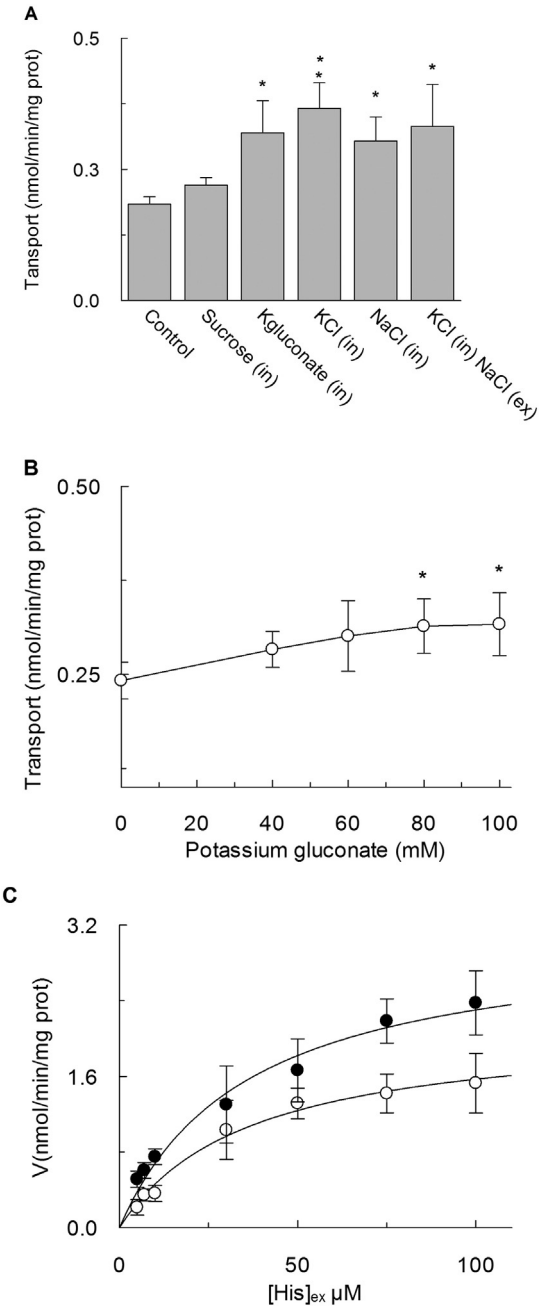

Fig. 7. Effects of intraliposomal salts on His_{ex}/His_{in} transport in proteliposomes. A) The reconstitution was performed as described in Section 2.4. Transport was started adding 5 µM [^{3}H]His to proteoliposomes containing 10 mM His and 100 mM of indicated salts. Sucrose at 200 mM was used as control of osmotic stress. Effect of 100 mM NaCl added to the extraliposomal compartment was also evaluated. Transport reaction was stopped at 30 min as described in Section 2.5. Results are mean ± S.D. from three independent experiments. B) Transport was started adding 5 µM [^{3}H]His to proteoliposomes containing 10 mM His and indicated concentrations of Potassium gluconate and stopped at 30 min as described in Section 2.5. Results are mean ± S.D. from three independent experiments. Student's two tailed unpaired *t*-test was performed on the sample without internal compounds (control); *p* values were symbolized as follows: $^*p < 0.05$; $^{**}p < 0.01$ (A–B). C) Dependence of the rate of His antiport. The transport rate at 15 min was measured adding [^{3}H]His at the indicated concentrations to proteoliposomes containing 10 mM internal His in the presence (●) or absence (○) of 100 mM Potassium gluconate. Data were plotted according to Michaelis - Menten equation. Results are mean ± S.D. from four independent experiments.

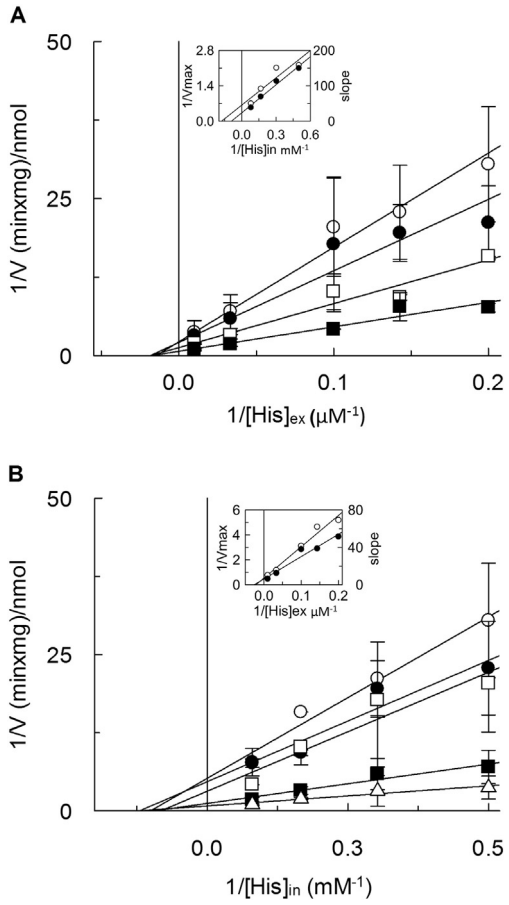

Fig. 8. Kinetics and Transport mechanism of the recombinant hLAT1. Data were analyzed by Lineweaver–Burk plots showing the dependence of reciprocal transport rate on reciprocal external A) or internal B) His concentrations. Transport reaction was stopped at 15 min as described in Section 2.5. In A), the concentrations of intraliposomal His were 2.0 (○), 3.3 (●), 6.0 (□), 12.5 (■) mM; the concentrations of external [^{3}H]His were 5.0, 7.0, 10, 33, 100 µM. In B) the same data of A) were plotted as function of the internal His concentration at external [^{3}H]His 5.0 (○), 7.0 (●), 10 (□), 30 (■), 100 (Δ) µM. In A–B the insets show the re-plots of the intercepts on the Y-axis (1/Vmax - ○) or the slopes (Km/Vmax - ●) from the primary plots as a function of internal A) or external B) His. Results are mean ± S.D. from three independent experiments.

4. Discussion

In spite of the more than 450 papers dedicated to LAT1(CD98) (from Pubmed with "LAT1 (OR) SLC7A5" keyword entry in "Title & Abstract") of the last 10 years, no or only predictive information is available on the structure/function relationships of this important transporter. Therefore, we have invested efforts in advancing the molecular knowledge of transport mechanism. Two different crystallized structures, one of AdiC (e.g. PDB: 3L1L) and the other of ApcT (e.g. PDB: 3GI9), can be used as distant homologous templates for hLAT1 comparative modelling. At the state of the art, the selection of the best template for modelling purposes is still challenging since the BLASTP and the HMM-based alignment are characterized by non-significantly different scores. We decided to base our modelling on the AdiC crystallographic structures, since more literature data supported this option [18,20,29]. Even though the homology model of LAT1 was built on the basis of AdiC, some relevant differences in term of molecular mechanism of substrate recognition are expected, since LAT1 accepts aromatic or aliphatic amino acids, while AdiC is mainly involved in interactions with the charged, Arg and Agmatine [2,29]. Indeed, W202 and W293 of AdiC are replaced in LAT1, respectively, by the more hydrophobic F252 according to Kyte-Doolittle [47] and by S342. These residues were previously predicted by bioinformatics to be involved in substrate recognition [18] but not experimentally proven, so far. In the present work, for the first time, the relationship of the F252 and S342 residues with substrate translocation has been demonstrated. In particular, F252 revealed to be essential as a gate of LAT1 as testified by disruptive

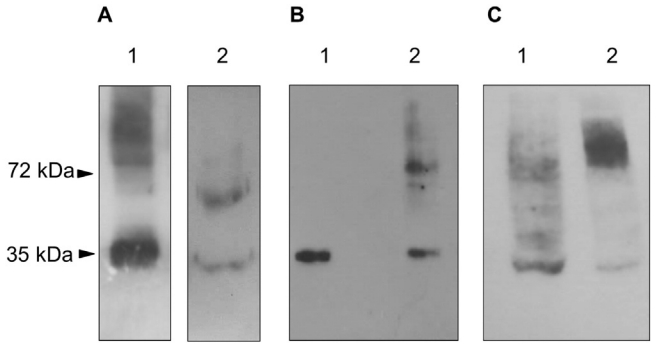

Fig. 9. Oligomeric state of recombinant and native hLAT1. In A) purified and functional hLAT1 (lane 1) or hLAT1 inserted in proteoliposomes (lane 2) was subjected to electrophoresis under mild denaturing conditions, using sarkosyl (0.1%) instead of SDS (0.1%) in all run buffers without reducing agents in sample buffer. In B) purified and functional hLAT1 has been treated with 2 mM Cu^{++}-phenanthroline (lane 2) compared to untreated control (lane 1). After stopping cross-linking reaction, samples were run on a SDS-PAGE 10% without reducing agents in sample buffer. Protein monomers and oligomers were detected by immunoblotting analysis using anti-His antiserum 1:1000 dilution as described in Section 2.7 (A–B). In C) native hLAT1 was extracted from SiHa cell membrane and subjected to electrophoresis under mild denaturing conditions (as in 2A) treated (lane 1) or not (lane 2) with 100 mM DTE before running. Protein monomers and oligomers were detected by immunoblotting analysis using anti-LAT1 antiserum 1:2000 dilution as described in Section 2.7. Western blots (A–C) are representative of three independent experiments.

effect of Ala substitution compared to F252W mutation and in analogy with structural data on AdiC [20]. However, the conservative substitution with W is not sufficient to restore proper affinity for substrate. An additional residue involved in substrate recognition and transport has been further identified, namely C335 which corresponds to C286 in AdiC (Figs. 1 and 3). This is mostly involved in substrate binding. Indeed, external Km increases up to 20 fold compared to WT. This result indicates that the thiol was the critical chemical group that is not present in Ala and that C335 represents a forefront residue for His binding. Another Cys residue was predicted to be part of the substrate binding site, namely C407. This residue, however, has a marginal role in substrate recognition since only the internal Km shows small variation upon mutation. The corresponding residue in AdiC is S357 (Figs. 1 and 3) whose side chain is more hydrophilic than that of Cys. Interestingly, AdiC in which this residue is mutated to Ala shows an affinity for substrate similar to that of WT as we observe in LAT1 [21]. Taken together, the results indicate: i) a switch from hydrophilic to neutral/hydrophobic substrate recognition between AdiC and LAT1; ii) that F252 is a gate element, allowing substrate entry in the translocation site playing, possibly, the same function as W202 in AdiC [20]; iii) that the other residues, i.e., S342 and C335 are responsible of substrate docking prior to translocation. Noteworthy, the prototype transporter with the same fold of LAT1, LeuT, shows critical residues more similar to LAT1 than AdiC, according to the more hydrophobic nature of LeuT substrates (not shown). This concept is also in agreement with predictions of a LAT1 wider binding site (smaller residues of the crucial amino acids) with respect to AdiC to accommodate larger amino acids [18].

C335A and C407A play a role in substrate handling and are not targeted by SH reagents either small, large, hydrophobic or hydrophilic, as shown by the unvaried sensitivity of C335A, C407A and C335/407A mutants to all these reagents. This means that the residues are not easily accessible by molecules other than substrates, i.e., the active site is accessible only upon substrate induced gating. Therefore, the high affinity of the transporter towards SH reacting compounds, mercurial or alkylating ones, is mediated by one or more of the other ten Cys residues. The mercury compounds do not interfere with the substrate path but impair conformational changes, according to the non-competitive inhibition caused by $HgCl_2$. Concerning the effect of K^+ and, at a similar extent, of Na^+ in stimulating the transport activity of LAT1 from the internal side, it might be due to a remnant cation binding site which is present in LeuT [48,49]. A similar effect by cations has been described for other membrane transporters of neutral amino acids, namely ASCT2, ASCT1 and B0AT1 which are stimulated/regulated by internal cations at physiological concentration [40,50,51]. Data on the kinetic mechanism of transport are in favor of a random simultaneous transport mechanism which implies formation of a ternary complex in which internal and external substrates are bound and translocated simultaneously towards opposed sides of the membrane. This type of mechanism cannot be easily explained by an alternating access model as that of LeuT [52,53] or APCS [54]. The simultaneous mechanism could however be explained by the existence of an oligomeric structure in which each single monomer can bind and translocate substrates from outside to inside or vice versa independently [40,41,55]. Data suggesting existence of hLAT1 dimeric structure are indeed in favor of the above described transport mechanism. Interestingly, AdiC, used as model and other similar eukaryotic transporters show also a dimeric organization [20,21,56–59]. Covalent dimer is observed upon treatment of the protein with S-S forming reagent; thus, it is likely that one (or more) Cys residue is located along the contact surface between the two monomers as highlighted by our model (Fig. 2) in which the residue C458 faces the homodimerization space, far from the C164 responsible of covalent interaction with CD98. Therefore, it can be hypothesized that also in cells hLAT1 can exist in a dimeric quaternary structure made by either homodimers of hLAT1 or dimers of the hLAT1/CD98 complex.

5. Conclusions

In this work, we improved the molecular knowledge on the human LAT1 transporter by using recombinant protein produced in *E. coli*, site-directed mutagenesis and transport assay in proteoliposomes. The residues F252, C335, S342 and C407 have been experimentally demonstrated to be critical for substrate binding and translocation shedding light on possible dimerization of the protein in cell membrane in analogy of APC transporters [20,21,56–59]. Since LAT1 is considered a valuable target for cancer therapy, the scenario resulting from these data represents also a step forward for studies aimed to identification of new potent and specific inhibitors that may have great outcome on human health.

Transparency document

The Transparency document associated with this article can be found, in online version.

Acknowledgments

This work was supported by grant from Italian MIUR, Ministero dell'Istruzione, dell'Università e della Ricerca [PON01_00937].

Appendix A. Supplementary data

Supplementary data to this article can be found online at http://dx.doi.org/10.1016/j.bbagen.2017.01.013.

References

[1] L. Mastroberardino, B. Spindler, R. Pfeiffer, P.J. Skelly, J. Loffing, C.B. Shoemaker, F. Verrey, Amino-acid transport by heterodimers of 4F2hc/CD98 and members of a permease family, Nature 395 (1998) 288–291.
[2] L. Napolitano, M. Scalise, M. Galluccio, L. Pochini, L.M. Albanese, C. Indiveri, LAT1 is the transport competent unit of the LAT1/CD98 heterodimeric amino acid transporter, Int. J. Biochem. Cell Biol. 67 (2015) 25–33.
[3] V. Ganapathy, M. Thangaraju, P.D. Prasad, Nutrient transporters in cancer: relevance to Warburg hypothesis and beyond, Pharmacol. Ther. 121 (2009) 29–40.
[4] L. Yang, T. Moss, L.S. Mangala, J. Marini, H. Zhao, S. Wahlig, G. Armaiz-Pena, D. Jiang, A. Achreja, J. Win, R. Roopaimoole, C. Rodriguez-Aguayo, I. Mercado-Uribe, G. Lopez-Berestein, J. Liu, T. Tsukamoto, A.K. Sood, P.T. Ram, D. Nagrath, Metabolic shifts

toward glutamine regulate tumor growth, invasion and bioenergetics in ovarian cancer, Mol. Syst. Biol. 10 (2014) 728.
[5] C. Colas, P.M.U. Ung, A. Schlessinger, SLC transporters: structure, function, and drug discovery, Med. Chem. Commun. 7 (2016) 1069–1081.
[6] B.C. Fuchs, B.P. Bode, Amino acid transporters ASCT2 and LAT1 in cancer: partners in crime? Semin. Cancer Biol. 15 (2005) 254–266.
[7] Y.D. Bhutia, E. Babu, S. Ramachandran, V. Ganapathy, Amino acid transporters in cancer and their relevance to "glutamine addiction": novel targets for the design of a new class of anticancer drugs, Cancer Res. 75 (2015) 1782–1788.
[8] Y. Zhao, L. Wang, J. Pan, The role of L-type amino acid transporter 1 in human tumors, Intractable Rare Dis. Res. 4 (2015) 165–169.
[9] Q. Wang, J. Holst, L-type amino acid transport and cancer: targeting the mTORC1 pathway to inhibit neoplasia, Am. J. Cancer Res. 5 (2015) 1281–1294.
[10] L. Pochini, M. Scalise, M. Galluccio, C. Indiveri, Membrane transporters for the special amino acid glutamine: structure/function relationships and relevance to human health, Front. Chem. 2 (2014) 61.
[11] M. Scalise, L. Pochini, M. Galluccio, C. Indiveri, Glutamine transport. From energy supply to sensing and beyond, Biochim. Biophys. Acta 1857 (2016) 1147–1157.
[12] R. Milkereit, A. Persaud, L. Vanoaica, A. Guetg, F. Verrey, D. Rotin, LAPTM4b recruits the LAT1-4F2hc Leu transporter to lysosomes and promotes mTORC1 activation, Nat. Commun. 6 (2015) 7250.
[13] M. Rebsamen, L. Pochini, T. Stasyk, M.E. de Araujo, M. Galluccio, R.K. Kandasamy, B. Snijder, A. Fauster, E.L. Rudashevskaya, M. Bruckner, S. Scorzoni, P.A. Filipek, K.V. Huber, J.W. Bigenzahn, L.X. Heinz, C. Kraft, K.L. Bennett, C. Indiveri, L.A. Huber, G. Superti-Furga, SLC38A9 is a component of the lysosomal amino acid sensing machinery that controls mTORC1, Nature 519 (2015) 477–481.
[14] S. Wang, Z.Y. Tsun, R.L. Wolfson, K. Shen, G.A. Wyant, M.E. Plovanich, E.D. Yuan, T.D. Jones, L. Chantranupong, W. Comb, T. Wang, L. Bar-Peled, R. Zoncu, C. Straub, C. Kim, J. Park, B.L. Sabatini, D.M. Sabatini, Metabolism. Lysosomal amino acid transporter SLC38A9 signals arginine sufficiency to mTORC1, Science 347 (2015) 188–194.
[15] J.M. Cantor, M.H. Ginsberg, CD98 at the crossroads of adaptive immunity and cancer, J. Cell Sci. 125 (2012) 1373–1382.
[16] L.R. de la Ballina, S. Cano-Crespo, E. Gonzalez-Munoz, S. Bial, S. Estrach, L. Cailleteau, F. Tissot, H. Daniel, A. Zorzano, M.H. Ginsberg, M. Palacin, C.C. Feral, Amino acid transport associated to cluster of differentiation 98 heavy chain (CD98hc) Is at the cross-road of oxidative stress and amino acid availability, J. Biol. Chem. 291 (2016) 9700–9711.
[17] E. Nakamura, M. Sato, H. Yang, F. Miyagawa, M. Harasaki, K. Tomita, S. Matsuoka, A. Noma, K. Iwai, N. Minato, 4F2 (CD98) heavy chain is associated covalently with an amino acid transporter and controls intracellular trafficking and membrane topology of 4F2 heterodimer, J. Biol. Chem. 274 (1999) 3009–3016.
[18] E.G. Geier, A. Schlessinger, H. Fan, J.E. Gable, J.J. Irwin, A. Sali, K.M. Giacomini, Structure-based ligand discovery for the large-neutral amino acid transporter 1, LAT-1, Proc. Natl. Acad. Sci. U. S. A. 110 (2013) 5480–5485.
[19] H. Ylikangas, K. Malmioja, L. Peura, M. Gynther, E.O. Nwachukwu, J. Leppanen, K. Laine, J. Rautio, M. Lahtela-Kakkonen, K.M. Huttunen, A. Poso, Quantitative insight into the design of compounds recognized by the L-type amino acid transporter 1 (LAT1), ChemMedChem 9 (2014) 2699–2707.
[20] X. Gao, L. Zhou, X. Jiao, F. Lu, C. Yan, X. Zeng, J. Wang, Y. Shi, Mechanism of substrate recognition and transport by an amino acid antiporter, Nature 463 (2010) 828–832.
[21] H. Ilgu, J.M. Jeckelmann, V. Gapsys, Z. Ucurum, B.L. de Groot, D. Fotiadis, Insights into the molecular basis for substrate binding and specificity of the wild-type L-arginine/agmatine antiporter AdiC, Proc. Natl. Acad. Sci. U. S. A. 113 (2016) 10358–10363.
[22] M. Galluccio, L. Pochini, V. Peta, M. Ianni, M. Scalise, C. Indiveri, Functional and molecular effects of mercury compounds on the human OCTN1 cation transporter: C50 and C136 are the targets for potent inhibition, Toxicol. Sci. 144 (2015) 105–113.
[23] S.N. Ho, H.D. Hunt, R.M. Horton, J.K. Pullen, L.R. Pease, Site-directed mutagenesis by overlap extension using the polymerase chain reaction, Gene 77 (1989) 51–59.
[24] M. Galluccio, P. Pingitore, M. Scalise, C. Indiveri, Cloning, large scale over-expression in *E. coli* and purification of the components of the human LAT 1 (SLC7A5) amino acid transporter, Protein J. 32 (2013) 442–448.
[25] L. Console, M. Scalise, Z. Tarmakova, I.R. Coe, C. Indiveri, N-linked glycosylation of human SLC1A5 (ASCT2) transporter is critical for trafficking to membrane, Biochim. Biophys. Acta 1853 (2015) 1636–1645.
[26] F. Palmieri, C. Indiveri, F. Bisaccia, V. Iacobazzi, Mitochondrial metabolite carrier proteins: purification, reconstitution, and transport studies, Methods Enzymol. 260 (1995) 349–369.
[27] E.M. Torchetti, C. Brizio, M. Colella, M. Galluccio, T.A. Giancaspero, C. Indiveri, M. Roberti, M. Barile, Mitochondrial localization of human FAD synthetase isoform 1, Mitochondrion 10 (2010) 263–273.
[28] L. Kowalczyk, M. Ratera, A. Paladino, P. Bartoccioni, E. Errasti-Murugarren, E. Valencia, G. Portella, S. Bial, A. Zorzano, I. Fita, M. Orozco, X. Carpena, J.L. Vazquez-Ibar, M. Palacin, Molecular basis of substrate-induced permeation by an amino acid antiporter, Proc. Natl. Acad. Sci. U. S. A. 108 (2011) 3935–3940.
[29] X. Gao, F. Lu, L. Zhou, S. Dang, L. Sun, X. Li, J. Wang, Y. Shi, Structure and mechanism of an amino acid antiporter, Science 324 (2009) 1565–1568.
[30] D. Van Der Spoel, E. Lindahl, B. Hess, G. Groenhof, A.E. Mark, H.J. Berendsen, GROMACS: fast, flexible, and free, J. Comput. Chem. 26 (2005) 1701–1718.
[31] Z. Guo, U. Mohanty, J. Noehre, T.K. Sawyer, W. Sherman, G. Krilov, Probing the alpha-helical structural stability of stapled p53 peptides: molecular dynamics simulations and analysis, Chem. Biol. Drug Des. 75 (2010) 348–359.
[32] H.J.C.P. Berendsen, J. P. M., W.F. van Gunsteren, A. DiNola, J.R. Haak, Molecular-dynamics with coupling to an external bath, J. Chem. Phys. 81 (1984) 3684–3690.
[33] S. Nosé, A unified formulation of the constant temperature molecular-dynamics methods, J. Chem. Phys. 81 (1984) 511–519.
[34] F. M., H. Eldesbrunner, R. Fu, J. Liang, Proceedings of the 28th Hawaii International Conference on Systems Science, 1995.
[35] Y. Fang, H. Jayaram, T. Shane, L. Kolmakova-Partensky, F. Wu, C. Williams, Y. Xiong, C. Miller, Structure of a prokaryotic virtual proton pump at 3.2 A resolution, Nature 460 (2009) 1040–1043.
[36] A. Krogh, B. Larsson, G. von Heijne, E.L. Sonnhammer, Predicting transmembrane protein topology with a hidden Markov model: application to complete genomes, J. Mol. Biol. 305 (2001) 567–580.
[37] R.J. Boado, J.Y. Li, C. Chu, F. Ogoshi, P. Wise, W.M. Pardridge, Site-directed mutagenesis of cysteine residues of large neutral amino acid transporter LAT1, Biochim. Biophys. Acta 1715 (2005) 104–110.
[38] Z. Yin, H. Jiang, T. Syversen, J.B. Rocha, M. Farina, M. Aschner, The methylmercury-L-cysteine conjugate is a substrate for the L-type large neutral amino acid transporter, J. Neurochem. 107 (2008) 1083–1090.
[39] C. Indiveri, A. Tonazzi, A. De Palma, F. Palmieri, Kinetic mechanism of antiports catalyzed by reconstituted ornithine/citrulline carrier from rat liver mitochondria, Biochim. Biophys. Acta 1503 (2001) 303–313.
[40] M. Scalise, L. Pochini, S. Panni, P. Pingitore, K. Hedfalk, C. Indiveri, Transport mechanism and regulatory properties of the human amino acid transporter ASCT2 (SLC1A5), Amino Acids 46 (2014) 2463–2475.
[41] C. Indiveri, L. Capobianco, R. Kramer, F. Palmieri, Kinetics of the reconstituted dicarboxylate carrier from rat liver mitochondria, Biochim. Biophys. Acta 977 (1989) 187–193.
[42] W.W. C., Stade state kinetics, The Enzymes, 2, 1970, pp. 1–65.
[43] O. Yanagida, Y. Kanai, A. Chairoungdua, D.K. Kim, H. Segawa, T. Nii, S.H. Cha, H. Matsuo, J. Fukushima, Y. Fukasawa, Y. Tani, Y. Taketani, H. Uchino, J.Y. Kim, J. Inatomi, I. Okayasu, K. Miyamoto, E. Takeda, T. Goya, H. Endou, Human L-type amino acid transporter 1 (LAT1): characterization of function and expression in tumor cell lines, Biochim. Biophys. Acta 1514 (2001) 291–302.
[44] Y. Kanai, H. Segawa, K. Miyamoto, H. Uchino, E. Takeda, H. Endou, Expression cloning and characterization of a transporter for large neutral amino acids activated by the heavy chain of 4F2 antigen (CD98), J. Biol. Chem. 273 (1998) 23629–23632.
[45] N. Reyes, C. Ginter, O. Boudker, Transport mechanism of a bacterial homologue of glutamate transporters, Nature 462 (2009) 880–885.
[46] I. Bartholomaus, L. Milan-Lobo, A. Nicke, S. Dutertre, H. Hastrup, A. Jha, U. Gether, H.H. Sitte, H. Betz, V. Eulenburg, Glycine transporter dimers: evidence for occurrence in the plasma membrane, J. Biol. Chem. 283 (2008) 10978–10991.
[47] J. Kyte, R.F. Doolittle, A simple method for displaying the hydropathic character of a protein, J. Mol. Biol. 157 (1982) 105–132.
[48] P.L. Shaffer, A. Goehring, A. Shankaranarayanan, E. Gouaux, Structure and mechanism of a Na^+-independent amino acid transporter, Science 325 (2009) 1010–1014.
[49] G. Khelashvili, S.G. Schmidt, L. Shi, J.A. Javitch, U. Gether, C.J. Loland, H. Weinstein, Conformational dynamics on the extracellular side of LeuT controlled by Na^+ and K^+ ions and the protonation state of Glu290, J. Biol. Chem. 291 (2016) 19786–19799.
[50] A.J. Scopelliti, G. Heinzelmann, S. Kuyucak, R.M. Ryan, R.J. Vandenberg, Na^+ interactions with the neutral amino acid transporter ASCT1, J. Biol. Chem. 289 (2014) 17468–17479.
[51] F. Oppedisano, C. Indiveri, Reconstitution into liposomes of the B degrees -like glutamine-neutral amino acid transporter from renal cell plasma membrane, Biochim. Biophys. Acta 1778 (2008) 2258–2265.
[52] D. Drew, O. Boudker, Shared molecular mechanisms of membrane transporters, Annu. Rev. Biochem. 85 (2016) 543–572.
[53] G. Rudnick, R. Kramer, R.D. Blakely, D.L. Murphy, F. Verrey, The SLC6 transporters: perspectives on structure, functions, regulation, and models for transporter dysfunction, Pflugers Arch. 466 (2014) 25–42.
[54] L.R. Forrest, R. Kramer, C. Ziegler, The structural basis of secondary active transport mechanisms, Biochim. Biophys. Acta 1807 (2011) 167–188.
[55] K. Khafizov, R. Staritzbichler, M. Stamm, L.R. Forrest, A study of the evolution of inverted-topology repeats from LeuT-fold transporters using AlignMe, Biochemistry 49 (2010) 10702–10713.
[56] F. Casagrande, M. Ratera, A.D. Schenk, M. Chami, E. Valencia, J.M. Lopez, D. Torrents, A. Engel, M. Palacin, D. Fotiadis, Projection structure of a member of the amino acid/polyamine/organocation transporter superfamily, J. Biol. Chem. 283 (2008) 33240–33248.
[57] Y. Fang, L. Kolmakova-Partensky, C. Miller, A bacterial arginine-agmatine exchange transporter involved in extreme acid resistance, J. Biol. Chem. 282 (2007) 176–182.
[58] Y. Alguel, S. Amillis, J. Leung, G. Lambrinidis, S. Capaldi, N.J. Scull, G. Craven, S. Iwata, A. Armstrong, E. Mikros, G. Diallinas, A.D. Cameron, B. Byrne, Structure of eukaryotic purine/H(+) symporter UapA suggests a role for homodimerization in transport activity, Nat. Commun. 7 (2016) 11336.
[59] G. Diallinas, Dissection of transporter function: from genetics to structure, Trends Genet. 32 (2016) 576–590.